Master Thesis, Department of Geosciences

Sedimentology, palaeontology and diagenesis of the Ordovician (Darriwilian) Svartodden Member (Huk Formation), Slemmestad, Oslo Region

Julie Guttormsen

UiO : Naturhistorisk museum

UNIVERSITY OF OSLO

FACULTY OF MATHEMATICS AND NATURAL SCIENCES

Front page photo: The Svartodden Mbr. at the Slemmestad IF arena locality, with the local cement factory seen in the distance.

UiO : Naturhistorisk museum

Sedimentology, palaeontology and diagenesis of the Ordovician (Darriwilian) Svartodden Member (Huk Formation), Slemmestad, Oslo Region

Julie Guttormsen

Master Thesis in Geosciences

Discipline: Geology

Department of Geosciences

Faculty of Mathematics and Natural Sciences

University of Oslo

November 1st , 2012

© Julie Guttormsen, 2012

This work is published digitally through DUO – Digitale Utgivelser ved UiO

http://www.duo.uio.no

It is also catalogued in BIBSYS (http://www.bibsys.no/english)

All rights reserved. No part of this publication may be reproduced or transmitted, in any form or by any means, without permission.

Acknowledgement

I would especially like to thank Professor Hans Arne Nakrem, who offered me a unique master thesis subject, with both elements of palaeontology and sedimentology. Thank you for being an excellent and always positive supervisor! I also greatly appreciate the good help from Dr. Øyvind Hammer and Krzysztof Hryniewicz, during discussions, analyses and feedback.

I owe Professor Nils-Martin Hanken a great thank you for teaching me about the petrography of limestones and about diagenetic studies, both in Tromsø and in Oslo. This thesis would not have been what it is if it was not for your help!

A special thank you goes to Dr. Björn Kröger, for being a great help in the identification of cephalopods.

I would also give a great thank you to Dr. Jan Audun Rasmussen for helping me identify conodonts.

To all the crew at NHM, I have very much enjoyed getting to know you and I will miss the good company at the museum. Thank you also for the job position as a museum guide during my studies.

To Nina Width, Lene Liebe and Liv Holmesland at the Slemmestad geology center; thank you for giving me the opportunity to convey what I study to the general public, I have very much appreciated it.

A great thank you also goes to my friends at Tøyen and Blindern; Geir, Ronny, Katrine, Andreas B., Håkon, Thine, Andreas G., Linn and Aubrey. Thank you for all good laughs and sorrows. I would also like to thank Stine and Linn-Torild for always telling me to „stay strong“.

The final thank you goes to my familiy. Thank you for all the support and for making it a joyful time when I come home to take a break.

Abstract

The Ordovician (Darriwilian) Svartodden Member of the Huk Formation in the village of Slemmestad in the Oslo Region, Norway, is a 2 m thick limestone unit, corresponding to the lower part of the Baltoscandic Orthoceratite Limestone. The unit is characterized by large and abundant orthoconic endocerid cephalopods in which *Proterovaginoceras incognitum* is the most dominant species recorded.

The main part of the fieldwork performed in this study was conducted at the now well-known outcrop near the Slemmestad IF arena, a bedding surface measuring approximately 1300 m^2. The Svartodden Mbr. was carefully logged with a particular focus on detecting firm- and hardgrounds. The macrofauna was recorded and cephalopod species were quantified. Current directions based on orientations of cephalopod conchs show a preferential current from a north-eastward direction. Extensive bioturbation can be witnessed from abundant trace fossils on the main bedding surface. Tunneling asaphid trilobites took advantage of the firmgrounds and produced most of the abundant *Thalassinoides* trace fossils. The main cause for this opportunistic behavior is linked to predation pressure from the abundant omnivorous nautiloid cephalopods.

New records and interpretations of firm- and hardgrounds based on field observations and element analysis by X-ray fluorescence (XRF) of the bulk unit are presented. Element concentrations of Fe, S, Mn and P are used to recognize the hardgrounds. The data suggest that firmgrounds evolved in combination with enrichment of phosphorus, which may be linked to cyclicities of upwelling, semi-emergence of the seafloor and a high accumulation of organic material. The Svartodden Mbr. is characterized by several firmgrounds formed as a result of very low net sedimentation rates and by early cementation. During the interpreted hardground period witnessed by the main bedding surface, truncated trilobite tunnels are believed to have been inhabited by microstromatolites, forming microbial linings growing from the tunnel peripheries. The microstromatolites are also present in other areas of the unit, either on cephalopod conchs or merely on the sediment surface.

Slabs were dissolved in acetic acid, and the acid resistant residue was analysed with respect to microfossils, authigenic minerals and microtektites. The recorded conodont species *Drepanodus arcuatus* and *Baltoniodus medius* are characteristic species of the *Eoplacognathus pseudoplanus* zone, previously reported from the Svartodden Mbr. Brachiopods belonging to the genera *Conotreta* and *Myotreta*, as well as bryozoans of the genera *Moyerella*, *Chasmatopora* and *Moorephylloporina* have also been recorded.

Isotopic variations of ^{13}C and ^{18}O has been recorded, however diagenetic alterations by hydrothermal circulating porewater have altered the samples with respects to the ^{18}O isotopes.

The diagenetic history of the unit based on studies of cements in cephalopod siphuncles and conchs, involves several stages of precipitation and dissolution of cements most likely caused by increasing burial depth and alternating CO_2 content in the pore water. Dolomitization is believed to have formed at different levels of burial, in the shallow and the deep realm.

Contents

1 Introduction

1.1 An exceptional locality at the Slemmestad IF arena

During the spring season of 2009 in the village of Slemmestad in the south-eastern part of Norway, volunteers from the football club Slemmestad IF in Røyken kommune cleared an approximately 1300 m² large rock surface from vegetation. They discovered that the rock surface contained hundreds of elongated, cone-like fossils. With help from the fire department, who cleaned the bedding surface free from soil and mud, the sports enthusiasts realized that the rock surface was in great condition to be examined by geologists.
Both the Natural History Museum (NHM) in Oslo and the local geology center in Slemmestad were informed about the discovery, and the locality was soon described by professionals as one of the largest fossil exposures in Norway.

Figure 1: Photo showing an overview of the Slemmestad football arena locality with the local mall in the background (photo: Ragnar Husum).

The elongated, cone-shaped fossils in the limestone at Slemmestad were quickly identified as large orthoconic nautiloid cephalopods, and the rock unit was identified as the Svartodden Member of the Huk Formation (previously called 3cγ of the former Etagen-system). The Svartodden Mbr. succession was formed during the Darriwilian stage of the Middle Ordovician, when Baltica was covered by an epicontinental sea (Bruton et al., 2010).

Located in the Oslo-Asker district, an area described in Bockelie (1982), the village of Slemmestad is an area with plenty of the Lower Palaeozoic epicontinental sediments ranging from the Upper Cambrian to the Upper Ordovician. The sediments are known for their fossil content including trilobites, graptolites and cephalopods, and several of the localities are often studied and visited by fossil hunters. The limestone-dominated Huk Fm. was extensively quarried in the Slemmestad area during the 19th and 20th century, and was utilized as an important raw material in the production of cement at the local cement factory in the village. Today, the Slemmestad IF arena locality acts as a popular exposure where fossil enthusiasts, geology students and the general public can enjoy studying the remarkably well-preserved, ancient sea bottom with so much of its former life present.

1.2 Purpose of thesis

The main purpose with this thesis is to make a palaeoenvironmental analysis of the Svartodden Mbr., based on studies of field data and rock samples collected from the Slemmestad IF arena locality. Some of the methods used in the study are core logging, X-ray fluorescence (XRF) showing elemental composition of the rock, dissolving the limestone in weak acid in order to analyze the acid resistant residue, and analysis of microfacies - the content of skeletal debris in the rock. The analysis will focus on the different groups contributing to the sediment buildup and the depositional history regarding formation of hardgrounds and firmgrounds, as well as the seafloor's control on the benthic fauna. The techniques used to identify all of these parameters are in the fields of geochemistry, palaeontology and sedimentology.

Having a rich content of fossil cephalopods, the Svartodden Mbr. is a rather characteristic limestone, and hence the cephalopods will be described in more detail. Aspects of the diagenetic history of the Svartodden Mbr. are also briefly studied, but will not be a main topic in the thesis. Hopefully, the interpretations and conclusions made in this thesis can contribute to the understanding of the Ordovician rocks in the Oslo Region, and to supplement the current ideas of the depositional environment on the western part of the Baltoscandic shelf during the Darriwilian. The study will also prove useful to those interested in learning more about the Slemmestad IF arena locality, having in mind the locality´s properties of being a place to convey geology to different kinds of audiences.

2 Geological framework

2.1 Regional Geology

The Ordovician Period lasted for 41 million years (485-444 Ma), and presents one of the most interesting periods of Earth´s time (Stanley et al., 2010) in the sense of evolution of life and plate tectonics. In Norway the Ordovician stratigraphic sequence occurs as allochtonous nappe units in the Caledonian belt, and as paraautochtonous successions in the Oslo Region and Digermulen in Finnmark (Bruton & Owen, 1982). The palaeocontinent Baltica (Figure 3), e.g. where Norway, Sweden, Denmark, Russia and the Baltic countries are situated, was positioned approximately 30 degrees south of the equator during Middle Ordovician time, and was bordered by two ancient oceans, the Iapetus Ocean in the west, and the Tornquist Sea in the south (Torsvik, 1998).

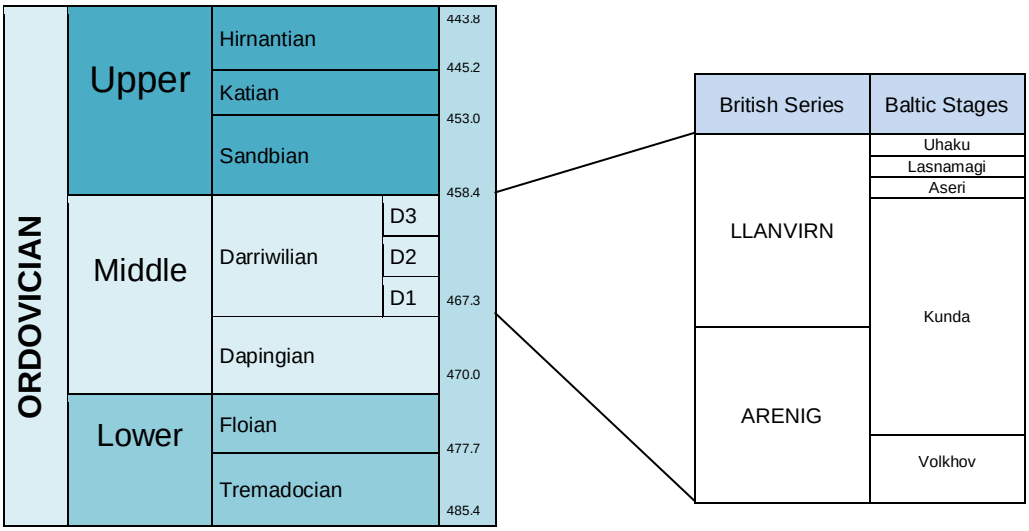

Figure 2: The Ordovician global timescale (from Gradstein et al., 2012), and British Series and Baltic Stages (from Bruton et al., 2010).

The Ordovician period is divided in the Lower, Middle and Upper Ordovician, and several global stages (Figure 2). The main global stage of interest to this study is the Darriwilian (467-458 Ma), which is further divided into three substages (D1, D2, D3).
The Baltoscandic successions were extensively studied by geologists during the 1970´s and 1980´s, which led to publications of several reports on different aspects of the geological history of the sedimentary units. Based on palaeomagnetic and faunal studies,

reconstructions of the palaeocontinents during Ordovician times have been presented by several authors (Perroud et al., 1992; Torsvik et al., 1995; Cocks & Torsvik, 2002). Most of the Earth's continents were located on the southern hemisphere (Figure 3), and since little life on land had yet evolved, several factors from atmospheric composition to weathering products were different from the modern standards. Volcanic activity caused by active seafloor spreading, as well as impacts from meteorites have been reported from Baltoscandia during the Ordovician (Sturesson, 2003; Schmitz, 2007).

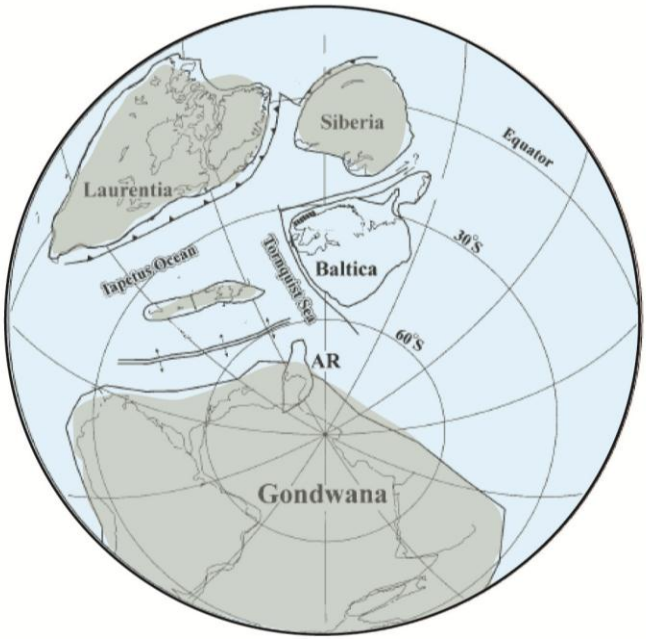

Figure 3: Configuration of the Earth´s continents during Middle Ordovician time, where Baltica was mainly covered by ocean (modified from Torsvik, 1998).

Jaanusson (1984) described the Ordovician period as a thallasocratic period with wide, flat seabeds and restricted land areas, most probably only represented by archipelagos in shallow epicontinental seas. Epeiric platforms (Figure 4), such as Baltica, were developed on the interior of major shelves, covering millions of square kilometers (Boggs, 2006).

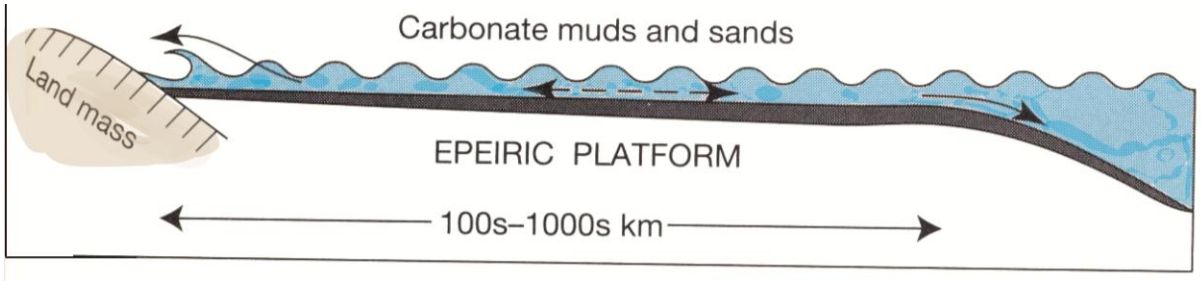

Figure 4: An epeiric platform characteristic of a wide, flooded continental shelf (modified from Boggs, 2006).

The Orthoceratite limestone

The lower part of the Baltoscandic Orthoceratite Limestone is characterized for its vast amount of orthoconic, endocerid cephalopods, formed during the Kunda Baltic Stage in the Darriwilian (Figure 2). In Norway, the so-called "Orthoceratite" limestone (the Huk Fm.) does not only contain orthocerid cephalopods, but a larger amount of endocerid cephalopods, hence the local stratigraphic term "Endoceras limestone" in the Oslo Region, first introduced by Størmer (1953). The Iapetus Ocean, situated to the west of Baltica, was approximately 5000 km wide, in which currents are believed to have transported various amounts of terrigenous sediments with provenance from exposed land areas on the west coast of the continent (Bruton & Owen, 1982). The Tornquist Sea, approximately 1100 km wide, was steadily closing by convergence of the continents Avalonia and Laurentia (Hansen & Harper, 2008).

Jaanusson (1976) divided the sequences of the Ordovician epicontinental sea into different confacies belts, based on the ideas of Männil (1966) on composite belts on the Baltoscandic shelf, which varies along the shelf with respects to fauna and sediments. Five confacies belts, illustrated in Figure 5, reflect ecologic zonations controlled by environmental factors, which also influenced the deposition of the sediments. The Oslo Region accordingly belongs to the Oslo belts, bordered by the Scandian belt to the east (Oslo-Scania), both belts being situated in the Caledonian foreland. The western border of the Oslo belt is however somewhat unknown (Bruton & Owen, 1982).

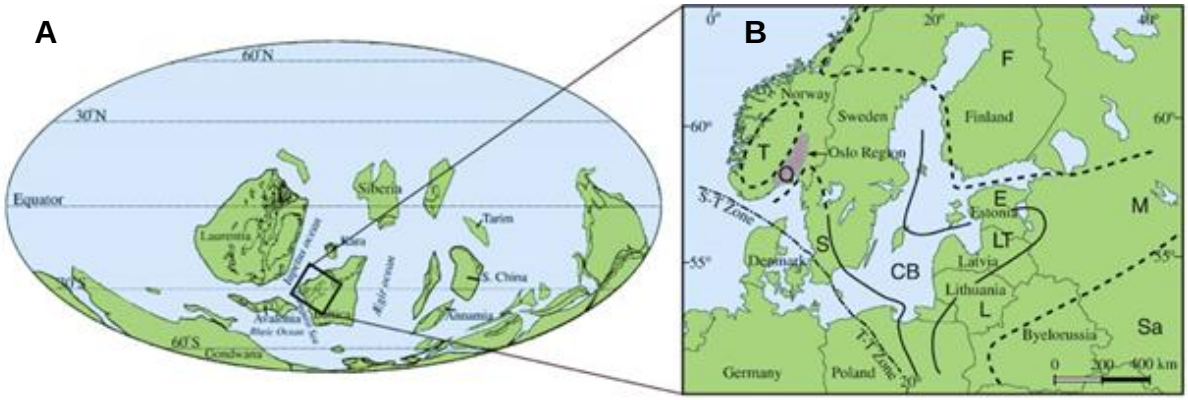

Figure 5: A: Palaeogeographic map with the distribution of continents during the Ordovician (modified from Cocks and Torsvik, 2004). B: The Baltoscandian Sea with the confacies belts O: Oslo, S: Scanian, CB: Central Baltoscandian, E: Estonian, L: Lithuanian; LT: Livonian tongue. Other abbreviations: T: Telemark Land, T-T zone: Tornquist-Teisseyre fault, S-T: Sorgenfrei-Tornquist fault, F: Fennoscandia Land, M: Moscow Basin, Sa: Sarmatia Land (from Hansen et al., 2009).

Before the onset of the Ordovician timeperiod, a major transgression had taken place in the southwestern part of Norway during the Early Cambrian. This gave rise to the deposition of dark organic rich shale superimposed on the subcambrian peneplane, today known as the black Alum Shale Formation. The platform area to the east in the central Baltic Region was uplifted and became subaerially exposed (Owen et al., 1990).

Most of the Baltoscandian successions show a clear break at the Cambrian - Ordovician transition. The succession in the Oslo Region is, however complete (Bruton & Owen, 1982). Continuing into Early Ordovician, the sea covered most of Norway, Sweden and an area east to the Baltic Sea, with the formation of the Tøyen Fm. in Norway and Sweden. By the Middle Ordovician, the sea had transgressed further east, and a shallowing of the sea level occurred in the Oslo belt and the Scanian belt, observed in the field as a transition from a graptolite shale environment during the Floian and Dapingian stages, to the the Huk Fm. (the Orthoceras limestone) typical of a carbonate dominated environment in the Darriwilian stage (illustrated in Figure 6).

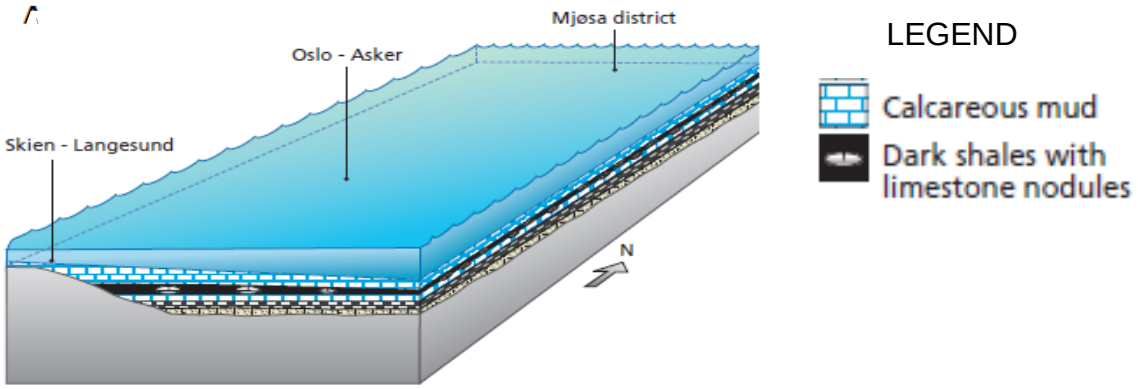

Figure 6: Early Ordovician depositional setting in the Oslo Region (modified from Ramberg et al, 2010).

While the seafloor during the Cambrian was mostly anoxic, favouring the preservation of organic matter, the environment changed in the beginning of the Ordovician with increased water circulation patterns, causing more upwelling of oxygenated and nutrient-rich waters (Nielsen, 2004). Epicontinental seas analogue to the one covering Baltica during the Ordovician can hardly be found anywhere on the Earth today, making it more difficult to understand the geological processes acting in an epicontinental sea depositional environment. However, the general opinion is that the relative sea level rarely reached a depth of more than 200 meters in the Oslo belt (Bjørlykke, 1974). Evidence indicates an

emergence of the Central belt (Figure 5) at the beginning of the Ordovician, as well as in other stages during the period. Lindström (1971) however, claimed that the Baltoscandic Ordovician deposits represent neritic or pelagic deposits, in a somewhat fairly deep epicontinental sea.

According to Jaanusson (1982) the epicontinental Ordovician sedimentary sequence of Baltoscandia is rather unusual with its intricate pattern of breaks in the deposition, and its particularily low sedimentation rate. This is represented by the relatively thin sequences of rocks less than 150-200 meters found in the Scania area and in Sweden. A relatively cold climate is believed to have been the main reason why the production of carbonate sediments was so low, by a net accumulation in Sweden and the East Baltic of about 0.1-0.9 cm/1000 years of clastic and carbonate sediment (Nielsen, 2004). In the Oslo Region however, sedimentation rates during the Ordovician were higher, locally represented by sequences with thicknesses up to 1000 meters (Bjørlykke, 1974). This might be due to the Oslo belt's closer proximity to the clastic source-area in the west, or due to a higher subsidence. The average sedimentation rate in the Oslo-Asker district during the Middle and Upper Ordovician was approximately 0.7 – 1.3 cm/1000 years (Bjørlykke, 1974). A typical offshore-nearshore succession in Sweden and Estonia is composed of a) dark graptolitic shales, b) calcilutitic limestones, c) calcarenitic limestones, d) argillaceous limestones, e) mudstones, marls and siltstone, f) carbonate-rich quartz sands (Nielsen, 2004).

Jaanusson (1982) also discusses the depositional relationship between shale and limestone units on Baltica, where the shale content in the west decreases while the calcium carbonate production in the east increases and vice versa, also known as competitive deposition. The terrigenous weathering products are thought to have their origin from an island area off the west coast of Baltica in the Iapetus Ocean, while the bulk limestone-mud is thought to have originated from the stable platform in the east (Bruton & Owen, 1982; Bjørlykke, 1974). The energy levels needed for the transport of suspended terrestrial material in the epicontinental sea on the Baltic platform can be explained in terms of several factors, as discussed by Bjørlykke (1974);

1. Wind-generated waves from the deep Iapetus Ocean that lose energy by friction with the seabottom as they enter and continue across the Baltoscandic shelf
2. Energy dissipation from the strong tidal currents from the Iapetus Ocean spreading

along the margin of the epicontinental sea

3. Deep water currents coming in to the epicontinental shelf for the replacement of evaporated water on the shallow platform
4. Any effect from the Coriolis force on ocean currents is thought to have only had minor significance on the currents in an epicontental sea.

These factors combined are believed to have ensured that the deep ocean waves and currents would compensate for the wave and current energy flowing in the opposite direction, out from the epicontinental basin. This also means that the weathering products of the eroded island arcs or landmasses in the Iapetus Ocean would be transported to the epicontinental shelf of Baltoscandia, as a landward transportation of suspended material. In addition, epicontinental seas are described as having depths no deeper than 200 m, with an average depth of 30-40 m or less, with a very low slope gradient of 20 cm/km. The prevailing winds could also have the ability to transport siliciclastic sediments through sandstorms etc. at higher wind velocities (Bjørlykke, 1974).

A palaeoenvironmental reconstruction of the Oslo Region during the Darriwilian based on faunal data in the Elnes Fm. was recently presented in Hansen et al. (2011). The reconstruction outlines the depositional environment of the Elnes Fm. (superimposed on the Huk Fm.), and geographically into eastern Sweden where the unit corresponds to the Holen Limestone Fm. The sea level at this time (late Kunda) was gradually rising, known as the Helskjer drowning (Nielsen, 2004). The Telemark and Trondheim areas (indicated in Figure 7) are believed to have been sub aerially exposed, probably acting as the main source-areas of siliciclastic material during pulses of tectonic uplift of the Caledonides. The Oslo Region formed the distal part of the foreland basin, while the Trondheim area acted as a main source of siliciclastic input on the shelf, an interpretation shared by several authors (e.g. Bockelie & Nystuen, 1985).

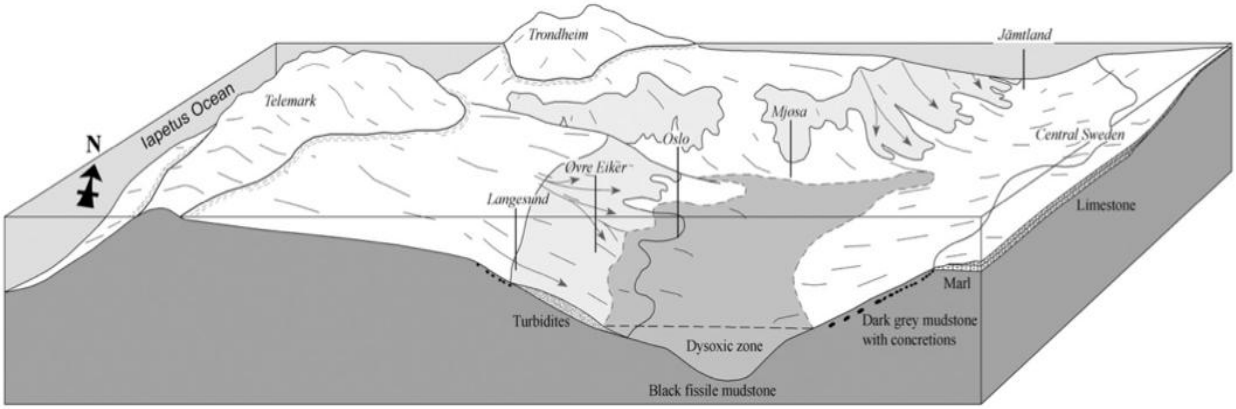

Figure 7: Middle Darriwilian palaeoenvironmental recontruction of west-Scandinavia, note that the figure is very much compressed, and that the shelf gradients are quite low (from Hansen et al., 2011).

2.2 Palaeogeography and palaeoclimate

During the Ordovician, the continental configuration of the landmasses representing Europe and the rest of the Earth´s continents was entirely different from the one of the modern world. Since the 1970´s, extensive work has been done to decipher the distribution of the world's continents and micro-continents during the Ordovician, a crucial parameter in the understanding of trends in biodiversity, climate and tectonics. Based on palaeomagnetic and faunal surveys, the position of Baltica during the Middle Ordovician is believed to have been between 30°- 60° on the southern hemisphere (Jaanusson 1973; Lindstrom 1984; Torsvik et al., 1995). Torsvik (1998) suggested a palaeogeographical position of the Norwegian sector of Baltica at approximately 30° during the Darriwilian (Llanvrin-Llandeilo boundary), as shown in Figure 3.

Sea levels, oceans and climate in the Middle Ordovician

Paleoclimatic reconstructions stretching back 465 million years in time are somewhat speculative, although certain conditions are more or less accepted by earth scientists. The climate is believed to have been a greenhouse climate with no ice caps, and a warm climate with tropical to warm temperate oceans (Barnes, 2004). An actualistic approach (Lindström, 1984) of how to discern the paleoclimate back in the Middle Ordovician, would be to make an analogue interpretation of todays climate on the same latitudes as where Baltica was

positioned during the Darriwilian. The present mean annual sea surface temperature at 30ºS is approximately 20ºC (Reynolds & Smith, 1995), possibly corresponding to the mean sea surface temperature at the same latitudes during the Darriwilian. Todays climate on 30ºS latitude is described as mild mid-latitude climate with desert areas (Aguado and Burt, 2007), although factors such as a different atmospheric composition, oceanic circulation system, high sealevels and a different configuration of the continents, could lower the credibility of this interpretation.

The oxygen content in the atmosphere-ocean system was apparently 50 % lower than that of today (Berner, 1994 *in* Barnes, 2004). The circulation in the oceans was mainly driven by evaporation and subduction of higher salinity waters on mid-latitudes due to the greenhouse conditions, rather than the present day dominating thermohaline circulation of water in high latitudes (Railsback, 1990).

Sea level changes in the Ordovician have been presented by Nielsen (2004), and it is believed that the low net deposition on the continental shelf did not affect local sea levels. In addition, the platform was tectonically stable, meaning that sea level variations reflected in the sediments are primarily representing eustacy. The Lower Ordovician condensed limestones from the Bjørkåsholmen Fm., found in the Oslo Region were apparently formed in a mid shelf environment, in relatively cold water temperatures. By the early Middle Ordovician, the carbonate deposition moved to the inner shelf. Warm water carbonates, typical for corals and of shallow water facies, were not deposited in the Oslo Region until the Late Ordovician (Nielsen, 2004). In his study, Nielsen also describes argillaceous limestones to represent shallow-water high stand deposits. Dronov et al. (2011) recently reconstructed sea level curves of the shallow water part of the Baltoscandic basin in Estonia. A marked highstand occurring during the Dapingian – early Darriwilian is marked by a widening of relatively deep-water marine red bed facies. The authors suggest that a mechanism of "highstand shedding" would transport calcitic material from the shallow shelf to deep-water settings during highstands. The production of calcium carbonate at this point is thought to have been on its maximum due to sea level highstand.

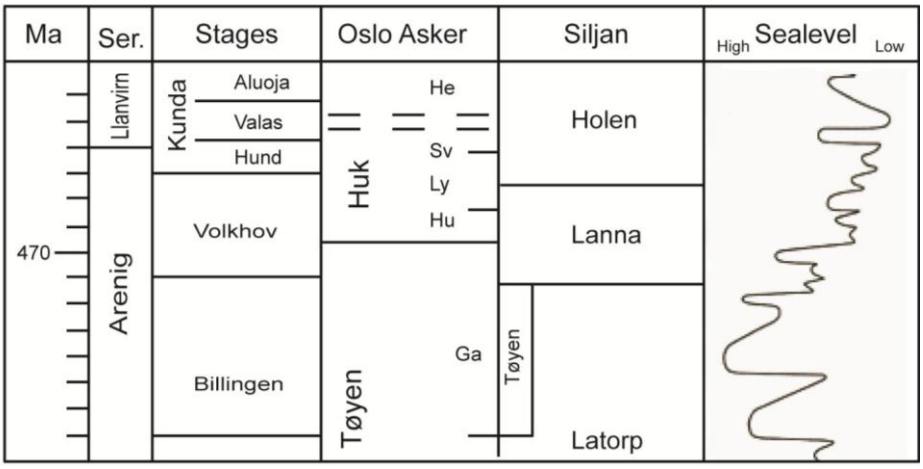

Figure 8: Sea level curve plotted with stratigraphic units in the Oslo-Asker district and in the Siljan district (Sweden), (modified from Nielsen (2004).

This assumption leads to the hypothesis that limestone deposits originally believed to represent lowstands, actually would represent periods of highstands. The lowstand of Baltoscandia during Middle Ordovician times, postulated by many geologists, is therefore considered to represent a possible artifact (Nielsen, 2004). The suggested sea level curve by Dronov et al. (2011) during the Darriwilian starts with a highstand at approximately 200 m which gradually sinks to approximately 130 m in the beginning of the Kunda Stage, rising again to a level of approximately 180 m, and resides during the end Kunda to a lowstand at approximately 100 m. By the end Darrriwilian, the sealevel has gradually increased to approximately 140 m. The sea level curve presented by Nielsen (2004) of the same time period in question shows a higher intensity of a fluctuating sealevel (Figure 8).

2.3 Tectonics

The deformation introduced by the Caledonian orogeny starting in the Upper Ordovician, greatly affected the Lower Palaeozoic deposits in the Oslo area. The deformation resulted in shortening of the Lower Palaeozoic sequence in the Oslo-Asker region, with the underlying Cambrian Alum Shale acting effectively as a thrust plane for the overlying sediments (Bruton & Owen, 1982). Foreland basin-type structural deformations are visible in the Oslo-Asker area, and the Huk Fm. in Slemmestad can be seen in several outcrops as extensively folded, faulted and thrusted (Figure 10).

The overall tectonic activity influencing the structural and depositional processes on Baltica during the Ordovician was quite extensive. Baltica rotated approximately 120° during Late Cambrian - Early Ordovician, but the amount of rotation declined in the Middle Ordovician (Torsvik, 1998). The submerged area between Scandinavia and Great Britain, named the British-Scandinavian geosyncline, contained volcanoes and island arcs that were active during the Early Ordovician (Holtedahl, 1920). This ocean area corresponds to the former Iapetus Ocean. Deposits of ash, today seen in Slemmestad in the Arnestad Fm. with a thickness up to 1 m, had their origin from the volcanoes on the island arcs in the Iapetus Ocean. Bentonites like in the Arnestad Fm. can be found in Poland, the Baltic countries, Great Britain and North-America. Near the Cambrian – Ordovician transition, the continents of Laurentia and Baltica started to converge, later resulting in the closing of the Iapetus Ocean (the Scandian Orogeny), with the obduction of ophiolites on to the present west-coast of Norway, and the final Caledonian continental collision later in Silurian times (Ramberg et al., 2010).

2.4 The Oslo Region

The Oslo Region is a graben structure, and extends geographically northwards from Langesundsfjorden to the northernmost part of the Mjøsa district, a distance of approximately 115 km north and south of Oslo. The width of the Oslo Region varies between 40 to 75 km, and the area is bordered to the east by major normal fault-zones (Bruton & Owen, 1982). The areas to the east are dominated by Precambrian rocks, while to the north the allochtonous Caledonian nappe units are preserved. The Oslo Region is well known for its unique variety of rocks (Figure 9), ranging from Cambrian, Ordovician, Silurian fossiliferous deposits, overlain by Upper Carboniferous sediments. Igneous rocks dated as late Carboniferous to early Triassic mark the event of extensional tectonics in the area (Ramberg et al., 2010).

The Lower Palaeozic rocks in the Oslo Region are preserved due to the graben-structure that formed during the Carboniferous - Permian extensional rifting of the supercontinent Pangea. The Oslo Region with its sediments subsided around 1000-2000 m, forming three subgrabens. The Lower Palaeozoic sediments became subsequently buried by erosional

material from the surrounding horst area and by volcanics and magmatic rocks (Størmer, 1953, 1967; Bockelie & Nystuen, 1985; Sundvoll & Larsen, 1994; Andersen, 1998).

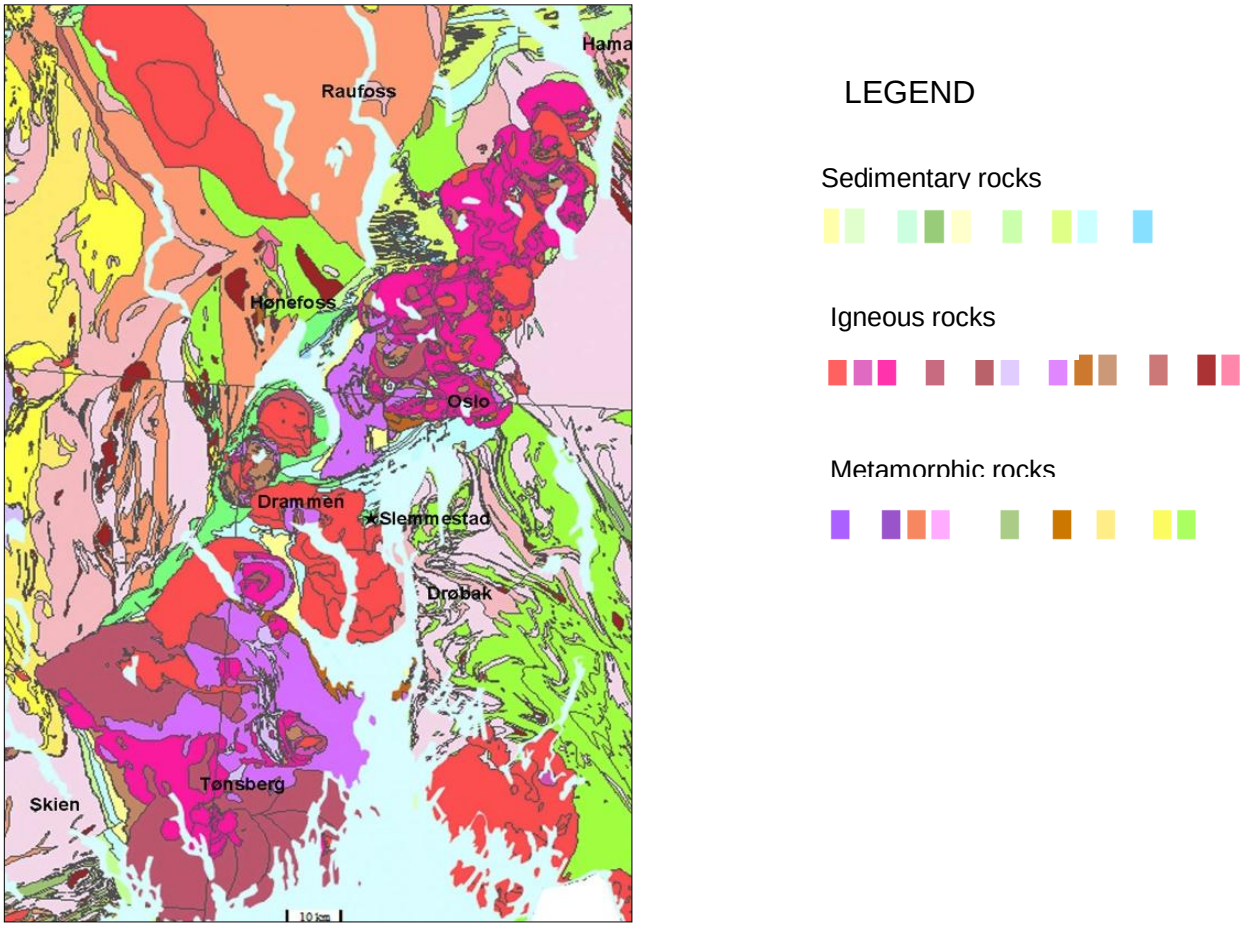

Figure 9: Geological map of the Oslo Region. Map source: NGU.

The Oslo Region was a subject of great study during the 19th century, with its wide selection of sedimentary rocks and fossils in the classic rift-setting of the Oslo Region. Known geologists and palaeontologists from the early history of geology in Norway, such as Theodor Kjerulf, Waldemar C. Brøgger and Johan A. Kiær contributed greatly to the mapping and interpretations of the Ordovician sedimentary sequences in the Oslo Region during the 19th and 20th centuries. Today the scores of geologic treasures found in the area are being conveyed between geologists, students and the general public.

2.5 Local geology in the Slemmestad area

Due to the Caledonian event, the Lower Palaeozoic succession in Slemmestad has been folded in trains and appears as closely imbricated thrust faults, where the limestone units often are faulted due to their brittleness (Morley, 1994). The structural geology and sedimentary units in the Slemmestad area are presented in Figure 10 below.

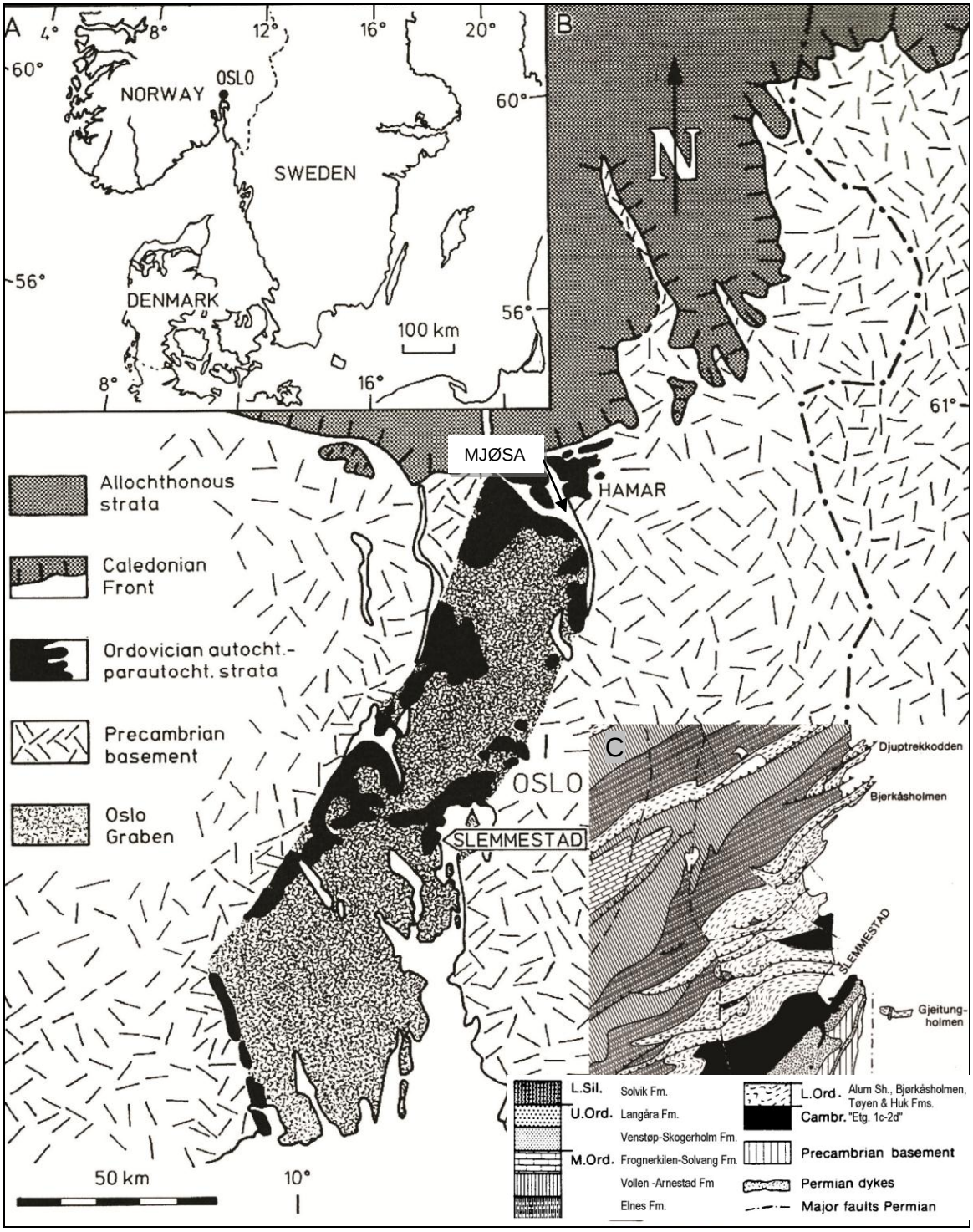

Figure 10: Geographic (A), regional (B) and local geological setting of the Slemmestad area (C). Modified from Rasmussen (1991) and Bockelie (1982).

2.6 Lithostratigraphic setting

The Huk Fm. and the rest of the Palaeozoic sequence in the Oslo Region were formally defined in Owen et al. (1990). The geochemistry and diagenetic history of the Huk Fm. were also described in an unpublished Cand.real. thesis by F. E. Skaar in 1972. The Svartodden Mbr. is the uppermost member of the Huk Fm., a biomicritic limestone unit, previously called the Orthoceras Limestone (Bjørlykke, 1974), although the Svartodden Mbr. in literature has been referred to as the Endoceras limestone (Størmer, 1953; Skjeseth, 1963; Svendsby, 1987). The average thickness of the Huk Fm. in the Oslo Region is approximately 7 meters (Owen et al., 1990), and the unit is exposed in outcrops from the Oslo-Asker area in the west to Gotland in Sweden to the east (Skjeseth, 1952). Correlations of the Ordovician successions were presented by Bruton et al. (2010), and they assign the Huk Fm. to the Volkhov and Kunda Baltic stage, and the Svartodden Mbr. within the transition between the Arenig and Llanvirn of the British time series (Figure 11).

<table>
<tr><th rowspan="2">Absolute age (Ma)</th><th rowspan="2">System</th><th rowspan="2">Series</th><th rowspan="2">Global Stages</th><th rowspan="2">British Series</th><th rowspan="2">Baltic Stages</th><th rowspan="2">North atlantic conodont biozones (Löfgren, 1995,2000)</th><th rowspan="2">Baltoscandian trilobite biozones (Nielsen, 1995)</th><th colspan="2">Lithostratigraphic units</th></tr>
<tr><th>Dalarna/ Öland (Sweden)</th><th>Oslo area (Norway)</th></tr>
<tr><td rowspan="13">460,9

468,1</td><td rowspan="13">ORDOVICIAN</td><td rowspan="13">MIDDLE</td><td rowspan="8">DARRIW-ILIAN</td><td rowspan="5">LLANV-IRN</td><td>Uhaku</td><td rowspan="3"></td><td rowspan="3"></td><td rowspan="8">Holen Limestone</td><td colspan="2">Elnes Fm.</td></tr>
<tr><td>Lasnamagi</td><td colspan="2">--- hiatus ---</td></tr>
<tr><td>Aseri</td><td rowspan="7">Huk Fm.</td><td rowspan="3">Svartodden Mbr.</td></tr>
<tr><td rowspan="4">Kunda</td><td rowspan="2">Eoplacognathus pseudoplanus</td><td>Megistaspis gigas</td></tr>
<tr><td>M. obtusicauda</td></tr>
<tr><td rowspan="2">ARENIG</td><td>Asaphus raniceps</td><td rowspan="2">Lysaker Mbr.</td></tr>
<tr><td>Lenodus variabilis</td><td rowspan="3">Lanna Limestone</td></tr>
<tr><td rowspan="3">DAPING-IAN</td><td rowspan="3">Volkhov</td><td>Baltoniodus norrlandicus</td><td>M. limbata</td><td>Hukodden Mbr.</td></tr>
<tr><td>P. originalis</td><td>M. simon</td><td rowspan="3">Galgeberg Mbr. (Tøyen Fm.)</td></tr>
<tr><td rowspan="2">FLOIAN</td><td>B. navis</td><td rowspan="2">M. polyphemus</td></tr>
<tr><td>Billingen</td><td>B. triangularis</td></tr>
</table>

Figure 11: Correlation of the studied sections in Slemmestad with the British, Baltic and Swedish sequences, and with conodont and trilobite biozones. Modified from Bruton et al, (2010); Kröger, (2012) and Tinn et al. (2006).

The Tøyen Formation

Mud from the rising Caledonides in the west, has been ascribed as the main source of the deposits making up the Tøyen Fm. together with the Huk Fm. considered as the laterally most extensive unit of the Ordovician Baltoscandic successions (Rasmussen & Bruton, 1994). The thickness of the Tøyen Fm. in the Oslo-Asker district is around 20.5 m (Owen et al., 1990). The Galgeberg Mbr. has a thickness of 12 m (Owen et al., 1990) and consists of shale and scattered limestone nodules. It underlies the massive Hukodden Mbr. of the Huk Fm., shown as a sharp lithologic boundary between the dark, muddy shale and the light, grey limestone.

The Huk Formation

The sedimentary sequence representing the tripartite division of the Huk Fm. (Figure 12) was first described by Brøgger (1882), and later the stratigraphy by Bockelie (1982). The "Orthoceras Limestone" (3c, 3cα-γ) of Brögger (1882) was the former name of the Huk Fm. until it was formally described and renamed by Owen et al. (1990). The Huk Fm. consists of the three subsequent members; the Hukodden Mbr., the Lysaker Mbr. and the Svartodden Mbr. The uppermost unit, the Svartodden Mbr. is the main theme of this study, and will be described in more detail in subsequent chapters. Outcrops of the Huk Fm. in the westernmost part of the Oslo Region have been reported from the Kongsberg area and from the Vestfossen area (Brögger, 1882), and the unit extends northwards from the Svartodden Mbr. in the Oslo-Asker district to the more shale rich Stein Fm. in the Mjøsa district. The unit thins southwards to the Rognstrand area in Skien-Langesund, where its thickness is no more than 2.4 m, compared to its thickness of 7.7 m at the Bjerkåsholmen locality in Slemmestad (Owen et al., 1990).

Exposed sections of the Huk Fm. can be traced eastwards into the Scanian confacies belt (Figure 5), and it evolves into the Holen Limestone Fm. in Sweden. The unit was formed during the Volkhov and Kunda Stages of Baltic terminology, and is equivalent to the Arenig-Llanvirn transition of British terminology (Bruton et al., 2010). The Huk Fm. also exists within allochtonous nappe units in the Caledonides of Norway and Sweden (Rasmussen & Bruton, 1994).

Svartodden Mbr. | Lysaker Mbr. | Hukodden Mbr.

Figure 12: The Huk Fm. at the Bjerkåsholmen locality.

Associated with a major sea-level fall in the Dapingian-early Darriwilian on Baltoscandia, the carbonate rock facies spread down-slope from the east on the platform, causing the formation of the laterally equivalent Komstad, Holen, Huk and Stein formations. The Swedish Komstad Limestone Formation, a tongue of the Orthoceratite Limestone, has been interpreted as an intercalated limestone in a generally shale-dominant depositional environment in the Scania-Bornholm area, southernmost Scandinavia (Nielsen, 1995). The Stein Fm. is a deeper lateral equivalent to the Huk Fm. and extends from the Ringsaker area in Norway, thinning eastwards to Andersön in Sweden (as the Isö Limestone) (Rasmussen and Bruton, 1994). In the lake Mjøsa area (Figure 10), the Stein Fm. shows a transitional zone of limestone into the Elnes Fm., possibly witnessing more persistent carbonate sedimentation in the area (Bjørlykke, 1974).

The Hukodden Member

The section of the Hukodden Mbr. at Bjerkåsodden shows a limestone that constitutes 24 beds of dark grey mud- and wackestone, with several discontinuity surfaces containing pyrite impregnations (Rasmussen, 1991). The abrupt transition from the underlying Tøyen Fm. to the Hukodden Mbr. is marked by the change in lithology from shale to the light coloured and weathered limestone. Along irregular bedding surfaces and pressure solutions seams, skeletal fragments are accummulated (Owen et al., 1990).

The Lysaker Member

The Lysaker Mbr. consists of 57 layers of nodular limestone surrounded by light grey and calcareous mud and siltstone (Rasmussen, 1991). The unit stands remarkably out compared to the under- and overlying units of massive limestones. Cyclic deposition is evident from the changing dominance of either limestone- or shale beds. The thickness of the Lysaker Mbr. varies in the the Oslo Region due to tectonically induced movement of the shale layers. The unit has a thickness of approximately 3.5 m at Bjerkåsholmen in Slemmestad (Figure 12). The Lysaker Mbr. has a remarkably high content of the asaphid trilobite *Asaphus expansus*, as well as brachiopods, ostracodes and echinoderms (Owen et al., 1990).

The Svartodden Member

The thickbedded, grey Svartodden Mbr. is believed to have formed in a highly oxygenated and high energy environment, representing a shallow palaeoenvironment compared to the overlying Elnes Fm. (Hansen et al., 2011). The dominance of endoceratid cephalopods is also considered to represent a shallow depositional setting of the Svartodden Mbr., possibly witnessing the shallowest sea level of all the members in the Huk Fm. The endoceratid association is characterized by having an abundance of more than 40 % endoceratid cephalopods and trilobite species, e.g. of the genera *Nileus* and *Megistaspis*, as well as orthid and sowerbyellid brachiopods (Hansen, 2009).

The lowermost part (0.2 m) of the Svartodden Mbr. is rich in brachiopods, and was termed by Brøgger (1882) as the "Porambonites bed". This bed is believed to mark the boundary between the *A. expansus* and the *A. raniceps* trilobite biozones, while the remaining Svartodden Mbr. represents the *A. raniceps* biozone. The basal part of the unit contains several phosphorite-stained seams (Nielsen, 1995). Abundant dissolution of the upper parts of cephalopod conchs has been described as omission surfaces, and the facies of the Svartodden Mbr. is interpreted to represent a shallow environment, somewhere above maximum storm wave base and below fair weather wave base. Early cementation of the seabottom has been reported, and current orientations are visible based on some of the largest cephalopods (Nilsen, 1985). Nielsen (2004) described the Svartodden Mbr. as having formed after an event of drowning, resulting in the deposition of purer carbonates, as was

the case in parts of Sweden with the deposition of the Komstad Limestone. This change in sea level is also known as the Basal Llanvirn Drowning Event (Nielsen, 2004).

The Elnes Formation

A marked shift in the depositional environment marks the boundary between the Svartodden Mbr. and the Helskjer Mbr. of the Darriwilian to locally Sandbian Elnes Fm., observed at the Slemmestad IF arena. A hiatus in the deposition between the two formations has also been inferred based on conodont and trilobite biostratigraphy (Rasmussen, 1991). In the central Oslo Region, the Elnes Fm. has a thickness of at least 80 m (Owen et al., 1990). The Helskjer Mbr. consists of dark grey to blackish mudstone, showing concretionary facies near its base. The water depth was between 50-200 m in a mid to outer shelf environment. The facies of the Helskjer Mbr. is described as a marl facies with limestone to compact marl, with few cephalopods and trilobite coquinas. Omission surfaces are hardly evident (Hansen et al., 2011)

2.7 Dating of the Svartodden Mbr.

Dating of the Ordovician Period has been an area of intense study by many geologists in the past decades, with different stages related to different palaoecontinents, such as Baltic and British terminology. The absence of several stratigraphically determined non-discrepant Rb-Sr and K-Ar isochron dates (Fitch et al., 1974) , as well as a marked faunal provincialism of the different continents (Servais et al., 2010) has also made this work problematic. In several publications, the Huk Fm. has previously been ascribed belonging to the Lower Ordovician Series (e.g. Rasmussen, 1991) making it important to keep in mind the previous changes in the Time Scale datings on sublevel correlations with global events, e.g. sealevel fluctuations and volcanic activity. In Bruton et al. (2010) the Huk Fm. was placed in the Middle Ordovician

3 Hardgrounds

Discontinuity surfaces are surfaces indicating a break in the sedimentation (Heim, 1924). There are many different terms describing characteristic features connected with the topic, e.g. hardgrounds, defined as centimeter-sized discontinuous surfaces caused by syn-sedimentary lithification. The hardground surface existed as hard seafloor for a long period of time during which it lithified, and eventually became covered by new deposits (Flügel, 2004). Hardgrounds are likely to be formed in depositional environments which have low sedimentation rates, condensed deposition and periods of non-deposition, combined with an early lithification.

Hardgrounds have been widely reported in Ordovician limestones in Baltoscandia (Jaanusson, 1961 and references therein), including in the Huk Fm. (Ekdale et al., 2002). The widespread development of hardgrounds during the Ordovician was probably related to the extensive precipitation of low-Mg calcite on shallow marine seafloors. Active dissolution of aragonite may have been the source of calcite cement, causing formation of hardgrounds (Wilson & Palmer, 1992). They have been well studied in Jurassic limestones from France and Switzerland (Hillgärtner, 1998), where a systematic approach of how to identify discontinuity surfaces and the processes active forming each type was presented.

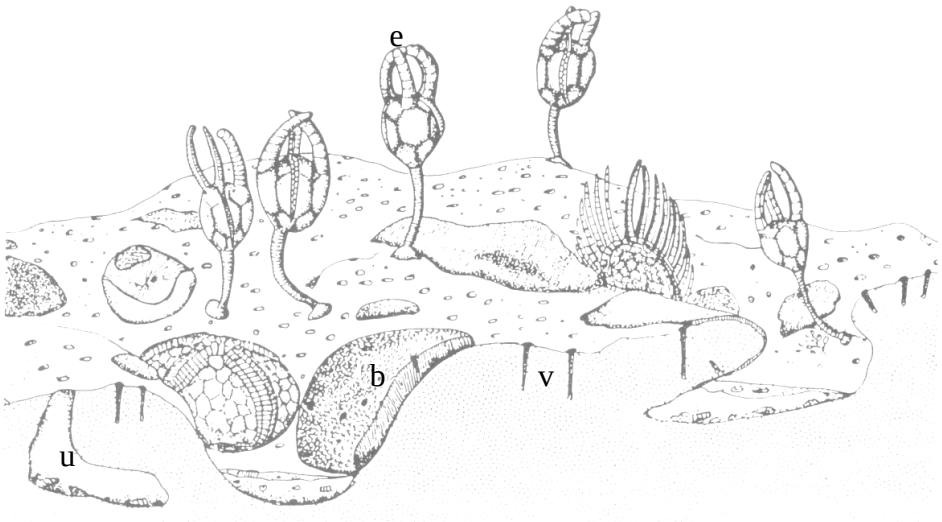

Figure 13: Reconstruction of a Middle Ordovician hardground community consisting of echinoderms (e), bryozoans (b), lithified burrows (u) and vertical borings (v) (modified from Brett & Liddel, 1978).

The controlling mechanism on the formation of hardgrounds is primarily condensed sedimentation, leading to alternating deposition and erosion of the seafloor. The three types of processes causing condensation are biological concentration, mechanical concentration and chemical concentration (Flügel, 2004). Condensed deposition is visible from intense bioerosion of hardgrounds, caused by boring and encrusting organisms (indicated in Figure 13). Mechanical concentration involves scouring, bypassing and sieving sediment, and occurs often in context with sea level fluctuations. Chemical concentration can occur as a consequence of dissolution of the sediments below the carbonate compensation depth, often combined with sea-level fluctuations, bioerosion and winnowing (Flügel, 2004).

3.1 Formation of hardgrounds

Being a result of condensation and omission, hardgrounds can be caused by several changes in a depositional system causing no net deposition. The formation processes of an incipient firmground and subsequently hardground, has been divided by Flügel (2004) into three stages:

I. A reduced sedimentation stage, marked by concentration of shells, encrusted and bored lithoclasts, in addition to iron crusts that have been reworked.
II. An omission stage, causing a bored, irregular and encrusted hardground. The surface also shows signs of truncation of burrows that were made before the omission event. Cavities and reworked breccias may also be present.
III. Formation of Fe/Mn or Fe crusts.

Wilson & Palmer (1992) state that in the cases of hardgrounds formed in calcite-precipitating seas, the rate of cementation was likely to happen within years or tens of years. This hypothesis is supported by experiments on bioerosion, which show that well bioeroded substrates such as skeletons and hardgrounds represent several years of depositional hiatus rather than months of hiatus (Bromley et al., 1990).

Factors related to the magnitude and speed of cementation are; porosity and permeability, supply of ions to precipitation sites, rates of pore water exchange, replenishment of the overlying sea water and its content of dissolved bicarbonate and calcium ions and the properties of the substrate on which calcite cement crystals nucleated (Wilson & Palmer,

1992). Recent hardgrounds are cemented by aragonite and/or magnesium calcite, while hardgrounds from earlier than the Permian are cemented by low-Mg calcite, although some cements may have been altered from aragonite or magnesium calcite during diagenesis (Wilson & Palmer, 1992).

Different controls affecting reduced sedimentation and subsequently the formation of a hardground are

I. Low input of carbonate mud due to drowning or emergence of the platform where it was produced
II. Low amount of nutrients
III. High and intense dissolution of carbonate and silica at the seafloor
IV. Scouring of the seafloor brought about by a change in bottom currents

Flügel (2004) also separates between long-lived and short-lived hardgrounds. The long-lived formation of hardgrounds is driven by extensive changes of environmental conditions e.g. shallowing, causing restricted seawater circulation preventing production of biogenic carbonate due to tectonic uplift or eustatic drop. Other environmental changes include increased salinity and deepening caused by tectonic subsidence or sealevel rise, to a level beyond the effective phototrophic zone. In the case of short-lived hardgrounds, causes might be changes in the sediment distribution pattern or climatic variations affecting storm activity.

Bioerosion, the biological breakdown of hard substrates by etching, boring, rasping and abrasion from organisms (Bromley et al., 1990) can also greatly affect the appearance of a hardground. The formation and burial sequence of a Middle Ordovician hardground described by Brett & Liddel (1978), shows how the community on the seafloor changes due to changes in the substrate (Figure 14). The initial soft seafloor was inhabited by burrowing brachiopods, and a succeeding firmground would mark the transition from a soft substrate to a hardground. The firmground sediments can be easily broken up and transported as cohesive intraclasts (Jindric, 1969; Hardie & Garret, 1977; Davis, 1979; *in* Flügel, 2004). The firmgrounds typically contain a network of burrows (Bromley et al., 1990), and the depth of formation of hardgrounds is highly variable, from subtidal environments, to shelves and ramps, and into slope and basinal settings (Wilson & Palmer, 1992).

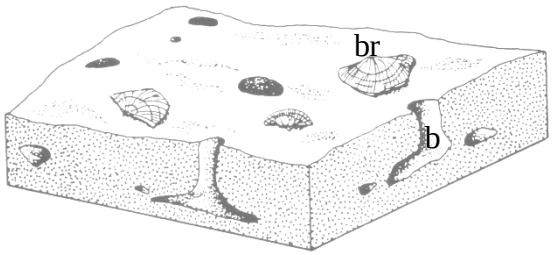

A: Soft bottom substrate; burrows (b) formed by brachiopods (br).

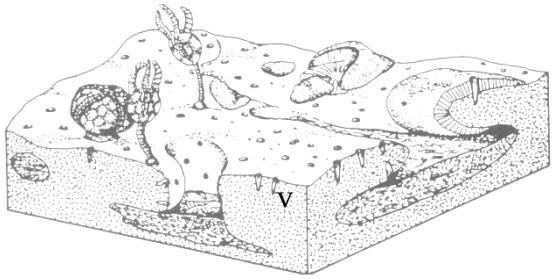

B: Hardground fauna with echinoderms and bryozoans. Formation of *Trypanites*-like borings (v) and infill of preomission burrows.

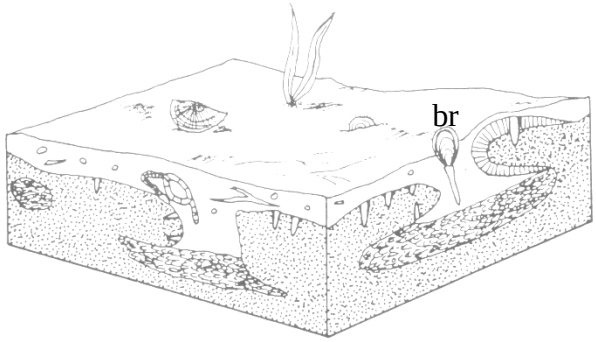

C: Burial of hardground and establishment of a new community of brachiopods (br) into the overlying soft substrate.

Figure 14: The evolution of a firmground to incipient hardground and the associated fauna (from Brett & Liddel, 1978).

3.2 Hardground identification

The appearance of hardgrounds can easily be confused with stylolites, omission surfaces and other discontinuity surfaces. Based on previous research on the topic, Flügel (2004) presented a series of criteria used in the recognition of hardgrounds, and these are summarized below;

- *Surfaces:* The upper contact of the hardground appears often either as a smooth or irregular surface, some showing pits and grooves. The smooth surfaces are formed by

abrasion and are often formed in shallow-marine high energy environments. Tepee-like expansion ridges and signs of corrosion are likely to occur on the upper surface of shelf hardgrounds. Absence of encrustations on these surfaces can indicate high energy conditions and a shorter omission period.

- *Contacts:* The upper contact of a hardground is commonly sharp, while the lower contact is more diffuse. Micritic microbial crusts may also cover the surface, and overlying sediment may fill cavities or borings.

- *Mineralization:* Crusts or impregnations may be mineralized on the uppermost layers of the hardground (Figure 15). The environment controls the form, composition and intensity of the mineralization. A shelf environment is likely to have hardgrounds with content of glauconite in burrows, in borings or cracks. Calcium phosphate salts (as phosphate stromatolites or cements) and iron hydroxides (limonite and goethite) may also mineralize the surface. Crusts composed of limonite are likely to represent long periods of omission and low-energy conditions.
  In the pelagic realm, manganese oxides are more common, and calcium carbonate may have been replaced by barite.

- *Borings:* Both micro- and macro borings are common on hardground surfaces (indicated in Figure 15), presenting palaeoecological information as well as sedimentological aspects, such as the consistency of the hardened seafloor, useful in the interpretation of environmental and depositional conditions.

- *Burrowing:* Associations of selected trace fossils marking changes in substrate types are often abundant in the overlying and underlying strata of a hardground. The relationship between borings, encrustations and bioturbation can indicate the change from a firm to hard seafloor. The cementation of the seafloor during the hardground formation would preserve the burrows as open galleries with hardened walls (Wilson & Palmer, 1992).

- *Microfacies:* Differences in biogenic content and texture of microfacies types in strata above and below a surface may represent a hardground.

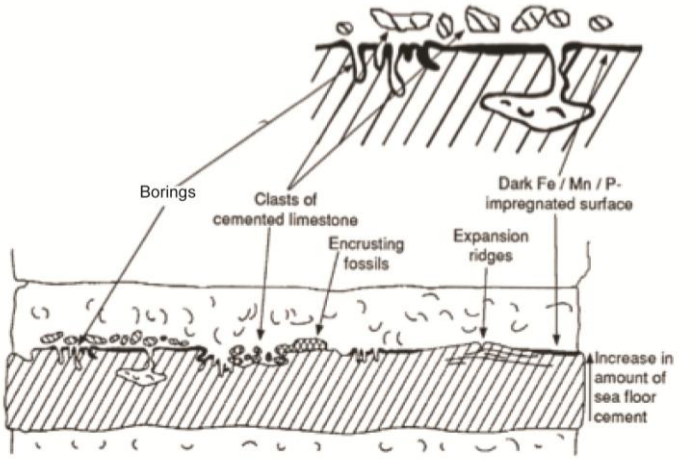

Figure 15: Illustration of characteristic features of a hardground (modified from Flügel, 2004).

- *Biogenic encrustations:* Hardgrounds are often inhabited by organisms which settle on the upper part of the hard substrate. The particular groups are bryozoans, oysters and brachiopods, while other common groups encrusting hard substrates are foraminifera, calcareous algae, serpulid polychaetes, corals and cirripeds. Crinoids, brachiopods and oysters are also abundant on firm substrates.

- *Cemented limestone clasts:* Clasts that are bored, appearing with sharp edges and with similar composition to the hardground, are often observed along the upper surface of the hardground and as infillings of depressions. The clasts have a complex origin, caused by reworking and erosion of the hardground.

- *Hiatus concretions:* Bearing signs of borings, encrustations and reworking, hiatus concretions can reflect several stages of deposition and burial, as well as excavation.

- *Carbonate cements:* Low Mg calcite cements appearing as blocky mosaics are common on most hardgrounds. Different shapes of cements are palisade-like fibrous cements and syntaxial rim cements.

- *Alternations of carbonate cements and hardground surfaces:* Multiple surfaces spaced millimeters apart can often indicate a hardground, associated with laterally expanding cement layers and crusts.

Common borings into the hardground surface are *Trypanites* (sipunculids, polychaetes and barnacles), *Petroxestes* (bivalves and bryozoans), *Gastrochaenolites* (bivalves) and *Entobia* (sponges) (Wilson & Palmer, 1992). Mineral staining on hardground surfaces and the burrows and borings that descend from them, is a common feature. Pyrite is most common in shallow water hardgrounds, and oxidizes readily to limonite in weathered sections (Wilson & Palmer, 1992).

Erosive sediment scour is a process which takes place where a growing hardground is overlain by a thin layer of loose sediment, which is jostled around on the surface, and remains uncemented. This sediment is likely to scour the hardground surface and truncate pre-omission burrows and large fossils imbedded in the lithified sediment (Wilson & Palmer, 1992).

4 Material and methods

4.1 Field work, field methods and carbonate classification

The main part of the fieldwork performed on behalf of this study was carried out during the summer 2011, and partly the spring 2012. Most of the fieldwork was done on the extensive bedding surface at the Slemmestad IF arena locality, approximately 500 meters from the village of Slemmestad in Røyken kommune, in the county of Buskerud (Figure 16). The locality is in close contact with infrastructure, and easily reached from the cities of Oslo and Drammen. GPS coordinates of the locality are: 5977619, 1048110.

The exposure of the Svartodden Mbr. at the Slemmestad football arena includes both its lower contact with the underlying unit; the Lysaker Mbr. of the Huk Fm., as well as the overlying Helskjer Mbr. of the Elnes Fm. (Figure 17). The Svartodden Mbr. is exposed with three bedding surfaces, where the uppermost surface is the largest and the most characteristic one, indicated in Figure 17.

Some localities displaying the whole Huk Fm. section located nearby in the village of Slemmestad were also visited for observations, such as the Bjerkåsholmen locality and the Djuptrekkodden locality. GPS coordinates of Bjerkåsholmen are 5979197, 1050277. GPS coordinates of the Djuptrekkodden are 5979369, 1050350. The localities are shown in the map below (Figure 16).

The entire Huk Fm.; the upper Svartodden Mbr., and partly the under- and overlying units, were logged at the two localities in the village of Slemmestad as shown in Figure 16. The complete Huk Fm. was logged at the Bjerkåsholmen locality in Slemmestad, while the Svartodden Mbr. was logged in detail (scale 1:10) and sampled at the Slemmestad IF arena locality. The logged section from Slemmestad IF arena is approximately 2.4 m, of which the Svartodden Mbr. constitutes 2.0 m with three distinct bedding surfaces exposed. The Svartodden Mbr. section was divided in six beds, of which bed 3, bed 4 and bed 6 show distinct bedding surfaces (Figure 17). Bed 6 (the uppermost bed of the Svartodden Mbr.) constitutes the main bedding surface of the locality.

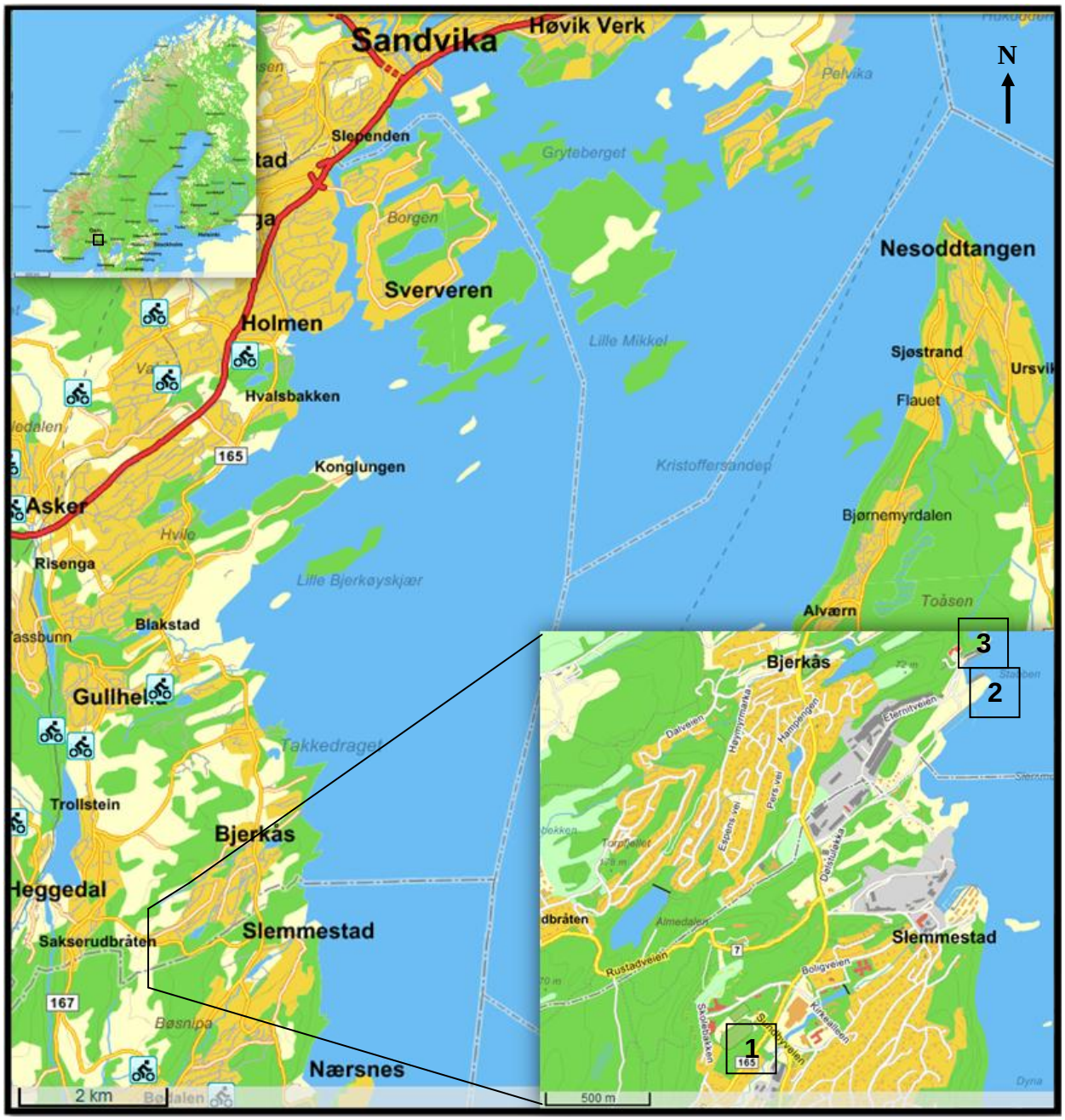

Figure 16: Map section of the Slemmestad area. Symbols: 1: Slemmestad IF arena locality, 2: Bjerkåsholmen locality, 3: Djuptrekkodden locality. Map source: Eniro Norge AS.

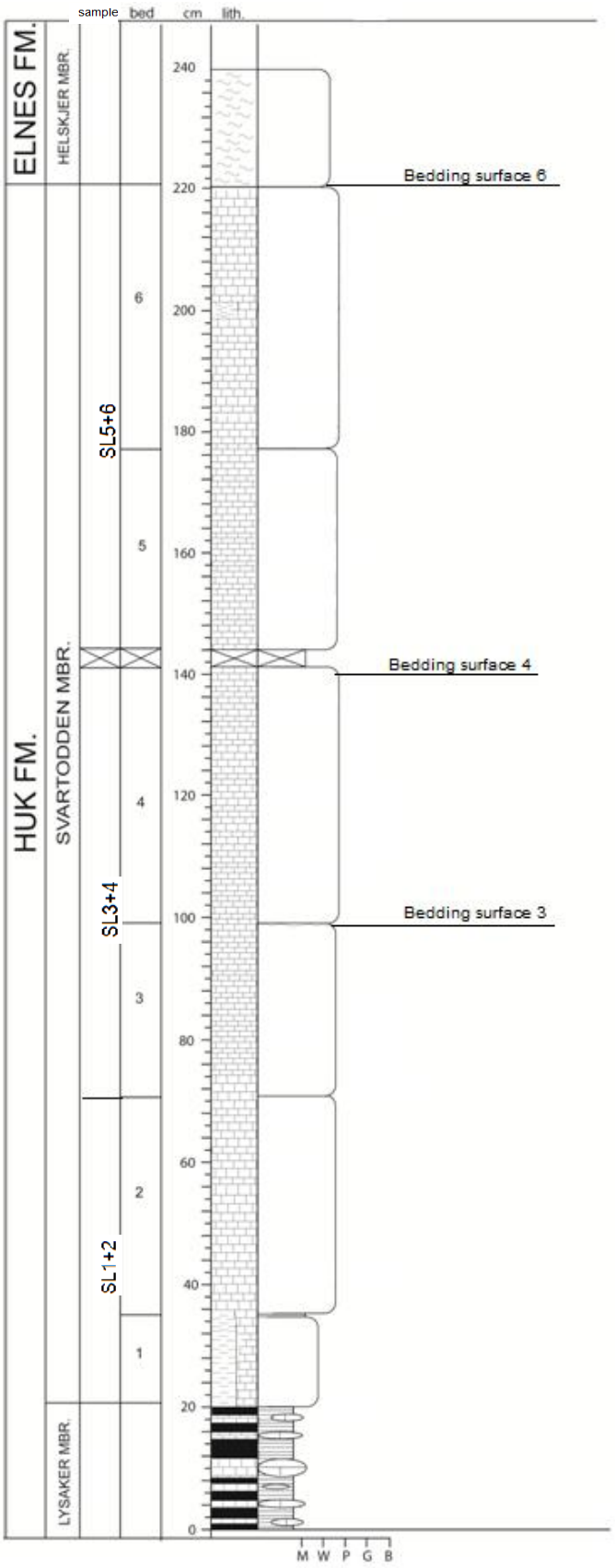

Figure 17: Simplified log of the Svartodden Mbr., the under- and overlying units, bedding surfaces and sampled sections.

The Dunham (1962) carbonate classification was used during the logging of the sections, based on whether the rock is mud-, grain-, matrix-, or component supported (Figure 18).

<table>
<tr><td colspan="4">DEPOSITIONAL TEXTURE RECOGNIZABLE</td><td rowspan="3">Original components were bound together during deposition… as shown by intergrown skeletal matter, lamination contrary to gravity, or sediment-floored cavities that are roofed over by organic or questionably organic matter and are too large to be interstice

Boundstone</td><td rowspan="3">DEPOSITIONAL TEXTURE NOT RECOGNIZABLE

(Subdivide according to classification designed to bear on physical texture or diagenesis.)

Crystalline carbonate</td></tr>
<tr><td colspan="4">Original components not bound together during deposition</td></tr>
<tr><td colspan="3">Contains mud
(particles of clay and fine silt)</td><td rowspan="2">Lacks mud and is grain-supported

Grainstone</td></tr>
<tr><td colspan="2">Mud-supported</td><td rowspan="2">Grain-supported

Packstone</td><td rowspan="2">Less than 10 percent grains

Mudstone</td><td rowspan="2">More than 10 percent grains

Wackestone</td></tr>
</table>

Figure 18: Dunham´s classification of carbonate rocks based on depositional texture (modified from Dunham, 1962).

The Wentworth grain-size scale has been used in this study for the classification of the siliciclastic components in the rock analysis. In the Wentworth classification scale, the particle size ranges from clay (1/256 mm), through medium sand (½ mm) to boulder size (256 mm). In this study, only grain sizes up to fine sand has been detected, hence a shortened version of the scale is presented in Figure 19 below.

Classification	Particle size
Clay	*< 0,004 mm.*
Silt	*0,004 – 0,063 mm.*
Very fine sand	*0,063 – 0,125 mm.*
Fine sand	*0,125 – 0,25 mm.*

Figure 19: The Wentworth classification of grain sizes (modified from Wentworth, 1922).

The area of the bedding surface with removed vegetation was measured with a levelling instrument for precise measurements of the surface. Six squares on the main (uppermost) bedding surface (2x2 m), and two squares (of same size) on the middle (top of bed 4) bedding surface were drawn out for statistical investigations (Figure 20).

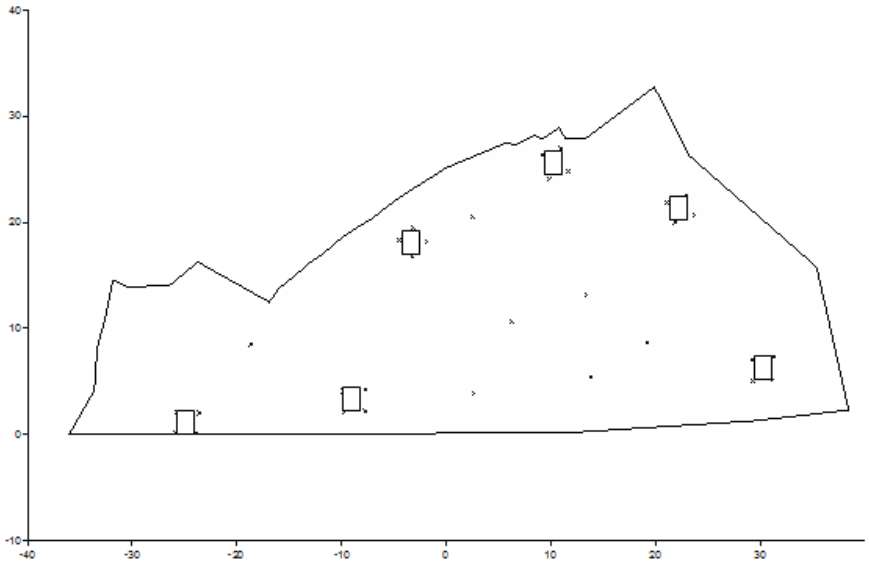

Figure 20: Precise measurement of the Slemmestad IF arena locality showing outlines of the six squares on bedding surface 6 that were studied.

Body fossils, trace fossils, and several geological features of the Svartodden Mbr. were photographed with a Nikon D3100 mirror reflex photo camera.
Cephalopod species were recorderecorded by using a cephalopod species key, compiled by Dr. Björn Kröger. Orientations of the apex of conchs were measured with a compass in each square and on the bedding surface of the Lysaker Mbr., later reproduced in the statistic software Past (Hammer et al., 2001) for the production of rose diagrams.

Blocks from the whole 2 m thick section were collected, in order to make an artificial core of the unit for geochemical purposes. Smaller samples were also collected for studies. Not all parts of the section could be sampled due to the locality now being considered for nature protection.

The logged sections were digitized in the computer software Adobe Illustrator CS4.

4.2 Preparation of slabs, core and thin section

Massive samples (30 x 40 cm) collected in the field were cut with a rock-saw into a core, although with some minor missing gaps between the beds. A total of 195 cm of core was cut

and compared versus the logged section. The core was polished with carbon polishing paper and later photographed.

21 samples for thin sections were cut out from the prepared core, at regular intervals through the section, and labelled. Additional 11 thin sections with interesting features were prepared. The samples cut in 3 x 2 x 1 cm, were polished with carborundum polishing paper, having a thickness of approximately 3 mm. In a thin section laboratory, the slabs were polished to a thickness of about 50 μm in order to become transparent, and glued to a glass slide measuring 2,7 x 4,7 cm. Results from thin section investigations are presented in Appendix 7.

4.3 Transmitted light microscope

A Leica DMLP microscope at NHM were used for analysis of thin sections. Photographs were taken with a digital Leica DC 300 camera, mounted on the microscope.

4.4 Microfacies analysis

The procedure of point counting on thin sections and acetate peels was carried out with a Leica DMLP microscope and a Swift model F automatic point counter, based on the method presented by Jaanusson (1972). The point counting of skeletal fragments and mineral grains was performed on 21 thin sections. 300 counts per thin section were identified for the component analysis of the rock. Points were counted in intervals of 0.2 mm. Both plain polarized and cross polarized light were used during the analysis.

4.5 Staining techniques

Differentiating between calcite, ferroan calcite, dolomite and ferroan dolomite in a carbonate rock is made possible by using Dickson´s staining method (Dickson, 1966). The staining solution was made by mixing 0.2 g Alizarin Red S with 100 ml 1.5 % hydrochloric solution, topped up to 500 ml with water. The thin sections were immersed in the solution for about 3-5 seconds. Afterwards they were dried in a drying cabinet for 24 hours. The staining solution

colours calcite and aragonite, while dolomite is kept unaltered (shown in Figure 21). The results from the staining are presented in Chapter 6.

Mineral type	Color after staining
Calcite	Varying through very pale pink to red
Ferroan calcite	Varying through mauve, purple to royal blue
Dolomite	No stain
Ferroan dolomite	Pale to deep turquoise
Quartz	No stain

Figure 21: Colour alterations after applying Dickson´s staining method on carbonate rocks (modified from Dickson, 1966).

4.6 Acid processing of samples

Layer 1 and 2, layer 3 and 4, layer 5 and 6 were grouped in three samples, namely the lower (SL1+2), middle (SL3+4) and upper units (SL5+6) of the Svartodden Mbr., presented in Figure 17. Each sample weighed 1.5 kg, and was dissolved in 10 % diluted acetic acid. The dissolved fraction between 500 – 63 μm was sieved, collected and dried after multiple stages of acid renewal. The samples were heavy mineral separated with the heavy liquid diodomethane diluted with acetone with a density of 2.92 g/ml (Figure 22), and the samples were later washed with acetone and dried.

Figure 22: Outline of the heavy mineral separation method.

The separated heavy fraction of the dissolved rocks was then weighed. Later the samples were analysed under a microscope, and microfossils and mineral grains were picked out from the samples.

4.7 Scanning Electron Microscope (SEM)

By using a scanning electron microscope (SEM), highly magnified images of the surface of a sample can be obtained (Goldstein, 2003). The SEM has in this study been used during investigations of conodonts, brachiopods, ostracodes and thin sections.

During SEM analysis, the surface of a sample (thin section, microfossil or crystal) is hit by an electron beam, first created by heating a wolfram filament and then by accelerating the electrons. By directing the electron beam onto the sample, secondary electrons (SE) are emitted. The registered secondary electrons, representing the electrons in the atoms outermost shells, provide an image of the surface topography (in 3D) of the sample, having a relatively low energy. By the use of an Energy Dispersive Detector (EDS), emitted X-rays from the sample are detected by selecting a specific area of interest. Immediately, one obtains information about the elemental composition and amount of each element of the analysed area, being particularly useful in the analysis of minerals. This method is known as the "point and ID" method, and is based on the elements emission of characteristic X-rays.

Imaging of microfossils and analysis of minerals was performed at NHM, with a Hitachi 3600N-model scanning electron microscope.

4.8 Cathodoluminescence (CL)

The CL microscopy work was carried out with a Nuclide Luminoscope microscope, an electron gun and a vacuum pump, at the University of Tromsø, guided by Dr. Nils-Martin Hanken. Images were recorded with a Leica camera. The electron gun was tuned at 13.5 kV and 1000 μA.

When a sample gets bombarded with electrons from an electron gun, it will emit photons (material and energy), which is described as the process of luminescence – a transformation of

energy into visible light. CL is a more specialized petrographic technique compared to reflection of light from a polished surface or the transmission through the mineral. The voltage and current were tuned to focus on carbonate minerals. The calcite, depending of its various content of trace elements, showed colours like orange and red (640 nm), as well as black, while the matrix shows a grey colour. The purpose of the CL-microscopy work was to gather information regarding the diagenetic history of the Svartodden Mbr., based on different stages of cementation, seen in the thin sections with a CL microscope.

A CL microscope has the advantage of showing the luminescence of minerals, i.e. minerals containing various amounts of trace elements, such as Mn^{2+} and Fe^{2+}, will give different colours. For instance, calcite crystals growing in an environment where the pore water is oxic would contain higher amounts of Mn^{2+}, which would be enriched in the calcite crystals. A calcite enriched in Mn^{2+} gives an orange colour to the crystals. However, with increased burial, the pore water will become slightly reducing, and Fe^{2+} will be absorbed and enriched in the crystal lattice of the precipitating calcite. The Fe^{2+} enriched calcite crystals give a grey-black colour in the CL microscope (Flügel, 2004).

4.9 X-ray fluorescence (XRF)

The XRF method utilizes the different elements ability in a sample to produce characteristic X-rays, following an irradiation of the sample by X-rays produced by an X-ray tube. By pointing an X-ray beam at the sample and ionizing its atoms, the specific elements in the sample will release characteristic X-rays of different energies. During this process, electrons from a higher shell (energy level) move to a vacancy in a lower shell (lower energy level), which has been made open by an external primary excitation X-ray from the X-ray tube. At the same time, the energy excess from the high level- to the low energy level in an atom gets released as characteristic X-rays which are unique to each specific type of atom. The characteristic X-rays are detected, and the specific elements and their concentrations are measured.

An Itrax core scanner at the University of Bergen was used for XRF scanning of the sampled and cut core of the Svartodden Mbr. The X-ray source had a 60 kV X-ray tube with a Cr-anode used during the data acquisition. The Cr tube can detect the following elements, with

concentrations in ppm: Mg, Al, Si, P, S, Cl, K, Ca, Ti, Mn, Fe, Br, Sr, Ba, Pb. The useful elements for the detection of hardgrounds, P and S, V, Fe and Ni could be detected with the Cr-tube. High precision on the analysis was achieved by having the scanner-point interval set to 1 mm. The tests were run with a counting time of 15 seconds per point, and each element was simultaneously scanned twice.

4.10 Magnetic susceptibility

Magnetic susceptibility logging was performed on the artificial core by a handheld magnetic susceptibility meter, a Kappameter of the KT series. The signal is measured in 1×10^{-6} [SI] units, i.e. a very sensitive signal. Magnetic susceptibility of rocks is a petrophysical parameter, which describes the type and amount of magnetic minerals. Ferromagnetic minerals are often indicators of geological processes, such as increased terrestrial input, and hence measurements of magnetic susceptibility are useful in environmental and depositional interpretations of rock sequences (Hrouda et al., 2009).

4.11 Mass spectrometry (^{18}O and ^{13}C stable isotopes)

Stable isotopic signatures from oxygen and carbon were obtained, with the purposes of performing stratigraphic correlations with regional $\delta^{13}C$ excursions, and analysing $\delta^{18}O$ for palaeoenvironmental interpretations (temperature and salinity).

10 samples were drilled out from the core of the Svartodden Mbr. for the extraction of oxygen (^{16}O and ^{18}O) and carbon (^{12}C and ^{13}C) stable isotopes. The samples were collected from each layer at regular intervals of approximately 20 cm, in order to get a range of the whole rock sequence. Carbonate samples were analysed for stable isotopes ($\delta^{13}C$ and $\delta^{18}O$) at the University of Bergen. Ground powdered samples were analysed on Finnigan MAT 251 and MAT 253 mass spectrometers coupled to automated Kiel devices. The data are reported on the VPDB scale calibrated with NBS-19. The long term analytical precision of both systems as defined by the external reproducibility of carbonate standards (>8 mg) over periods of weeks to months exceeds 0.05‰ and 0.1‰ for $\delta^{13}C$ and $\delta^{18}O$, respectively.

5 Palaeontology

The Ordovician period holds one of the greatest evolutionary events in the history of life on Earth (Webby, 2004) with the establishment of much of the evolving marine life. During a time interval of approximately 25 Myr from early to mid Ordovician time, the world's second largest radiation of diversity occurred, known as the Great Ordovician Biodiversification Event (Servais et al., 2010).

The fossil fauna can provide important information regarding sedimentary processes e.g. hardground formation, current directions, sedimentation rates and cementation history. Important groups known from the Ordovician fauna are benthic trilobites, bryozoans, stromatoporoids, brachiopods, echinoderms, conodonts and ostracodes, several illustrated in Figure 23. Common features in Baltoscandic successions are trace fossils such as macroborings in hardgrounds or tunnel networks into semi lithified firmgrounds. These phenomena are good recordings regarding conditions in a depositional environment.

Figure 23: Life on an Ordovician seafloor. A: trilobite, B: crinoid, C: cephalopod, D: graptolites (illustration by B. Bocianowski).

In this section, a short literature study of the fossil groups present in the Svartodden Mbr. is presented. The cephalopods are given a greater emphasis in their description than the other groups, due to their dominant appearance in the rock unit. Classification to genus-level regarding observed fossils and to species level on cephalopods, conodonts and acrotretid brachiopods, will be attempted. Microfacies analysis of thin sections shows the relative distribution of skeletal grains from calcium carbonate secreting organisms through the unit. The abundant trace fossils found in the Svartodden Mbr. will also be presented and discussed.

5.1 Previous work

This section will focus on published sources covering aspects of palaeontology; the groups of fossils that were abundant in the planktonic water column and on the benthic seafloor during the deposition of the Svartodden Mbr. during the Darriwilian. Characteristic features of the different animal groups associated with the Svartodden Mbr., are based on the collected references in Benton & Harper (2009).

5.1.2 Brachiopods

Brachiopods are bivalved filter feeders, often attached to hard substrates by a pedicle. During the Ordovician, brachiopods thrived on shelves, ramps and in slope environments (Flügel, 2010), and were the most dominating of the low-level suspension-feeding benthos (Benton & Harper, 2009).Taxonomic studies of brachiopods in Lower and Middle Ordovician rocks in the Oslo Region are few. Exceptions are the works of Spjeldnæs (1957). Early to Middle Ordovician brachiopod faunas diversified in great extent in Baltoscandia and the varying facies belts experienced different faunas due to changes in fluxes of immigrant species and the changes in latitude of Baltica (Harper & Mac Niocaill, 2002). The most pronounced diversification took place in the shallow water communities (Harper & Mac Niocaill, 2002). The lower part of the Svartodden Mbr. was distinguished by Brögger (1882) as the *Porambonites* Beds, being rich in brachiopods. Hansen & Bruton (2009) reported small dalmanellid brachiopods as a constituent of the endoceratid faunal association.

Phosphatic inarticulate brachiopods of the order Acrotretida have been reported from Middle Ordovician limestones inVästergötland and Dalarna, Sweden (Holmer, 1989). The phosphatic brachiopod species recorded in the Svartodden Mbr. equivalent Holen Fm. are *Scaphelasma* sp., *Numericoma? spinosa, Hisingerella? ungulcula, Conotreta? mica, Tornyelasma* sp., *Biernatia* sp., *Eocunulus* spp., *Myotreta* aff. *crasse and Paterula* spp. Several of the species are illustrated in Figure 24. Variation in phosphatic inarticulate brachiopod assemblages across the various confacies belts reflects different ecological factors in the different belts (Holmer, 1989).

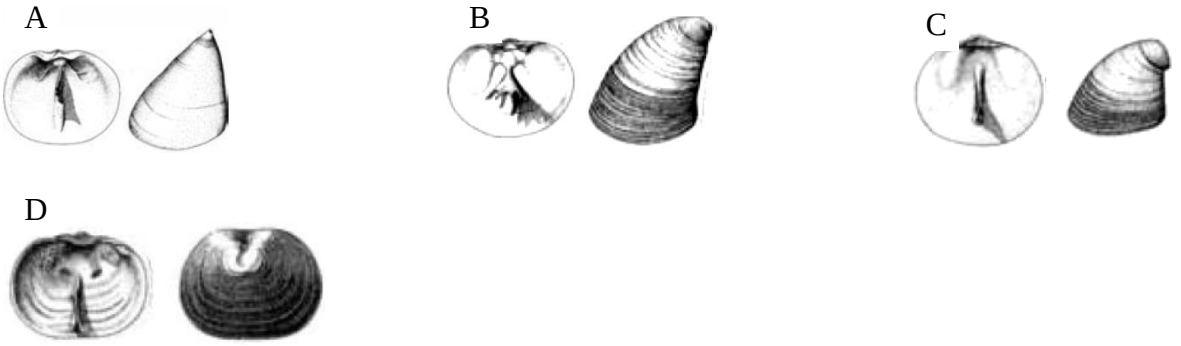

Figure 24: A: *Conotreta? mica* B: *Numericoma? spinosa* C: *Myotreta* aff. *crasse* D: *Scaphelasma* sp. nov. a (From Holmer, 1989).

Most of the acrotretaceans belonged to the benthic epifauna, and different strategies were employed by the brachiopods of attaching themselves to different substrates. Some were likely to attach themselves to small scattered skeletal grains, while others had an encrusting mode of life using algae as substratum, eg. *Eoconulus.* A free-lying mode of life, using spines for stabilization was a strategy of some species, eg. *Acanthambonia portanensis.* This species had hook-like spines and were attached to minute cylindrical objects, possibly sponge spicules. None of the acrotretaceans are known to have had an infaunal life habit (Holmer, 1989).

5.1.3 Bryozoans

Bryozoans are millimeter- to several centimeter- sized colonial, marine organisms that are active suspension feeders, with a fossil record since the Early Ordovician (Benton & Harper, 2009). The tiny individuals or the zooids are usually less than 1 mm in diameter. They often have a horseshoe-shaped or circular lophophore containing a ring of many tentacles. The individual zooid is enclosed by a calcareous exoskeleton (Benton & Harper, 2009). The bryozoans are distributed on seafloors from the tidal area to bathyal depths (Flügel, 2010). The Stenolaemata and its five orders (Trepostomata, Cystoporata, Cyclostomata, Fenestrata and Cryptostomata) were common in Ordovician limestones (Benton & Harper, 2009). Bryozoans are first recorded in the Baltoscandic platform from the Volkhov Stage (Middle Ordovician), present in sediments from eastern Russia, Estonia and Poland (Taylor & Ernst, 2004).

5.1.4 Gastropods

Gastropods are mostly benthic mobile organisms, with a wide range of feeding strategies, e.g. grazing herbivores or detritus feeders. They are mainly known as snails and slugs with or without an external skeleton (Benton & Harper, 2009). The main gastropod groups during the Ordovician were Archaeogastropoda, Mimospirina, Euomphalomorpha and Macluritoidea (Frýda & Rohr, 2004). Ordovician microgastropods (< 1 mm) have been reported from the Huk Fm. (Ebbestad & Isakar, 2004), and can often be found in acid dissolved residue due to phosphatic infilling of the shells.

5.1.5 Cephalopods

The class Cephalopoda belongs to the phylum Mollusca; animals that are usually un-segmented and soft-bodied (Benton & Harper, 2009). The majority of Recent cephalopod species belong to the subclass Coleoidea, are covered by soft parts and have an inner or no skeleton. However, in the Early Palaeozoic, most cephalopods had exterior shells, and were probably the most diverse group of nektonic predators (Kröger & Mutvei, 2004). Some had coiled evolute shells, while others had simple straight, cone shaped shells (orthocones). The only cephalopod genus with an exoskeleton alive today, is the coiled *Nautilus* of the subclass Nautiloidea, found in the Indo-Pacific region. The evolution and ecology of the cephalopod groups living in the Middle Ordovician will in this section be briefly described. For a more comprehensive background on cephalopods, see Moore (1964) and Boardman et al. (1987). Due to their rapid evolution, both external and internal shells of fossil cephalopods are good stratigraphic proxies (Moore, 1964).

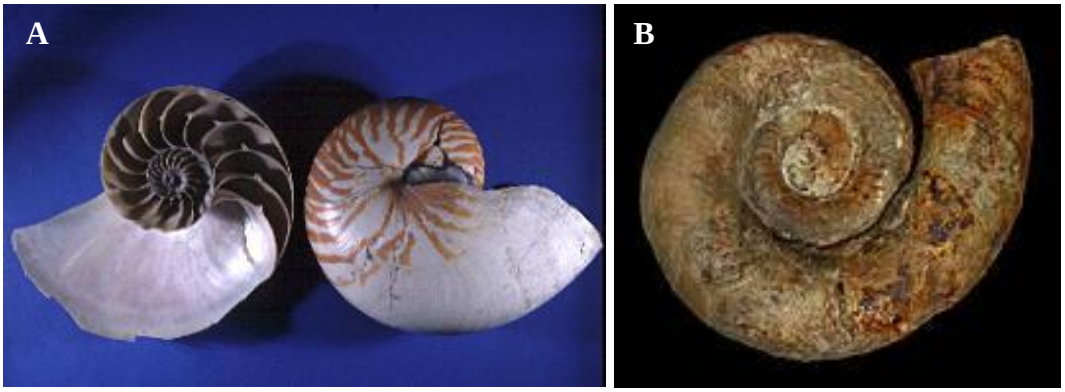

Figure 25: A. The extant *Nautilus*
Source: Natural history museum, Oslo.
B. Specimen of the extinct order Tarphycerida
Source: Musum für naturkunde, Berlin.

Cephalopod morphology

Since the only extant cephalopod with an external shell is the coiled shelled genus *Nautilus*, this group is used in the understanding of extinct cephalopod morphologies and soft parts. Important organs, soft and hard parts in *Nautilus* that are believed to have been shared by the extinct cephalopods, are gills, a funnel, the siphuncle and the phragmocone (Figure 26). Buoyancy regulation of the extinct cephalopods is believed to have been the same as that of *Nautilus*, having gas-filled chambers with an intersecting siphuncle which can transport water or gas through the chambers in order to keep the cephalopod floating and vertically oriented in the water column.

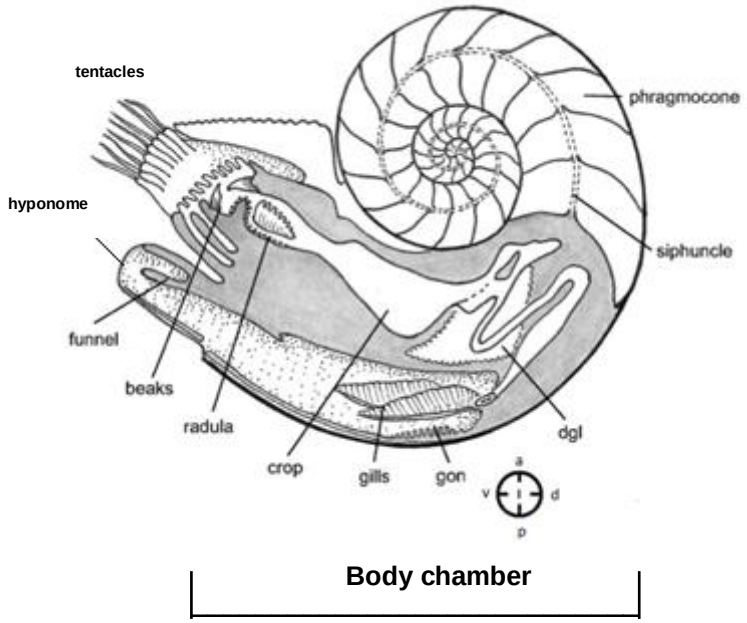

Figure 26: Diagrammatic section through soft and hard parts of *Nautilus.* Bodyplan abbreviates: a = anterior, p = posterior, v = ventral, d = dorsal. Modified from Kröger et al, (2011).

The funnel (hyponome) of the *Nautilus* is used for propulsion or swimming, by squeezing out water and hence the cephalopod will move backwards in the water, also described as jet propulsion. *Nautilus* has primitive "pin-hole" eyes. Sexes are separate, and cephalopod eggs are big and contain more yolk than usual in other mollusks (Moore, 1964). The function of the arms or the tentacles in living cephalopods is to assist the animals` balance, swimming, and capture of prey. The body chamber is the outermost chamber, being secreted by the mantle. The head holds an internal cartilaginous skeleton, enclosing the central nerve system, balance

organs and the attachment of the hyponome (Moore, 1964). Fossil cephalopod conchs had a variety of different shapes, illustrated below in Figure 27.

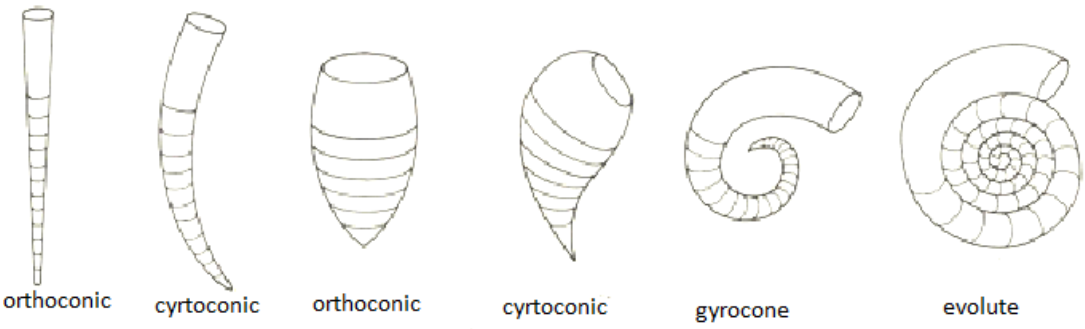

Figure 27: Some common cephalopod conch shapes (Modified from Moore, 1964).

In nautiloid cephalopods, each chamber is separated from adjacent chambers, by a layer of calcareous material between them, which is called the septum. The suture is the area where each septum is cemented to the outer cephalopod shell, and its appearance (form or pattern) is used in classification of the nautiloids (Benton & Harper, 2009). General morphology of orthoconic conchs is shown in Figure 28.

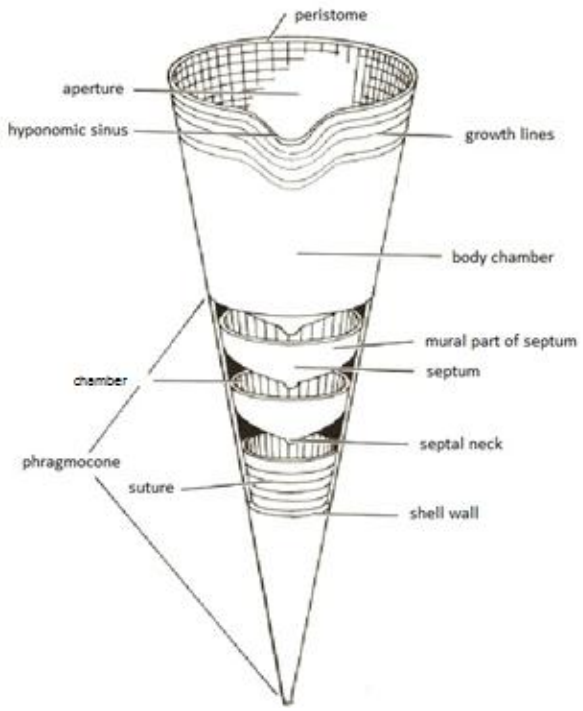

Figure 28: Diagrammatic figure of an orthoconic conch (modified from Moore, 1964).

Cephalopod evolution until the Middle Ordovician

The major classes of mollusks, such as the Cephalopoda, are believed to have diverged in the early Cambrian. The ancestor of the Cephalopoda was apparently a benthic monoplacophoran-like mollusc, with a high conical mineralized shell which later evolved septa that divided the chambers in the conchs. The orders Orthocerida, Ellesmerocerida, Plectronocerida and Discosorida, had evolved by Early Ordovician time. A high variation in shapes and sizes of cephalopod conchs can be seen in the fossil record from this time on. The orders Ellesmerocerida, Plectronocerida and Discosorida are regarded as the stem group Cephalopoda, and went extinct during the Carboniferous. The order Orthocerida on the other hand, is believed to be the ancestor of the extant *Nautilus*, although the Orthocerida went extinct in the Late Triassic (Kröger et al., 2011).

The Ordovician was significant for the nautiloid cephalopods, and the nautiloids reached their greatest diversity and greatest size in shallow marine carbonate facies environments in subtropical and tropical climates (Frey et al., 2004).
During the Early Ordovician, faunas containing the orders Ellesmerocerida, Endocerida and the coiled Tarphycerida, extensively diversified. Further into the Middle Ordovician, an expansion of the orders Endocerida, Actinocerida and Orthocerida continued, while the orders Discosorida, Pseudoorthocerida and Oncocerida evolved (Frey et al., 2004). The order Endocerida with the family Endoceratidae was highly abundant on the Baltoscandic shelf, with more than 40 genera during the early-mid Ordovician (Moore, 1964). The endocerids can be distinguished by the appearance of their endosiphuncular cements that consists of calcareous, conical sheaths (Moore, 1964).

The subclass Endoceratoidea contained species representing many Ordovician mega fossils, and during the Middle Ordovician the class represented the largest known invertebrates, evidenced by an endoceratid shell reaching 9-10 m in length (Doyle, 1996). The group consists of mainly orthoconic conchs (a few are cyrtoconic), with siphuncles that are cement-filled, large and often marginal (Moore, 1964). The endoceratids show a remarkable decline in diversity in Upper Ordovician and Silurian rocks (Boardman et al., 1987). The coiled order Tarphycerida persisted through the Ordovician and into the Silurian (Moore, 1964).

Figure 29 illustrates the evolution of some cephalopod orders from the Cambrian and onwards.

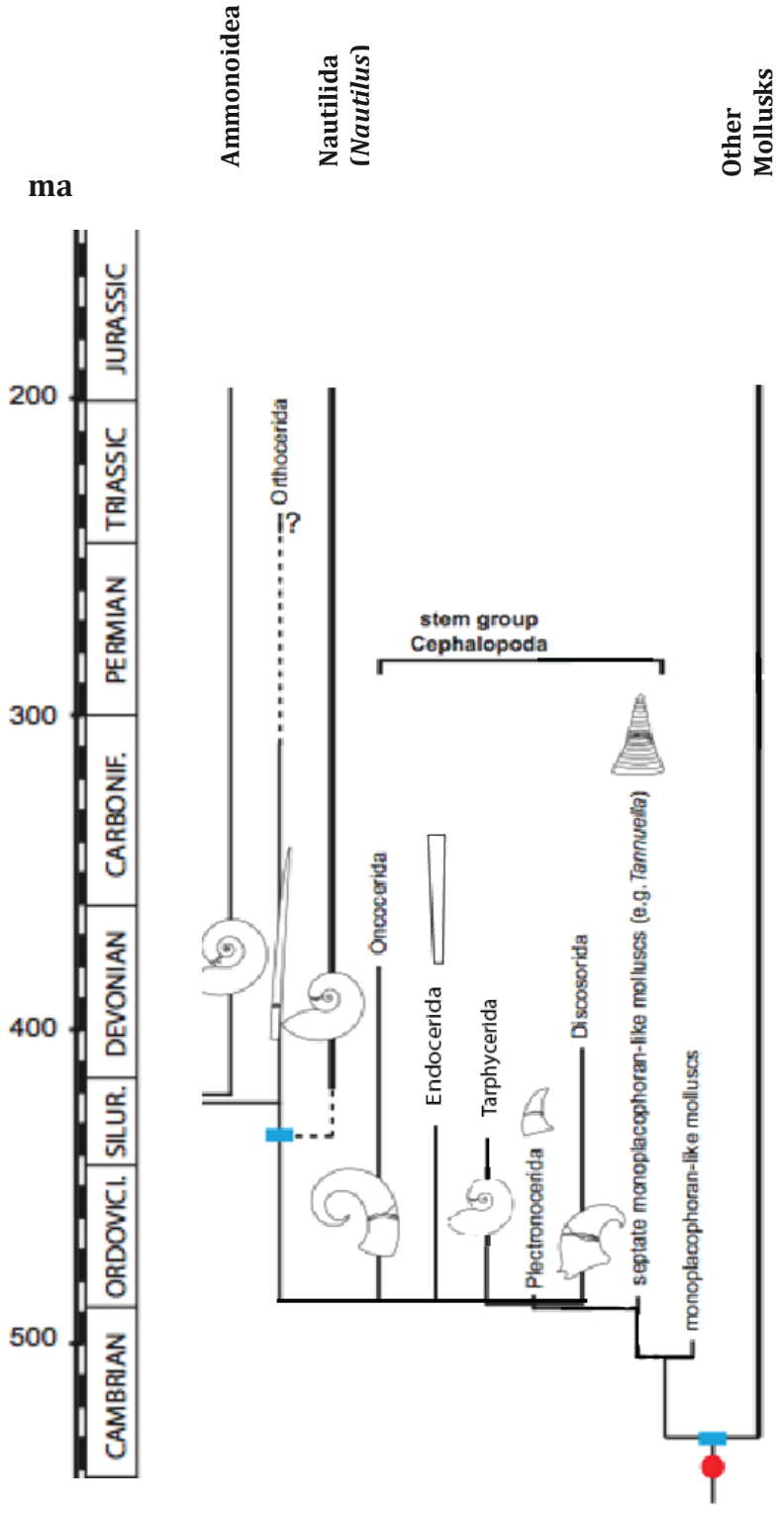

Figure 29: Time tree of cephalopod evolution until the Devonian, with selected cephalopod orders (modified from Kröger et al., 2011).

Cephalopod paleoecology

Conch morphology (Figure 28) is often used in the interpretation of habitats of fossil nautiloids, in which equilibrium of the cephalopod shell plays a major role in the understanding of the alignment of the cephalopod. Different modes of life from a benthonic, crawling style to horizontal propulsion, was mainly controlled by the cephalopods ability to achieve equilibrium between water and gas in the chambers and its weight.
A complicating factor in the interpretation of paleoecology of fossil nautiloids is that their conchs were likely to drift for long periods after the death of the animal. Organic decay of its soft parts and disintegration of the conch would postpone the process of the conch sinking, so that tides and ocean currents could transport them far away from their habitat, known as *post mortem* distribution. Most endocerids had lamellae or endocones that progressively developed from the apical end of the siphuncle, in order to obtain equilibrium between the total weight of the animal and the gas in the chambers. Hence, the axis of the endocerids was in a horizontal position. Most cephalopods of the orders Endocerida, Actinocerida and Orthocerida are longiconic orthocones which secreted primary mineralized cameral precipitates as siphuncular cements. The secretion of the cements was progressive, starting from the apical end of the phragmocone and further in the adoral direction. This also led to a stronger apical end of the conch, which could be favorable since the cephalopods were swimming backwards (Moore, 1964).

Strength of the septum of Endocerida against implosion of the water column was calculated by Westermann (1973) and the conchs had a sea depth tolerance down to 450 m.

Taphonomy and depositional mechanisms

Old age and decease may have been the main reasons for death of the Middle Ordovician nautiloids. Being carnivores and relatively large in size, the cephalopods were probably capable of escaping many threats in the water. However, there are several unknown factors, such as competition within and between groups and whether there were any superior carnivores feeding on cephalopods. Some cephalopods, as the Recent *Nautilus,* had colour markings, a feature that bears direct relationship to light intensity (Moore, 1964).

Several depositional parameters can be deduced from observations of nautiloid orthoconic cephalopods. After death, the nautiloids are believed to have been floating in the water for long periods, as is the case with the living *Nautilus* (Reyment, 1968).

Three mechanisms causing the conchs to sink were suggested by Raup (1973): a) they stranded on a shoreline, b) the density of the shells became higher than that of seawater due to flooding of the phragmocone, or c) encrusting organisms on the conchs added enough weight to cause sinking (Raup, 1973). While floating, orthoconic conchs are believed to have remained in a position with its siphuncle side pointing towards the seafloor, and the length axis in a position of 60° (Reyment, 1968). It is believed that while floating, the gas filled chambers eventually were filled with water, gaining a higher weight than the surrounding water, causing it to sink. According to Reyment (1970), after the shell had sunk to the sea-bottom, it would stay upright on the seafloor for a long time, caused by the remains of cameral gas. Figure 30 illustrates the position of the floating conchs in the water column and their alignment in the sediment after stranding on the seashore.

However, the theory of a floating position with the apex towards the sea surface may not have been the case with the endocerids due to their ability to secrete mineral cements in the siphuncle. Hence, when the animal died, the siphuncle would represent the point of highest gravitation, and eventually point towards to the seafloor when the soft parts were decayed.

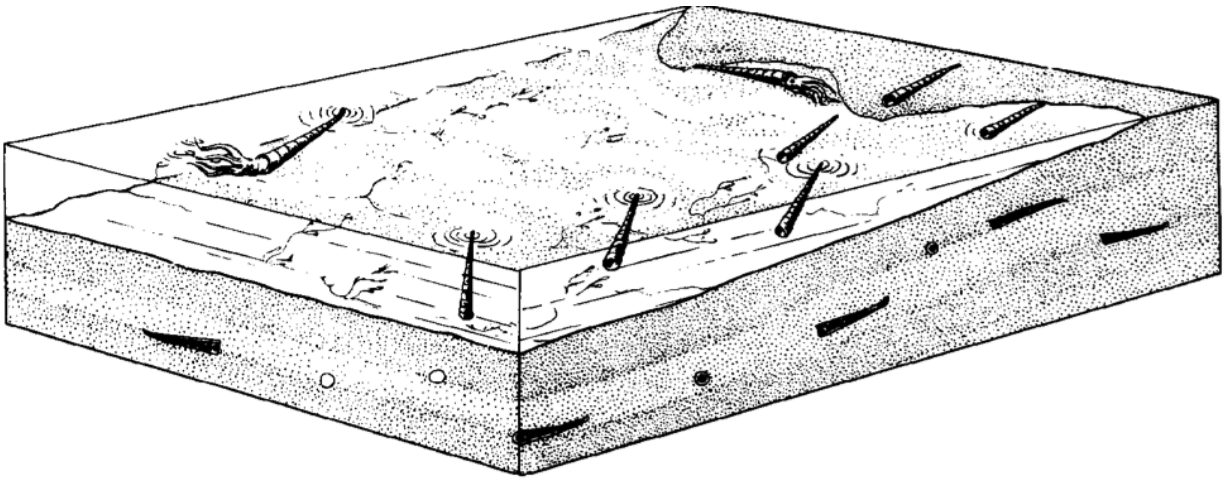

Figure 30: Floating habit of orthoconic conchs. The apex was filled with gas and would keep the conch from sinking for long a time interval (from Reyment, 1968).

5.1.6 Trilobites

The segmented exoskeletons of trilobites, an extinct subphylum of arthropods, were potentially great sediment contributors often due to frequent molting of exoskeletons during growth of the animal. Nielsen (1995) studied and compared trilobite distribution from the Hukodden Mbr. and the Lysaker Mbr. of the Huk Fm. with the stratigraphic equivalent Komstad Fm. in the Scania-Bornholm area in Sweden. Trilobite recordings from the Svartodden Mbr. were however not included in the study, but based on previous works. According to Nielsen (1995) the genus *Asaphus* is abundant in the Huk Fm., being a common genus from Eastern Baltica which became abundant in the Baltoscandic area in the early times of the Kunda Stage (Middle Ordovician) (Nielsen, 1995). In addition, *Megalaspis grandis* and *Asaphus striatus* have been identified in the Svartodden Mbr. (the former 3 cγ) in Slemmestad (Størmer, 1953).

The *A. expansus* trilobite biozone spans the Hukodden Mbr., the Lysaker Mbr. and partly the Svartodden Mbr. of the Huk Fm. The transition from the *A. expansus* biozone to the *A. 'raniceps'* Zone is located in the lowermost part (20-30 cm) of the Svartodden Mbr. based on Størmer (1953), who identified the trilobite *A. raniceps* in the upper beds of the Svartodden Mbr. Sea level reconstructions indicate a maximum lowstand at this biozone boundary (Nielsen, 1995).

A. expansus Zone	*A. ´raniceps´* Zone	Recorded in the Svartodden Mbr.
Megistaspis (M.) elongata *Dysplanus centrotus* *Niobe (Niobe) schmidti* *Asaphus expansus* (infrequent) Ptychopygids (infrequent) *Illaenus sarsi* (infrequent)	*Asaphus ´raniceps´* *Asaphus striatus* *Illaenus aduncus* *Stygina* sp.	*Megalaspis grandis* *Asaphus striatus* *Bronteopsis holtedahli* *Asaphus ´raniceps´* *Illaenus aduncus* *Megistaspis* *Ampyx nasutus*

Figure 31: The two trilobite zones which span the Svartodden Mbr. (based on Nielsen, 1995) and recorded trilobites in the unit (based on Skjeseth, 1953; Størmer, 1953; Nielsen, 1995 and Hansen, 2009).

Trilobites as constructors of open tunnel networks of the trace fossil *Thalassinoides* have been reported in the Huk Fm. equivalent Holen limestone in Sweden (Cherns et al., 2006). *In situ*

preservation in tunnels of more than 90 specimens of *Asaphus* trilobites combined with the genus' functional morphology strengthens the assumption of trilobites as Middle Ordovician tracemakers.

5.1.7 Ostracodes

Ostracodes are crustacean arthropods with small bivalved carapaces. The group has a fossil record since the Early Cambrian (Benton & Harper, 2009). Ostracodes are able to swim, crawl or burrow at the sediment-water interface, and they are mostly benthic (Benton & Harper, 2009). The Middle Ordovician ostracode fauna in Baltoscandia is described by several authors, including Henningsmoen (1954), who studied ostracodes in the Oslo Region. However, the study did not include the Huk Fm., which at that time was placed in the Lower Ordovician (Etage 3c) hence little is known about the ostracodes in the unit. Middle Ordovician ostracodes have been described from the time equivalent (Kunda Stage) Holen Limestone Fm., Västergötland in Sweden (Tinn & Meidla, 2001).
The ostracode fauna in the Holen and Lanna limestones of Sweden proved to be rich and diverse, containing species including *Conchoprimitia gammae, Unisulcopleura punctosulcata, Tallinnellina lanceolata, Elliptocyprites nonumbonatu, Glossomorphites digitatus, Longiscula curvata, Pinnatulites procerus, Brevivelum avelata,* and *Aulacopsis simplex* (Tinn & Meidla, 2001).

5.1.8 Echinoderms

Echinoderms comprise several classes, among the Crinoidea (sea lilies) were abundant in calcium carbonate platforms. These organisms consist of a high number of calcified plates making up their body walls in a five-fold symmetry, which disarticulate after death. They are equipped with a water vascular system, pentameral symmetry and tube feet (Benton & Harper, 2009). Crinoids can become several meters in length, are composed by a holdfast (root), a stem and an upper calyx (mouth, anus and arms). The majority of fossil forms were almost certainly included in the shallow water sessile benthos, and the class has an age ranging from the Early Ordovician to the present day (Benton & Harper, 2009).
Bockelie (1984) presented the stratigraphic distribution of some Ordovician echinoderm

classes in the Oslo Region, in his work on the Diploporita of the order Cystoidea. The study shows that the class Rhombifera is present in the Svartodden Mbr. (Bockelie, 1984).

5.1.9 Conodonts

Kohut (1972) was the first to establish the conodont biozonations of the Huk Fm. The particular biozone of the Svartodden Mbr. is the *Eoplacognathus? variabilis* zone. This conodont biozone is defined by the interval between the first appearance of *Eoplacognathus? variabilis* and the first appearance of *Eoplacognathus suecicus* (Löfgren 1978 *in* Rasmussen 1991). Characteristic species from this interval are *Protopanderodus rectus, Drepanodus arcatus, Drepanoistodus basiovalis, Eoplacognathus? variabilis, Scalpellodus gracilis, Baltonodus medius* and *Microzarkodina parva* (Rasmussen, 1991). Within the *E.? variabilis* zone, a subzone named the *E.? variabilis- Microzarkodina parva* Subzone is defined by the first appearance of *E.? variabilis* and first appearance of *Microzarkodina ozarkodella* (Löfgren, 1978 *in* Rasmussen, 1991).

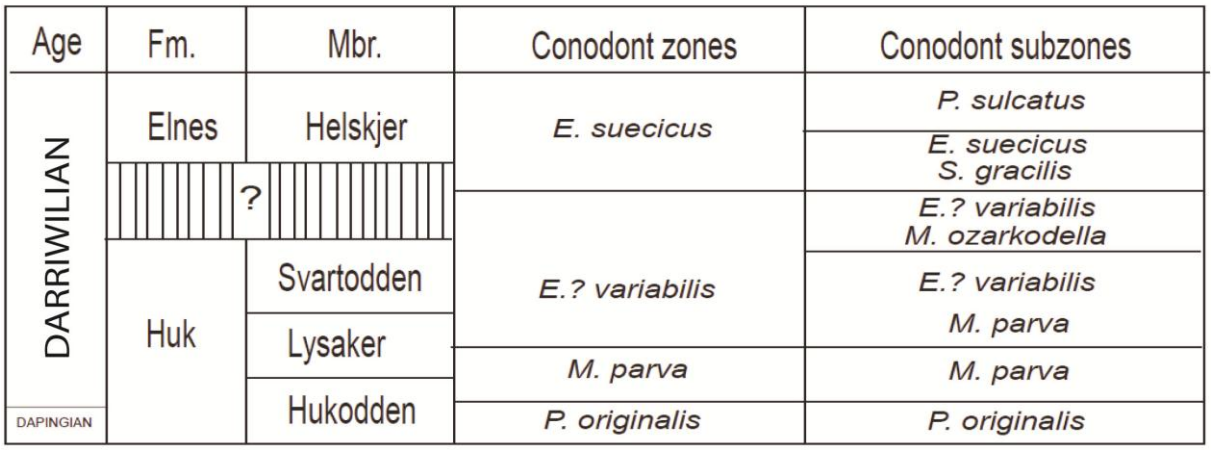

Figure 32: Correlation table. Chronostratigraphy and lithostratigraphy after Bruton et al. (2010), and conodont zones after Rasmussen (1991).

Epstein et al. (1977) introduced the concept of conodont Colour Alteration Index (CAI), based on experiments showing that colour change in conodonts is a consequence of depth and duration of burial, in context with geothermal gradients (Epstein et al., 1977). The colour change in the calcium phosphatic conodont elements is irreversible, and extends from pale yellow to black or colourless, depending on the degree of burial and heating.

Bergström (1980) and Rasmussen (1991) used conodonts as tools for bureal temperatures on Lower Palaeozoic rocks in the Oslo Region and in the Huk Fm., respectively.

Colour alteration in field collections	CAI	Temperature range °C
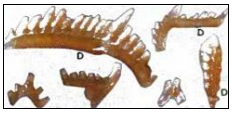	1	< 50° - 80°
	1,5	50° - 90°
	2	60° - 140°
	3	110° - 200°
	4	190° - 300°
	5	+ 300°

Figure 33: The six stages of colour change in conodont elements (modified from Epstein et al., 1977).

5.2 Results

The abundance of body fossils in the Svartodden Mbr. is a characteristic feature compared to the rest of the Huk Fm. By far, the cephalopods dominate the main bedding surface at the Slemmestad IF arena locality, but also the scores of trace fossils tell us that the activity on the seafloor was extensive, during the deposition of the sediments. Other fossils observed in the Svartodden Mbr. are trilobites (that are mostly fragmented), gastropods and brachiopods. A more representative image of the diverse fauna embedded in the Svartodden Mbr. has been obtained, based on microfacies analysis. This section presents the recordings of fossils and data obtained by field investigations of the Svartodden Mbr. at the Slemmestad IF arena locality. An analysis of thin sections, microfacies and fossil content from the acid insoluble residue is also presented.

5.2.1 Field observations

Microstromatolites

Along the periphery of the canal-looking trace fossils on bedding surface 6 (see Figure 17 for stratigraphic level) one can see growth lamellar-like structures stained with a brown colour, probably oxidized crusty material (Figure 41). These structures have been identified as microstromatolites. Coherent microstromatolites can be traced several meters along the walls of the trace fossils, and the growth structures are similar on both sides of the canal walls, illustrated by Figure 41.

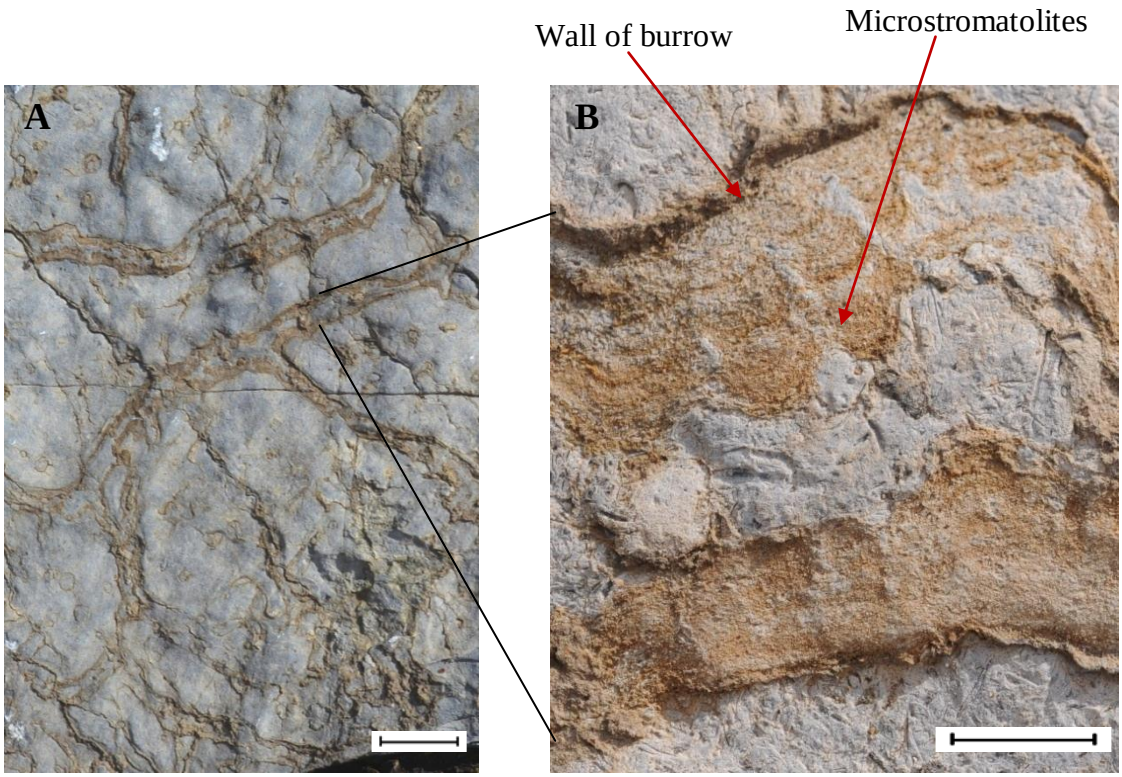

Figure 41: A. *Thalassinoides* (Type 1) trace fossils with microstromatolites near the tunnel peripheries. Scale bar = 10 cm. B. Close up view of growth like structures along the periphery of Type 1 trace fossils, identified as microstromatolites. Scale bar = 0.5 cm.

Microstromatolites which grew on the conchs of cephalopods are also present on bedding surface 6. These stromatolites are approximately 5 cm long, and up to 6 cm wide, growing from the conch-opening. Microstromatolites with a circular shape and possible concentric growth-films of oxidized material can also be encountered on bedding surface 6, such as Figure 42 below. Sizes range from approximately 4-7 cm in diameter. Dark coloured linings are visible on the inner circle of the microstromatolites.

Figure 42: Possible microstromatolites with a dark stained inner rim. Scale bar = 2 cm.

Brachiopods

A few complete brachiopod specimens are observed in outcrops of bed 1, as shown in Figure 43. These specimens are classified to belong in the genus *Porambonites,* based on descriptions by Spjeldnæs (1953). No brachiopod specimens were recorded in the overlying beds.

Figure 43: Specimen of the genus *Porambonites,* in bed 1. Scale bar = 0.5 cm.

Bryozoans

No bryozoans or ostracodes were identified during field studies of the unit.

Gastropods

Gastropods are not commonly present in the Svartodden Mbr. at the Slemmestad IF arena locality, and only one specimen has been observed during field studies.

Cephalopods

Species recorded in the Svartodden Mbr.

The vast numbers of fossil cephalopods from the longiconic orthoconic order Endoceratida found in the Svartodden Mbr. covering the Oslo Region, can also be traced eastwards to Sweden in the Huk Fm. equivalent Holen and Lanna Limestones, also known as the Vaginoceras Limestone. A cephalopod identification key (Appendix 1) was provided by Dr. B. Kröger, and was used to identify cephalopods in the Svartodden Mbr. Based on siphuncle and chamber morphology, the distinct species can be identified.

Coiled species of the order Tarphycerida, and species of Endocerida with straight shells, occur in the Svartodden Mbr. however, the orthocone nautiloid species *Proterovaginoceras incognitum* (Figure 44) dominate the rock by far. The observed straight species belonging to the order Endoceratida identified in the Svartodden Mbr. are the following: *Proterovaginoceras incognitum* and *Anthoceraas buchi* (formerly termed *Endoceras vaginatum*).

In the upper unit, bed 6, the following species from the order Tarphycerida were identified; *Holmiceras kjerulfi, Estoniceras ariense?, Estoniceras kundense, Estoniceras perforatum* and *Estoniceras imperfectum*. Only 11 specimens from the order Tarphycerida have been identified, some of the present in Figure 45. The following Table 2 shows the observed species and their stratigraphic and geographic distribution, while Figure 44 and 45 are photos of some of the identified species in the Svartodden Mbr.

Table 2: Cephalopod species recorded in the Svartodden Mbr. and their geographic and stratigraphic distribution (from Moore, 1964 and Kröger, 2012).

Straight/ coiled	Order	Species	Geographic extent	Stratigraphic distribution
Straight	Endocerida	*Proterovaginoceras incognitum* (previous name: *Endoceras belemnitiforme*)	Baltoscandia	M. Ord.
Straight	Endocerida	*Anthoceraas buchi* (previous name: *Endoceras vaginatum*)	Baltoscandia N. Am-NW. Australia-Sibiria	M. Ord
Straight	Tarphycerida	*Holmiceras kjerulfi*	Baltoscandia	M. Ord.
Coiled	Tarphycerida	*Estoniceras perforatum*	Baltoscandia	M. Ord.
Coiled	Tarphycerida	*Estoniceras kundense*	Baltoscandia	M. Ord.
Coiled	Tarphycerida	*Estoniceras imperfectum*	Baltoscandia	M. Ord.

Counting of the different cephalopod species was performed on 5 squares (2x2 m) on bedding surface 6, and on 3 squares on bedding surface 4. All the specimens were identified as *Proterovaginoceras incognitum* (Figure 44). The area studied on bedding surface 4 was smaller than that of bedding surface 6. No specimens of the order Tarphycerida have been observed on the bedding surfaces of bed 3 and 4.

Order: Endocerida

Figure 44: *Proterovaginoceras incognitum*

Order: Tarphycerida

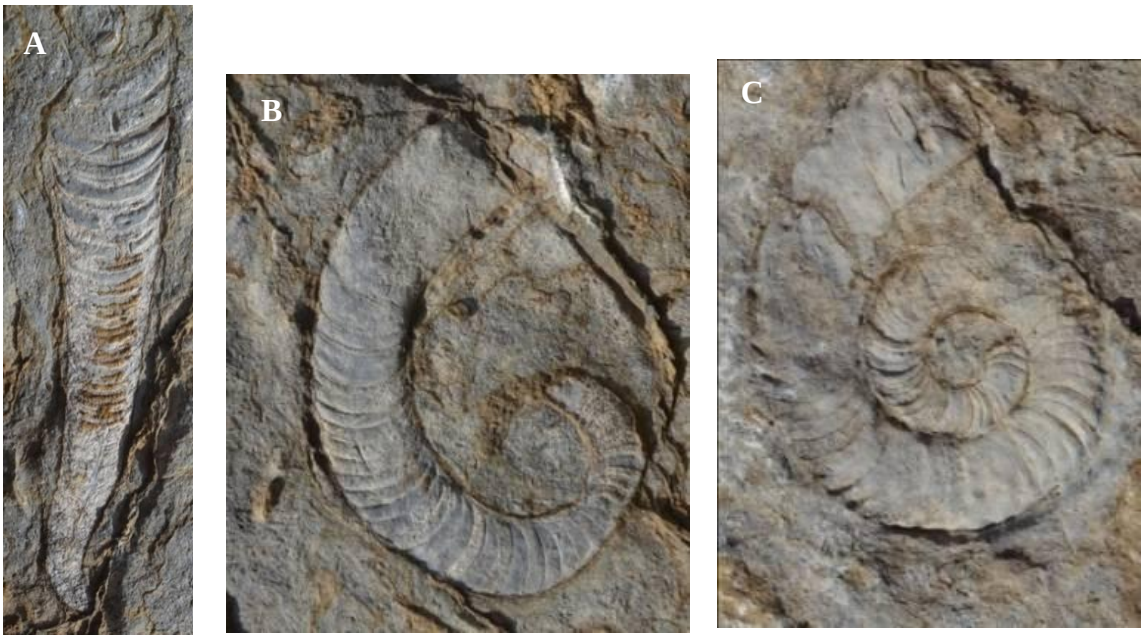

Figure 45: A: *Holmiceras kjerulfi* B: *Estoniceras ariense?* C: *Estoniceras imperfectum*

Cephalopod apex directions in palaeo-current studies

As previously discussed by Skaar (1972), the palaeo-current directions in the Svartodden Mbr. can be interpreted from preferred cephalopod orientations. Among others, Nagle (1967) established a theory based on experiments with orientations of straight shells that the apex of the cephalopod conchs would preferably orientate against the main current direction. However, broken cephalopod shells did apparently orientate with the apex downstream. Based on this, the orientations of cephalopod conchs were measured only on specimens longer than 30 cm. Palaeo-current reconstructions based on cephalopod orientations were performed on the uppermost bedding surface of the underlying Lysaker Mbr., on the bedding surface of bed 4 and on the bedding surface of bed 6, of the Svartodden Mbr., see Figure 17 for stratigraphic levels. The paleontological statistics software PAST (Hammer et al., 2001) was used in the preparation of rose diagrams, presented in Figure 46 below. The continental rotation of Baltica since the Middle Ordovician may implicate the recorded palaeo current directions.

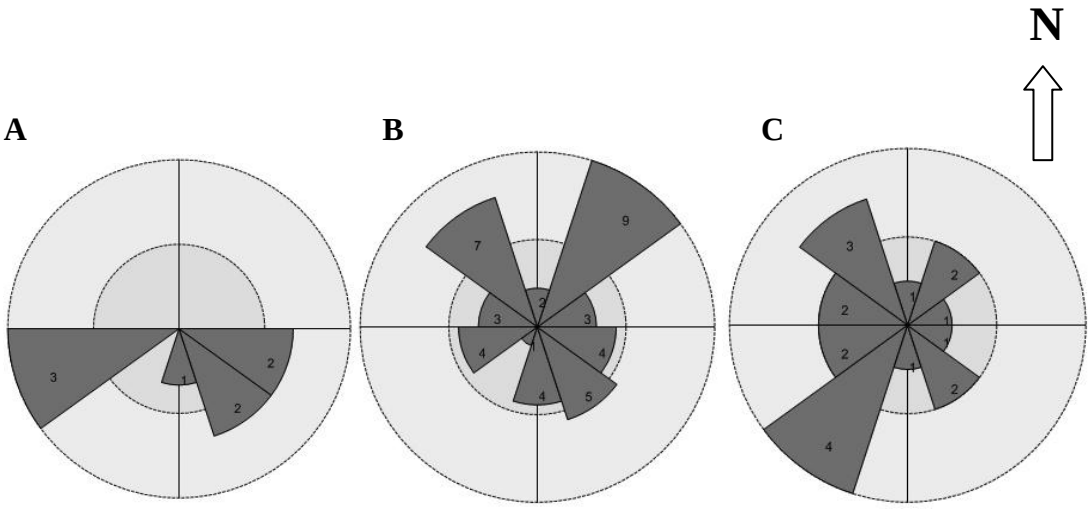

Figure 46: Rose diagrams of apex directions on cephalopod shells on A: the uppermost bedding surface of the Lysaker Mbr., B: Bedding surface 4 of the Svartodden Mbr., C: Bedding surface 6 of the Svartodden Mbr.

Several peculiar patterns of cephalopod assemblages on the bedding surfaces 4 and 6 were encountered. One example is a star-shaped pattern (Figure 47).

Figure 47: Star-shaped conch accumulation on bedding surface 4. Scale bar = 5 cm.

Siphuncle orientations in vertical section

According to Reyment (1968), the orientation of the siphuncle in orthoconic nautiloids, can be used as an indicator of rolling action by swash currents after the conchs have stranded. Conchs positioned with the siphuncle located underneath the shell (at the 270° resting position), were probably buried in quiet conditions on the seafloor, compared to rolling conchs where the siphuncle orientation deviates from the normal resting position (Reyment, 1968). Based on observations, the cephalopod siphuncles in vertical section in Slemmestad show an average orientation of 270°, on the resting side of the cephalopod (Figure 48).

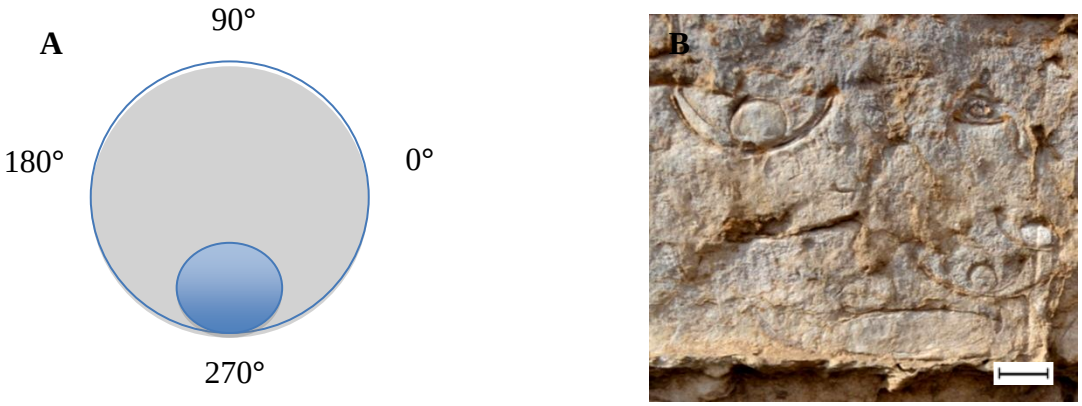

Figure 48: A: Siphuncle positions B: Conchs in vertical section of bed 6. Scale bar = 1 cm

Vertically imbedded conchs

Calcite-mineralized circles of unknown affinity are a common feature on bedding surface 6 of the Svartodden Mbr. (Figure 49). Approximately 100 specimens have been observed. Diameters of the circles range from 3-15 cm. The walls are approximately 0.5 cm thick. The rims of the shapes are often black in colour (Figure 50). One specimen was collected, and was cut and polished, in order to identify the depth of the walls. The cut and polished sample of the calcite ring shows that the diameter of the ring increased 0.5 cm down into the rock. In vertical view, the shape appears as a bottleneck as illustrated in Figure 49 C.

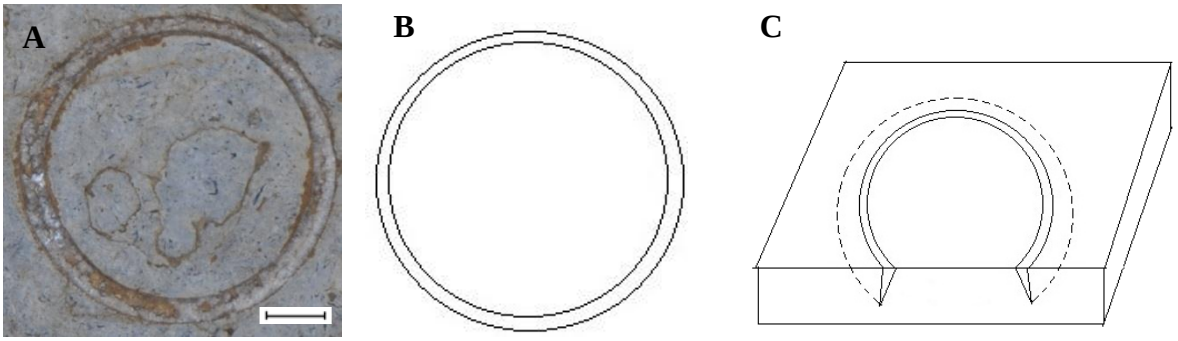

Figure 49: A: Field photo of calcite ring. B: Drawing of collected specimen C: Cut specimen with dashed line indicating vertical extension. Scale bar = 1 cm

At the Bjerkåsholmen locality, the circles have a positive relief of approximately 1 cm above the bedding surface. The walls are black in colour (Figure 50).

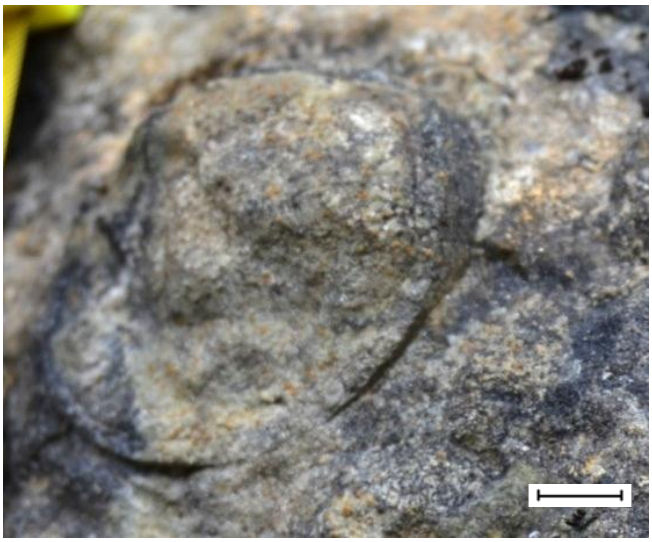

Figure 50: Specimen from Bjerkåsholmen with positive relief. Scale bar = 1 cm.

Trilobites

Fragments of thin trilobite exoskeletons are common features in the Svartodden Mbr., and appear black in colour (Figure 51). Compared to the many complete trilobites in the underlying Lysaker Mbr., the Svartodden Mbr. shows few trilobite specimens that are fully preserved.

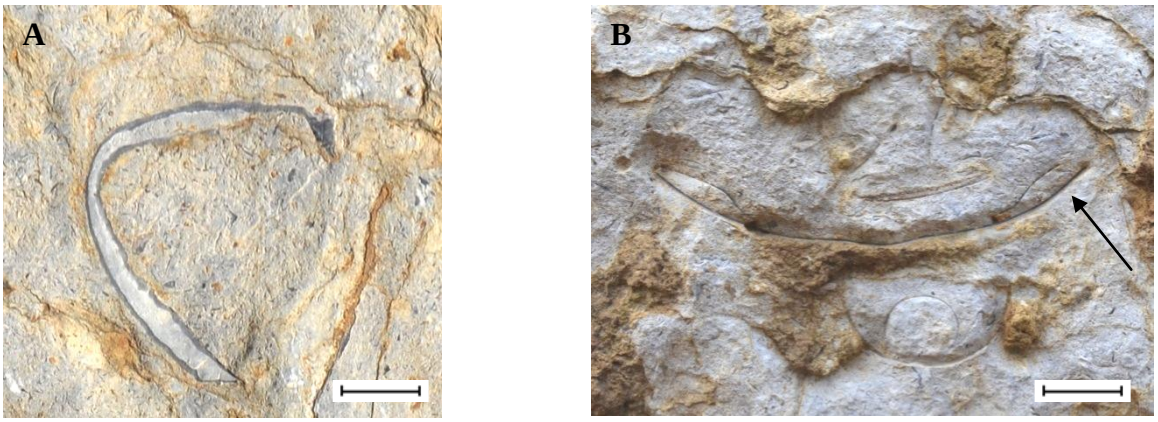

Figure 51: A: Possible pygydium segment in oblique longitudinal section. B: Black coloured possible thorax segment in in cross section. Scale bars = 1 cm.

On bedding surface 6, a possible trilobite imprint with a spiny looking outline (Figure 52) is observed. The specimen is 5 cm long and 2.5 cm wide. Its rim consists of a dark material, similar to that of trilobites.

Figure 52: The possible outline of a trilobite on bedding surface 6. Scale bar = 1 cm

Ostracodes, echinoderms and conodonts

No ostracodes, echinoderms or conodonts were identified during field studies of the unit.

Trace fossils

Trace fossils in the Svartodden Mbr. can be recognized both from field observations, slabs and observations from thin section analysis. The trace fossils are regarded as the only elements which for certain are preserved *in situ*. The field recordings will here be described in detail.

Both horizontal and vertical trace fossils are visible on the bedding surfaces of the Svartodden Mbr. (Figure 53 and 56). Two different sets of horizontal endogenic burrows are identifiable on bedding surface 4 and 6, and are named Type 1 and Type 2 trace fossils for convenience.

Figure 53: Type 1, *Thalassinoides* trace fossils on bedding surface 6. Scale bar = 10 cm.

Type 1 trace fossils comprise 2-5 cm wide canals, continuous and branching, stretching continuously over several m^2 across the bedding surface (Figure 53). The branching patterns are in some areas showing Y- and T- shaped patterns, with partly larger interconnecting chambers in junctions. The traces are distinguished from the surrounding, grey limestone by a positive relief, having a brown and oxidized appearance. In certain areas of bedding surface 4

and 6, an enrichment of dark mud fills the burrows in the limestone. Here the trace fossils are more visible, as they appear in a 3D network. Branched canals are also visible. Wall linings are present, approximately 2 mm thick. The Type 1 trace fossils are tentatively identified as *Thalassinoides* isp.

Type 2 trace fossils are maze-like, often appear as tunnels, or elongated paths on the bedding surface. They are thinner than Type 1 trace fossils, with diameters of approximately 2 cm or less. They extend horizontally on the bedding surface approximately 10-20 cm, and show varying branching angles (Figure 54). They are brown in colour probably caused by oxidation of the tunnel-infills, and consist of fine-grained material. The trace fossils have an epirelief of approximately 0.5 cm. This trace fossil is identified as *Thalassinoides bacae* (Ekdale & Bromley, 2003). The tunnels often appear alongside the eroded cephalopod conchs.

Figure 54: Type 2, *Thalassinoides bacae* trace fossils on bedding surface 6. Scale bar = 5 cm.

The trace fossils are accompanied by closely spaced vertical, short shafts, appearing as burrow openings (Figure 55) of *Thallasinoides bacae*. The vertical burrow openings are abundant on bedding surface 6, seen as circular shapes of brown colour (Figure 55 A) on the horizontal plane, contrasting with the light yellow colour of the surrounding limestone on

weathered surfaces. The burrows have a positive epirelief in horizontal view on weathered bedding surfaces. Sizes range from 1- 2.5 cm in diameter. Depth of the burrows extends approximately 3 cm down into the substrate. The rims of the burrows are enriched in pyrite, as seen in Figure 55 B. No sampled specimens of the burrows cut skeletal fragments, i.e. they can be regarded as burrows in a semi lithified substrate, and not borings. In vertical section, vertical burrows may bend and appear horizontally along bedding planes (Figure 55 D). A circular "tunnel" can be seen in Figure 55 C. The peripheries of the burrows are covered with abundant cube shaped pyrite crystals.

Determining the ichnological identify of the burrows presented in Figure 55 below is complicated, but the trace fossils are believed to represent *Thalassinoides bacae* burrows.

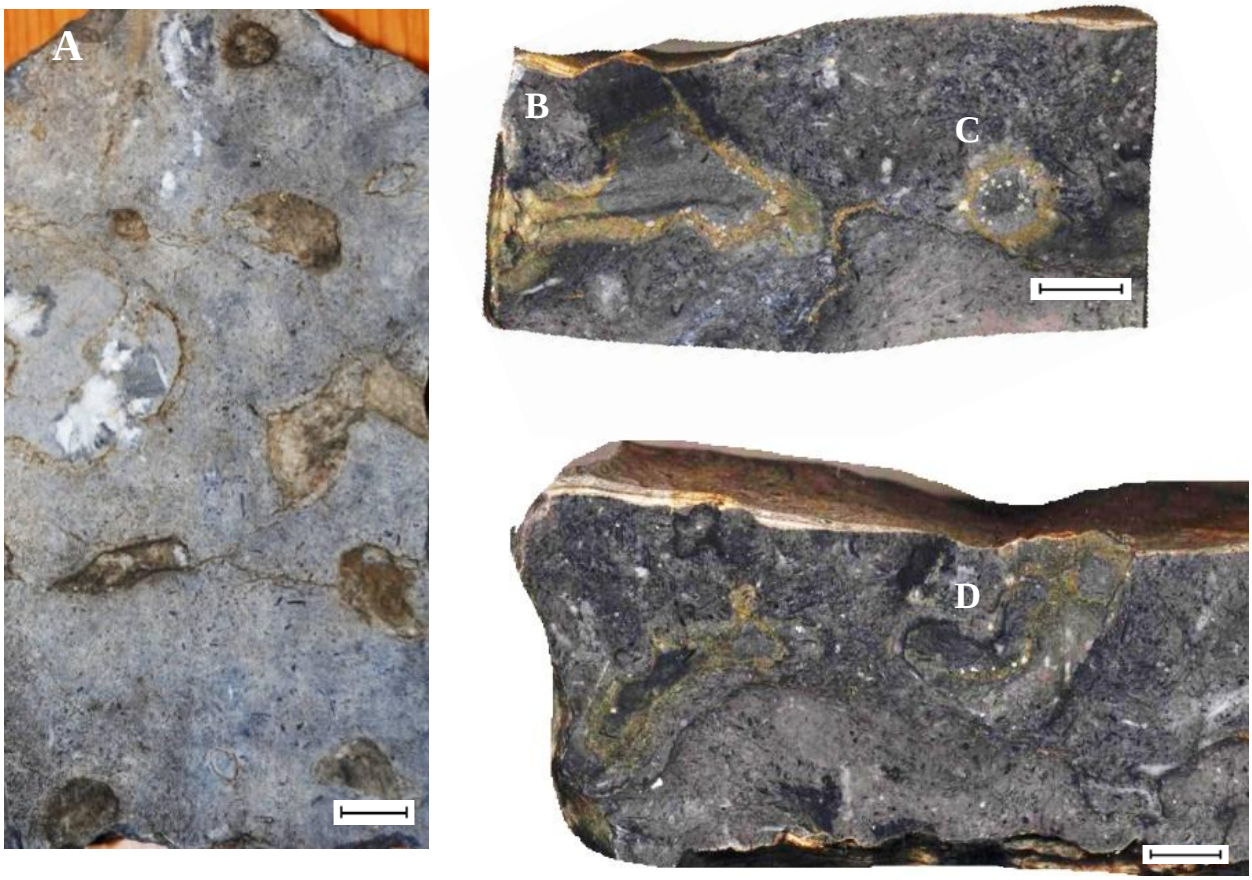

Figure 55: A. *Thalassinoides bacae* in horizontal view, the traces appear as circular and elongated.
B. Vertical *Thalassinoides bacae* which bends (PMO 221.626).
C. Horizontal tunnel, identified as *Thalassinoides bacae* (PMO 221.625).
D.Cross section of a turning tunnel of *Thalassinoides bacae* (PMO 221.622).
Scale bars = 1 cm.

The fine grained material infill of *Thalassinoides bacae* in Figure 55 B is laminated with darker silty material. The upper infill of the trace fossil in Figure 55 B is very fine grained and dark coloured, and could possibly represent phosphate. Thin sections were prepared from the vertical burrows of *Thalassinoides bacae*, and subsequently analysed with a microscope. Any borings cutting through bed boundaries could indicate hardgrounds, however no such borings were found. Borings that cut skeletal material have only been identified in thin sections. Elongated tunnel shapes, as seen in Figure 55 are also associated with the *Thalassinoides bacae* trace making organisms.

In vertical section, thin laminae of brown oxidized crusts form ragged, horizontal lines, each line traceable approximately 50 m (the entire length of the outcrop). Vertical *Skolithos* burrows are filled with brownish material visible along the horizontal lines (Figure 56).

Figure 56: Vertical trace fossils filled with brown coloured material along bed boundaries. The trace fossils are identified as *Skolithos*. Scale bar = 10 cm.

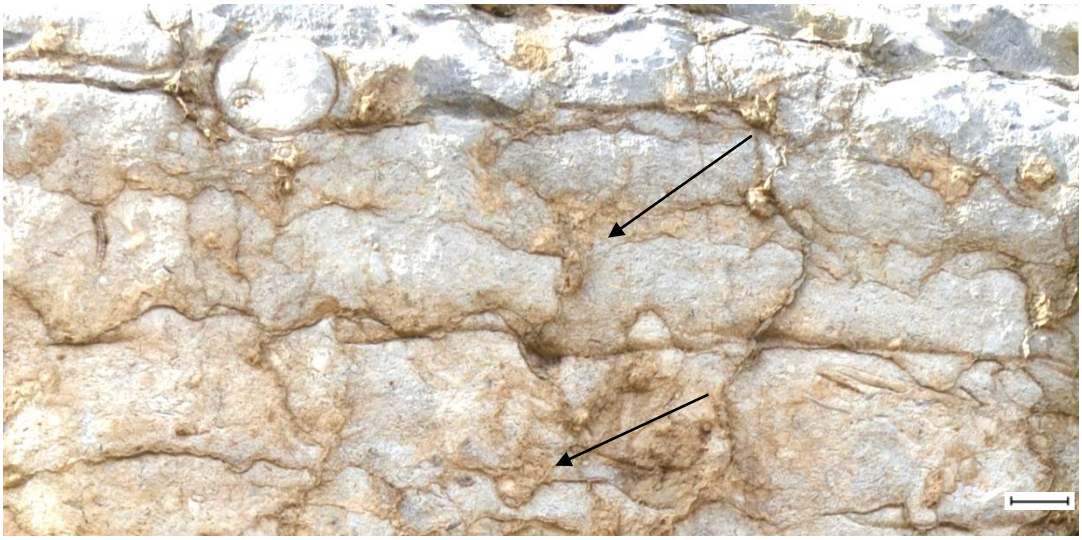

Figure 57: Close up view of bedding parallel trace fossils in vertical section of bed 6, several identified as truncated *Skolithos* traces. Scale bar = 2 cm.

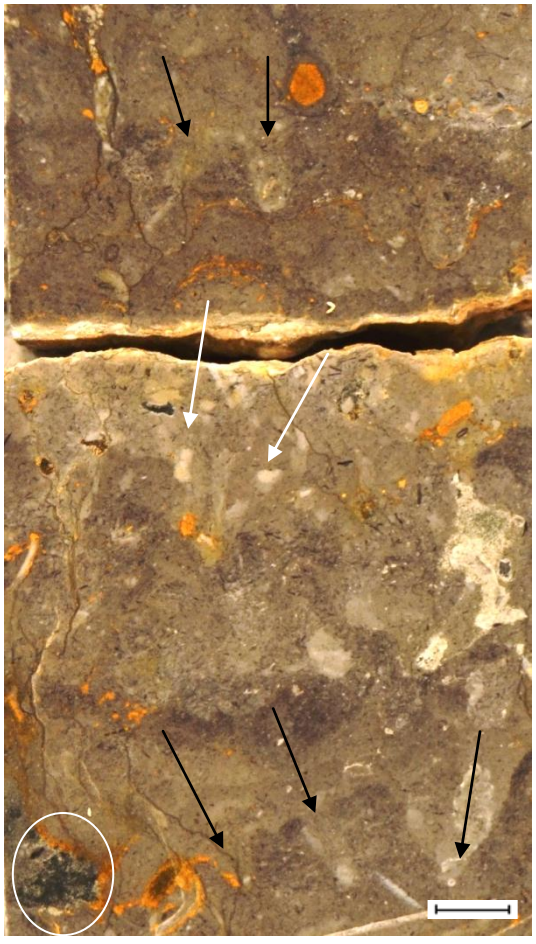

In Figure 58 of the polished core, several borings indicate boundaries of lithological contrasts. The *Skolithos* burrows, being 2-3 cm long, have penetrated into darker material, indicated by the black arrows in the figure. They are also jagged and irregular. In Figure 58, three stages of borings are present. The observed borings are present in bed 5, in the interval 135-145 cm from base of the core (see Figure for stratigraphic level).

White coloured, mm-sized borings occur frequent in the middle section of the photo, marked by the white arrows. A dark area, approximately 1 cm in diameter is present in the left corner of Figure 58 (shown in the white circle), and might represent phosphate due to its dark colour.

Figure 58: Polished slab with *Skolithos* as pre-omission burrows, filled with sediment shown by the arrows. Scale bar = 1 cm.

5.2.2 Microfacies

21 thin sections from intervals of the artificial core were analysed with a petrographic microscope, by point counting. Plane- and cross-polarized light were used to distinguish between fossil groups, e.g. by single cell extinction with polarized light in echinoderms. 300 counts in each thin section were recorded. Skeletal grains from the following groups were identified and counted (in relative decreasing order of abundance): ostracodes, echinoderms, trilobites, brachiopods, bryozoans and cephalopods. More detailed taxonomic identifications have not been done, except from identification on phyla-level of bryozoans. A few, possible observations of conodonts were assigned to unidentifiable grains. No faecal pellets, intraclasts or ooids were identified in the thin sections.

The results from the point counting are presented in Figure 59, followed by a short description of observations from the point counting analysis.

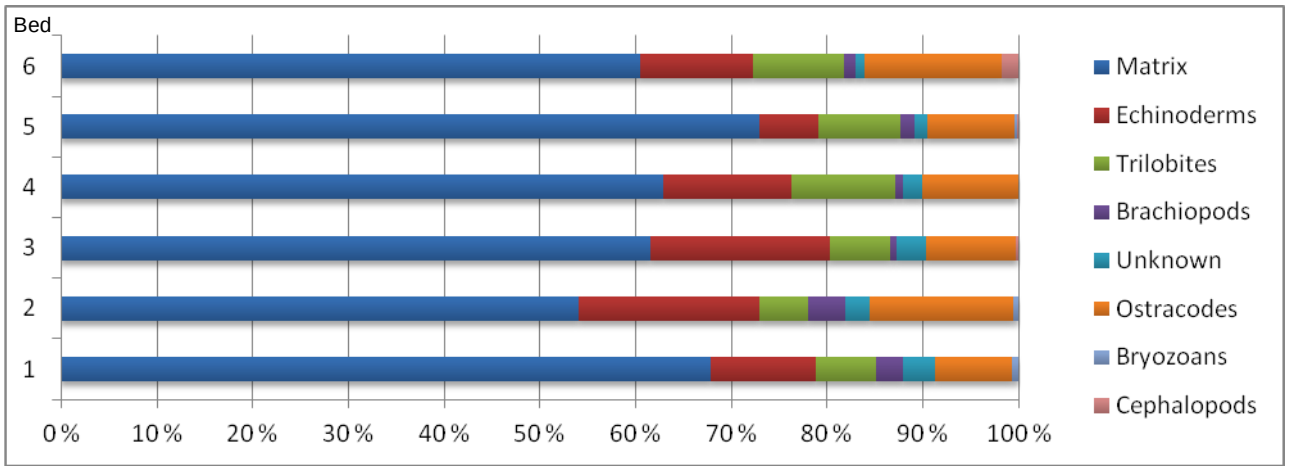

Figure 59: Amount in percentage of matrix, skeletal groups and unidentified skeletal grains in bed 1-6 of the Svartodden Mbr.

Matrix

The rock matrix in the Svartodden Mbr. consists of micritic sediment and clay particles concentrated as stylolites. The matrix content is approximately 60 % but increases in bed 5 and 6 towards an average of 70%. Matrix infill in the conchs of cephalopods is common.

Brachiopods

Brachiopod shell appearance in thin section often show a foliated lamellar structure, as seen in

Figure 60. The high content of brachiopod shell fragments in bed 1 and 2 gives a good correlation with the previously discussed ”*Porambonites* bed” in the lowermost part of the Svartodden Mbr., originally described by Brögger (1882). Various shell structures in brachiopods are observed, including impunctate shells devoid of pores (eg. PMO 221.485).

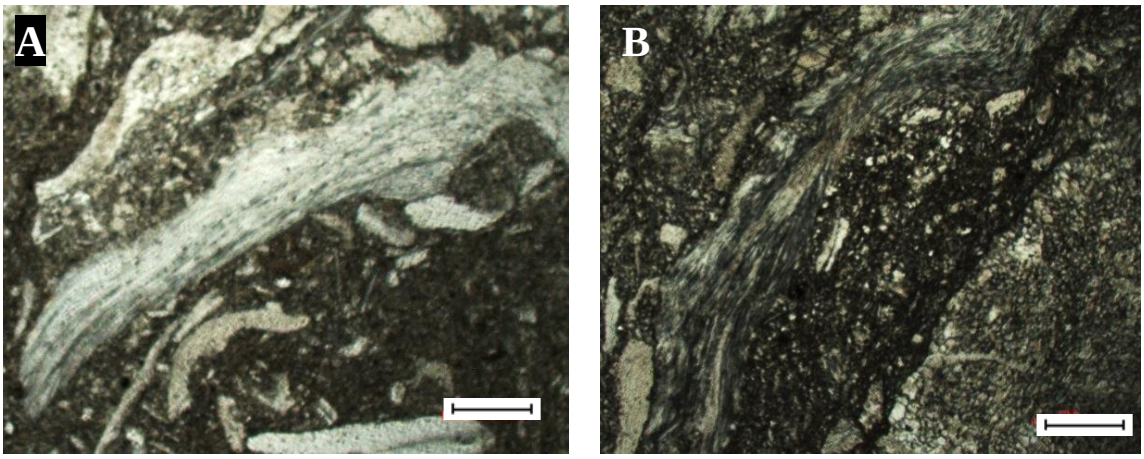

Figure 60: Impunctate brachiopod skeletal fragments in thin section. A. PMO 221.481. B. PMO 221.468. Scale bars = 50 µm.

Bryozoans

This group appears randomly with few fragments throughout the section. Sizes of colonies and fragments range from 50-150 µm in diameter. Specimens from the orders Cryptostomida, Cystoporida and Trepostomida were discovered in thin sections by Dr. Andrej Ernst, Albrecht Universität zur Kiel. The observed genera are the following; *Moyerella* (PMO 221.469), *Chasmotopora* (PMO 221.472) and *Moorephylloporina* (PMO 221.490).

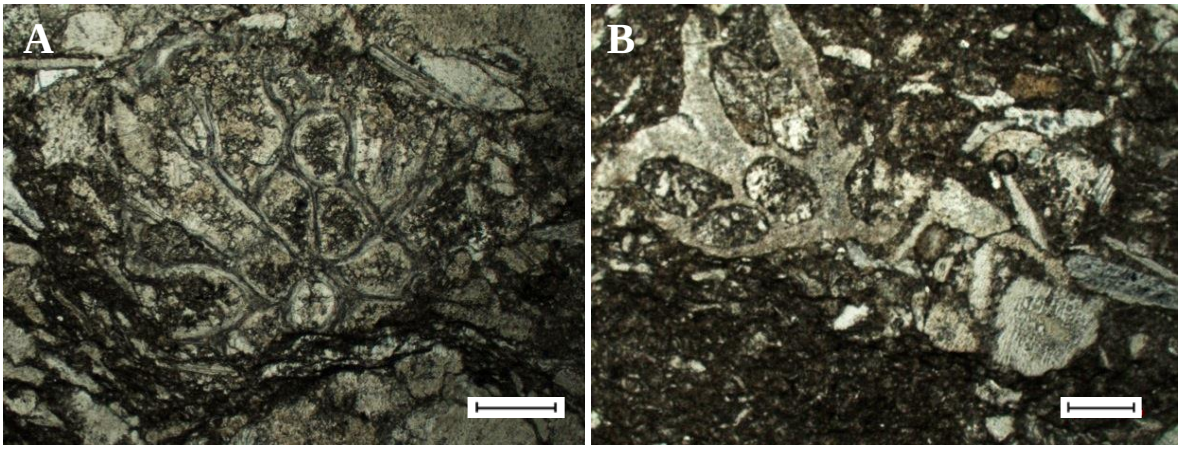

Figure 61: Bryozoans in thin section. A. PMO 221.467. B. PMO 221.469. Scale bars = 50 µm.

Gastropods

Two gastropod specimens were observed in thin sections PMO 221.478 and PMO 221.482. These were not identified on a higher taxonomic level.

Cephalopods

Cephalopod conchs observed in thin section show a primary aragonitic mineralogy which subsequently has been altered and recrystallized by calcite (see also Chapter 6). The dissolution of conchs is illustrated in Figure 62, where more than half of the conch has corroded, marked by the abrupt transition from grey to black matrix. Several conchs also show completely cement filled siphuncles. No disarticulated fragments from cephalopod conchs were identified in thin section. The conchs are filled with sediment, with the same grain types as the surrounding matrix. Figure 62 also shows a stylolite (pressure solution seam), vertically cutting through the cemented siphuncle. The dark lamina shown in the upper part of the thin section, are horizontal stylolites.

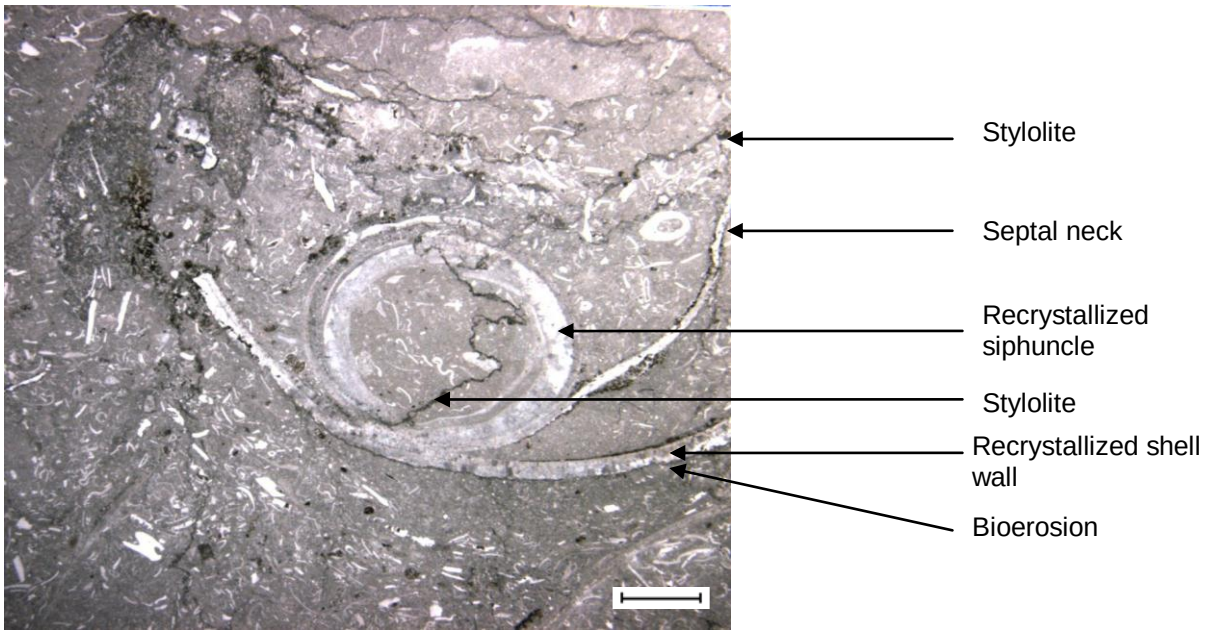

Figure 62: Dissolution, cementation and stylolitization of a cephalopod conch (PMO 221.483). Scale bar = 0.4 cm.

Trilobites

In thin section, this group displays an undulating light extinction, and fragments have a ´sheperd's hook´ shape (Figure 63). The abundance of trilobite fragments increases through bed 1-4, and shows a lower abundance in bed 5 and 6.

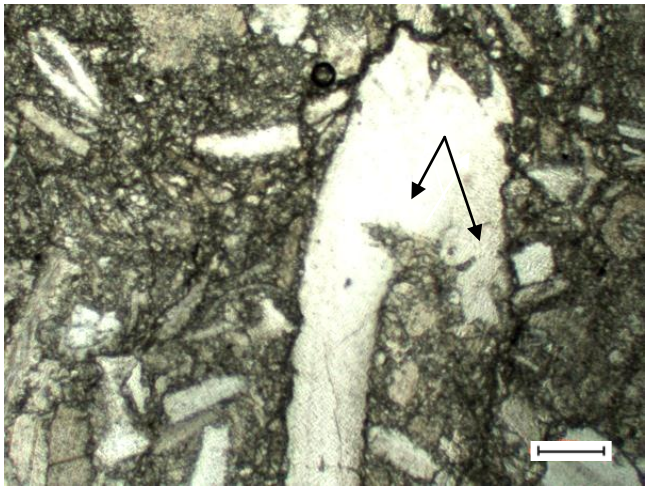

Figure 63: Trilobite fragment in thin section, with micro-borings (arrows). PMO 221.466. Scale bar = 50 µm.

Ostracodes

Ostracodes in thin section show the same light extinction in crossed polarized light as trilobites, although fragments are most often smaller in size. Sizes range from 50 to 150 µm, and the group is present in thin sections through the entire unit. Their carapaces show minor bioerosion and possible *Trypanites* borings, as shown in Figure 64. The group constitutes approximately 3-18 percent of the bioclasts.

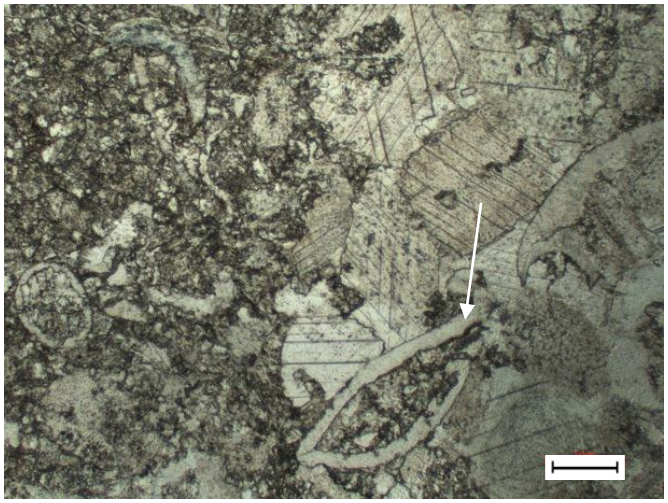

Figure 64: Ostracode valves in thin section, marked with arrow. PMO 221.472 Scale bar = 50 µm.

Echinoderms

Crinoid grains represent the most dominant group of echinoderms in the analysed samples, and fragments are exemplified below in Figure 65. Echinoderms are great sediment contributors in the unit, representing 10 – 20 % of the skeletal grains.

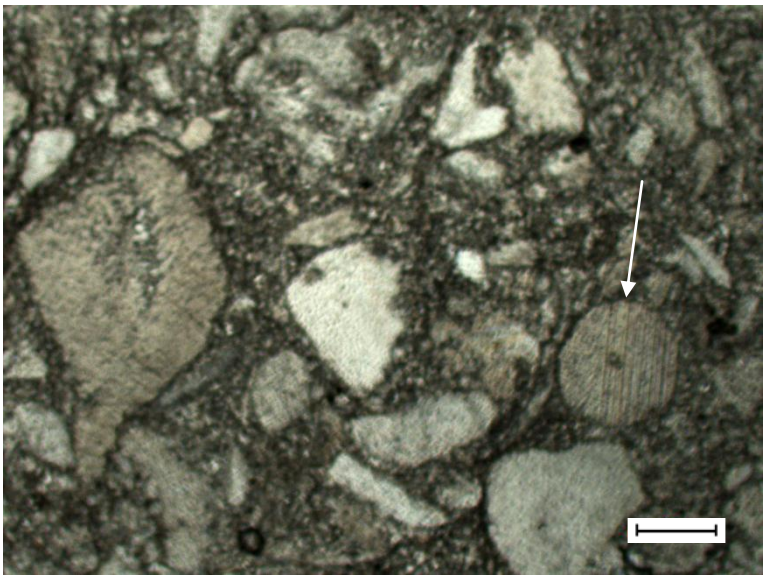

Figure 65: Crinoid fragment (arrow). PMO 221.472. Scale bar = 50 µm.

5.2.3 Acid insoluble residue

Microfossils obtained from the Svartodden Mbr. are the groups found in the acetic acid insoluble residue, such as ostracodes, inarticulate brachiopods and conodonts. See Chapter 4 for the method used. Table 1 summarizes the groups of fossils and their abundance, identified from the acid insoluble residue. No glauconitic grains were identified in the samples. The fossil abundance in the samples is divided in low, medium and high, where low corresponds to 1-5 specimens, medium corresponds to 6-10 specimens and high corresponds to 11 or more specimens.

Table 1: Statistics from the insoluble acid residue of sample SL1+2, SL3+4 and SL5+6.

Sample	Weight (kg)		INSOLUBLE SAMPLE RESIDUE							
		Weight (g)	Dolo-mite	Pyrite	Quartz	Fossil abundance			Conodont elements	Other fossils
						low	medium	high		
SL5+6	1,5	61	X	X	X			X	150	Ostracodes, inarticulate brachiopods
SL3+4	1,5	47	X	X	X			X	181	Ostracodes, inarticulate brachiopods, crinoids
SL1+2	1,5	46	X	X	X			X	111	Ostracodes, inarticulate brachiopods, crinoids

Bioclasts of uncertain biological affinity

Unidentifiable objects picked from the acid insoluble residue were investigated with a SEM. Elemental composition of the specimens presented in Figure 34 below are presented in Appendix 6. The specimens PMO 224.360/B and PMO 224.360/C are calcium phosphatic. Similar skeletal grains to B and C presented in Figure 34 are present in all samples of the acid insoluble residue.

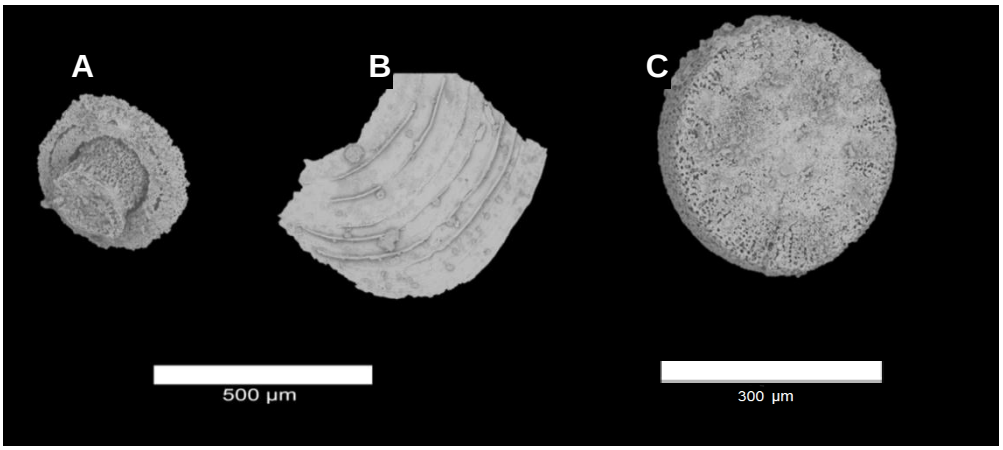

Figure 34: Bioclasts in the acid insoluble residue. A. Unidentified, PMO 224.360/A. B. Possible brachiopod grain, PMO 224.360/B. C. Possible crinoid grain, PMO 224.360/C.

Inarticulate brachiopods

Four specimens of inarticulate phosphatic brachiopods, measuring approximately 0.5 mm long, were studied and photographed with the SEM (Figure 35). Taxonomic identifications were based on the works by Holmer (1989) who identified phosphatic brachiopods of the order Acrotretida in the Lanna Fm. and Holen Fm. of Sweden. Bad preservation of the valves causes some uncertainty regarding the taxonomic identifications. Inarticualated brachiopods are not present in sample SL1+2 (see stratigraphic level in Figure 17).

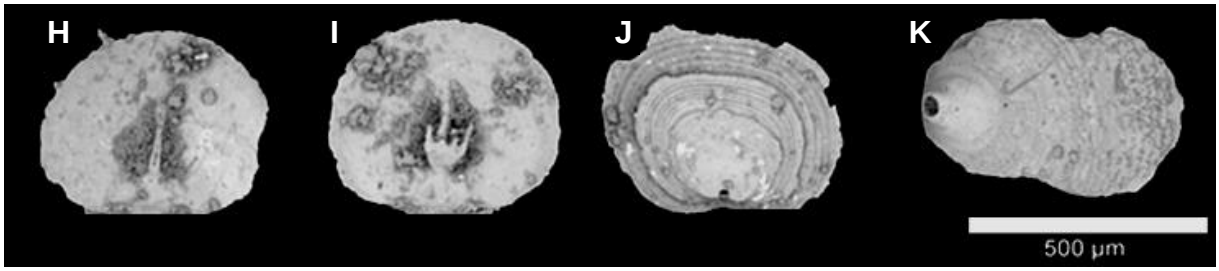

Figure 35: Suggested taxonomic identifications of acrotretid brachiopods. H. *Conotreta* (PMO 224.360/H). I. *Conotreta* (PMO 224.360/I). J. *Myotreta* (PMO224.360/J). K. *Biernata* (PMO224.360/K).

Ostracodes

Due their relatively small size and dark colour, ostracodes are not easily recognized in the field. However, in the acid insoluble residue, ostracodes were present due to phosphatization of the shells. The ostracode valves were picked and analysed in a scanning electron microscope. The specimens measure approximately 0.5 mm, possibly showing muscle scars and dimorphism (Figure 36). Based on studies of ostracodes from the Huk Fm. equivalent Lanna Fm. and Holen Fm. in Sweden (Tinn & Meidla, 2001), the specimens could, however not be identified. Ostracodes have been recorded in all of the samples.

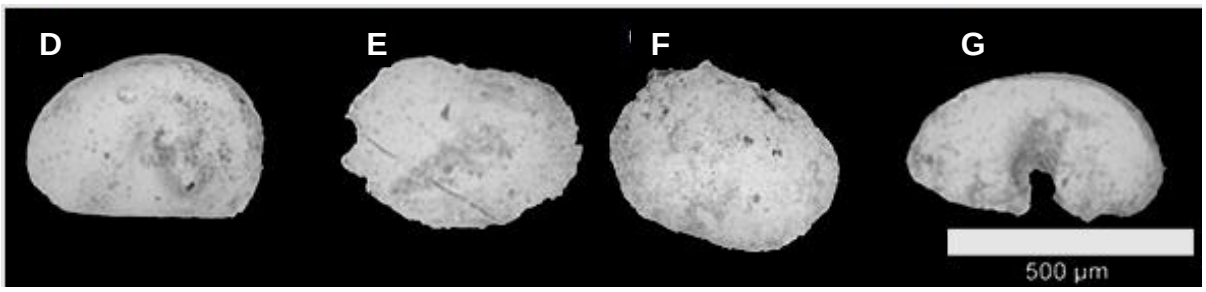

Figure 36: Unidentified ostracod specimens from the acid insoluble residue. D. PMO224.360/D. E. PMO224.360/E. F. PMO224.360/F. G. PMO224.360/G.

CAI and conodonts

In the present study, three stratigraphic levels comprising the whole Svartodden Mbr. were analysed with the purpose of finding conodonts. The conodont species in the three sampled units (SL1+2, SL3+4 and SL5+6) were picked from the heavy mineral separated samples. More than 400 conodont elements were counted in the acid insoluble residue, of the Svartodden Mbr. The extracted conodonts have a colour alteration of CAI 4, illustrated in Figure 37 below.

Figure 37: Colour photos of preparated conodonts, showing a CAI of 4.

Due to the limited extent of this master thesis, a systematic taxonomic identification was only performed on a few well preserved conodonts. The different conodont species were identified, in order to deduce the same conodont biozone as of that presented in Rasmussen (1991). Most of the conodont specimens in Figure 38 and Figure 40 were identified by Dr. Jan Audun Rasmussen from the University of Copenhagen. A few of the specimens in Figure 39 were identified based on taxonomic descriptions in Löfgren (2000; 2003; 2004) and Rasmussen (1991; 2001).

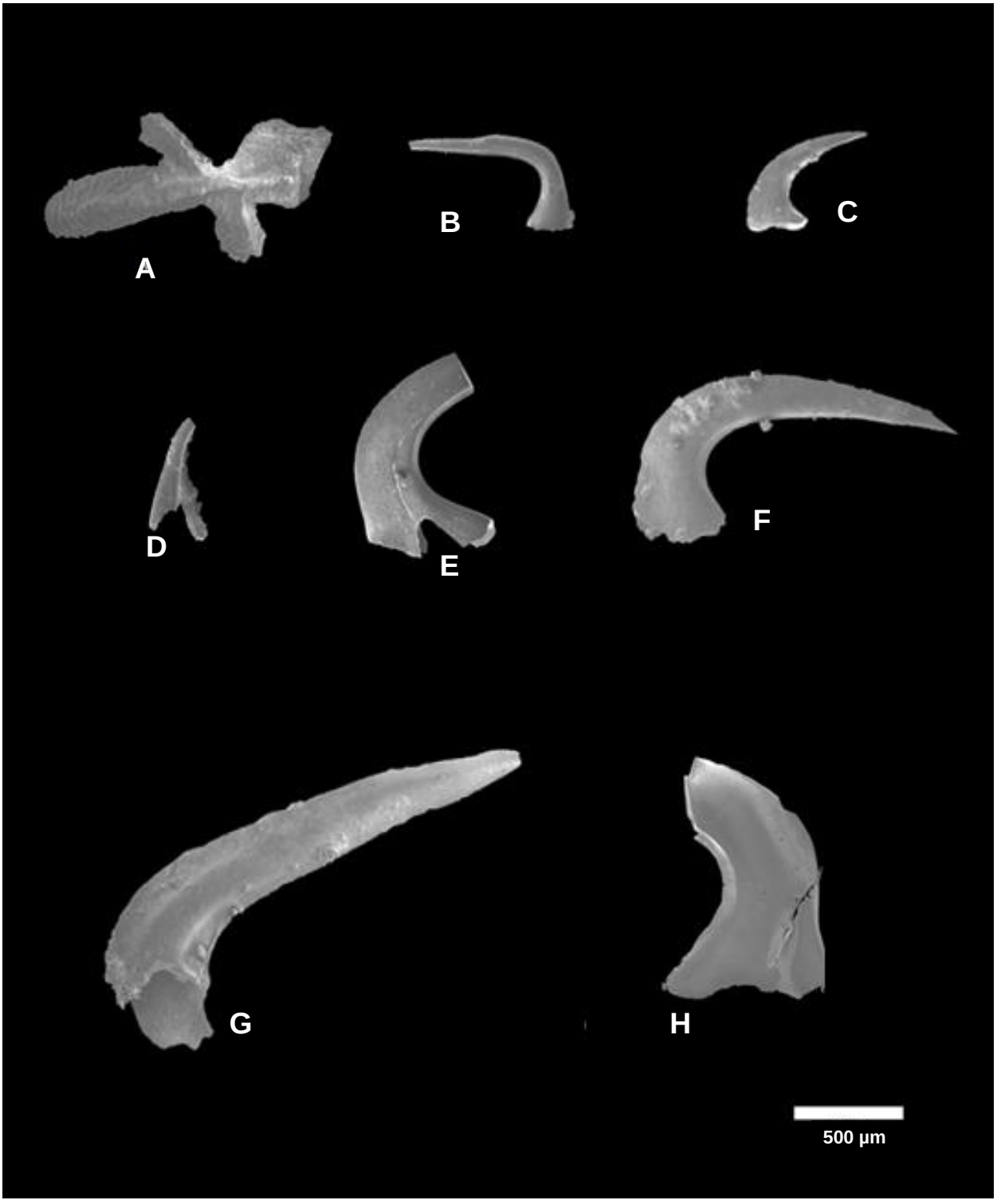

Figure 38: Specimens from sample SL 1+2.
A: *Dzikodus hunanensis*, PMO 224.363/A.
B: *Semiacontiodus cornuformis*, PMO 224.363/B.
C: *Drepanoistodus* sp, PMO 224.363/C.
D: *Baltoniodus medius*, PMO 224.363/D.
E: *Drepanodus arcuatus*, PMO 224.363/E.
F: *Drepanodus arcuatus*, PMO 224.363/F.
G: *Drepanodus* sp, PMO 224.363/G.
H: *Drepanodus planus*, PMO 224.363/H.

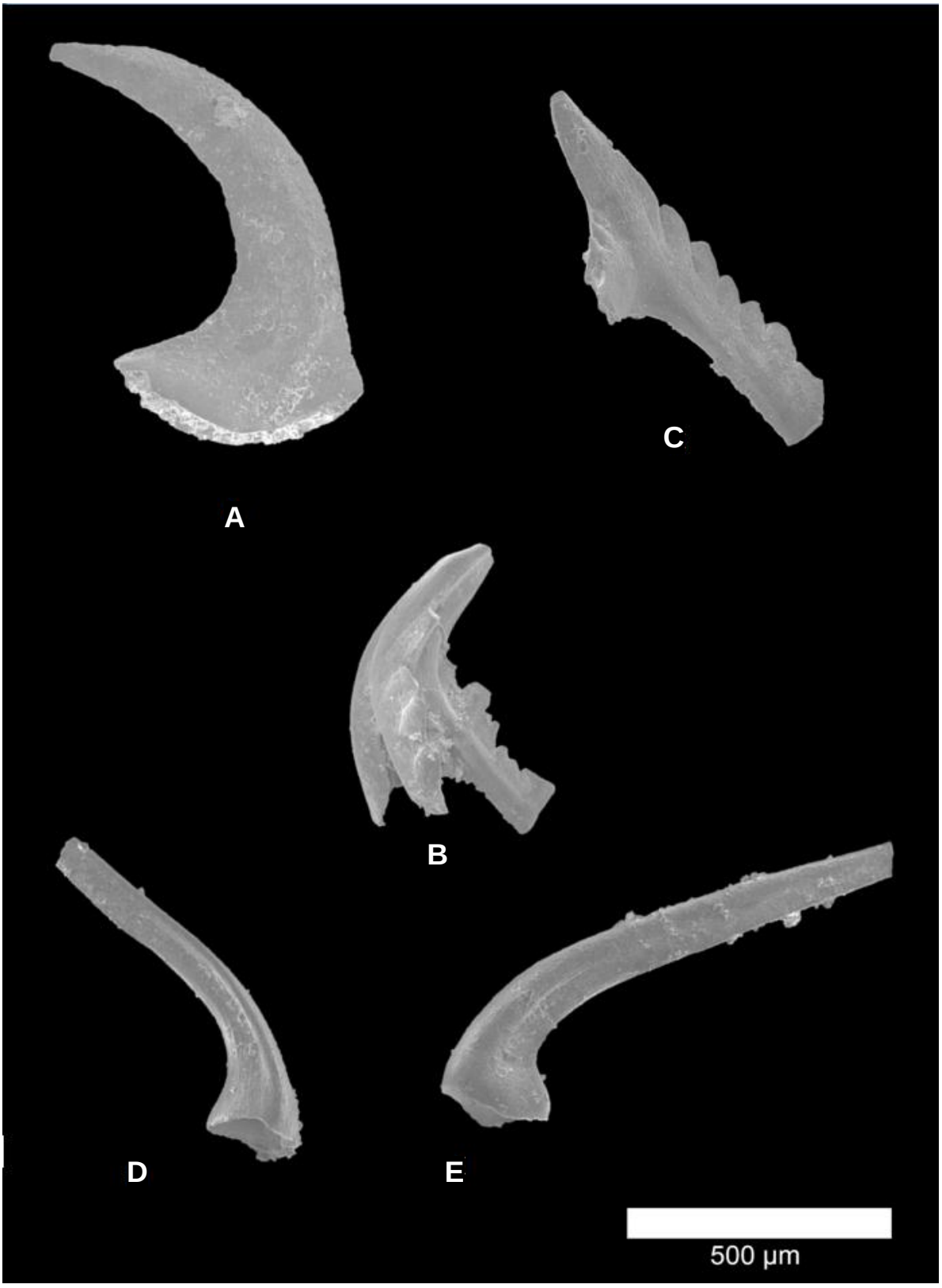

Figure 39: Specimens from sample SL 3+4
A: not identified, PMO 224.362/A. B: *Polonodus* ? cf. *tablepointensis*, PMO 224.362/B.
C: not identified, PMO 224.362/C. D: *Semicontiodus corniformis*, PMO224.362/D.
E: *Semicontiodus corniformis,* PMO 224.362/E.

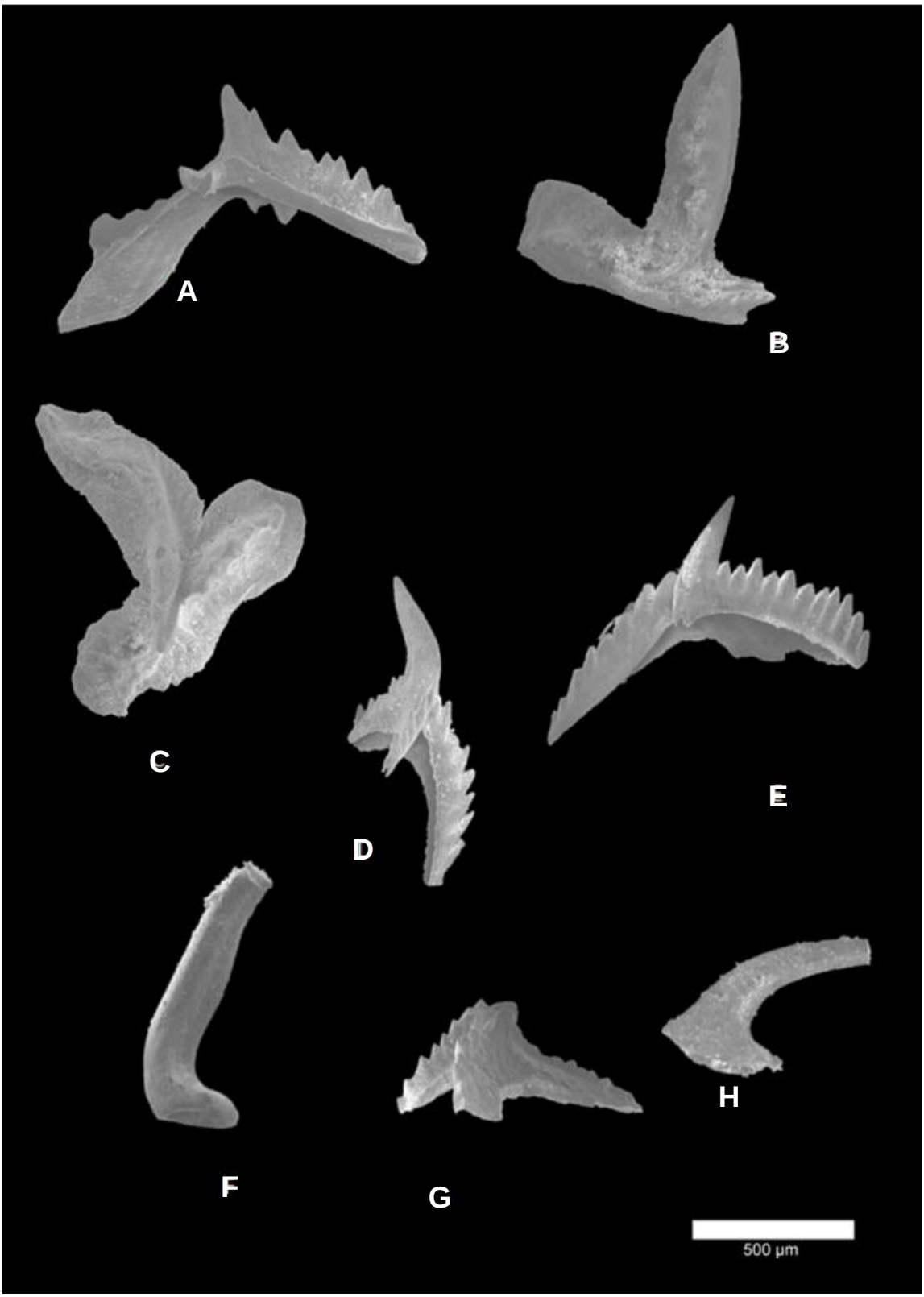

Figure 40: Specimens from sample SL 5+6.
A: *Baltoniodus medius*, PMO 224.361/A. B: *Yangtzeplacognathus crassus*, PMO 224.361/B.
C:*Polonodus clivosus*, PMO224.361/C. D: *Baltoniodus medius*, PMO224.361/D.
E: *Baltoniodus medius*, PMO224.361/E. F: *Semiacontiodus cornuformis*, PMO 224.361/F.
G: *Lenodus cf. variabilis*, PMO224.361/G. H: *Drepanodus arcuatus*, PMO224.361/H.

5.3 Discussion

Based on literature studies, field observations, microfacies and acid insoluble residue, a discussion of the results above follows here.

5.3.1 Micrite

The fine grained carbonate matrix surrounding skeletal fragments in the Svartodden Mbr. is regarded as micrite. Fragments smaller than 0.03 mm have been identified as micrite, based on the classification of Dunham (1962). According to Flügel (2004), the carbonate mud produced on ancient carbonate platforms is believed to have formed during inorganic precipitation. However Pratt (2001) discusses the origin of Lower Palaeozoic lime mud to have formed from the decomposition of the cyanobacterium *Girvanella*. The lithification of these minute particles of algae was caused by cementation and neomorphism, changing the primary composition into low-Mg calcite, removing any traces of original texture. Hence, the mud became a microcrystalline mosaic of micrite (Pratt, 2001). Previously suggested sources of micrite are the disintegration of shells and algal bioclasts by bioerosion, spontaneous whitings from calcification of organic matter and suspended picoplankton, as well as mineralizing marine organisms (Pratt, 2001). Submarine eroded material causing winnowing of the sediment surface is also presented as a possible contributor of micrite (Flügel, 2004). The micrites observed in thin sections of the Svartodden Mbr. are identified as allomicrites; described by Flügel (2004) as to have originated from destroyed invertebrate skeletons and algae, calcareous plankton, bioerosion and eroded carbonates.

5.3.2 Microbial mats and microstromatolites

The intricate brown coloured patterns on the peripheries of the inferred trilobite tunnels on bedding surface 6 are believed to be the remnants of microstromatolites – fossilized layers of microbial mats formed by authigenic phosphatization on the seafloor. Chacón & Martín-Chivelet (2008) described phosphatic stromatolites from the Palaeocene in Spain, and associates these with hardground events and submarine hiatuses in pelagic environments. The stromatolites studied in Spain are believed to have grown in open marine settings, at the

sediment-water interface, while there was low sediment input and a high flux of dissolved ions and phosphorus. The nature of bacterial growth in the stromatolites was accompanied by the trapping and binding of fine-grained particles in the suspended water, with a considerable low growth speed and in aphotic conditions (Chacón & Martín-Chivelet, 2008).

Two hypotheses could explain the formation of the microstromatolites in the trilobite tunnels, based on the observations presented in Chapter 5.2.

The first suggested interpretation of the microstromatolites is that they grew into open space from the tunnel peripheries, underneath the seafloor. The tunnels were likely to have been kept open and free from loose sediment by the activities of trilobites. However, several negative factors regarding the growth conditions of the microstromatolites are associated with this "buried tunnel" hypothesis. The absence of sunlight in the tunnels would be a limiting factor to the cyanobacteria producing the microstromatolites.

Secondly, the trilobites would be likely to feed from the microstromatolitic films, reducing their growth and influencing their appearance. Finally, if the microstromatolites inhabited the tunnel walls when the tunnels were free from trilobites, the tunnels were likely to get filled with sediment, removing the open space needed for the microstromatolites to grow.

A second proposed environmental condition preferable to microstromatolitic-growth is a hardground substrate setting. In the event of no net accumulation of sediments, winnowing of loosened cemented grains could abrade and scour the seafloor, and truncate trilobite tunnels. The vertical edges seen on the tunnel peripheries (Figure 41) are believed to be present due to the more weathering resistant habit of the wall linings of the tunnels. The subsequent hardground substrate and the tunnels could be an ideal habitat to microstromatolites, with the tunnel-linings promoting growth. One negative factor regarding this proposition is that the eroded tunnels would act as grooves, likely to be filled with bottom current transported sediments. However, it could be possible that the bottom transport in the particular area was at a minimum, allowing the microstromatolites to grow into the open, eroded tunnels.

Chemosynthetic bacteria which benefitted from methane produced by the rotting of organic material into methane and hydrogen sulphide might also have thrived in the tunnels. The fact that the bacteria live in conditions without sunlight, strengthens the theory of their possible

presence in the tunnels.The high concentration of crystallized pyrite observed in burrows may also be related to the release of hydrogen sulphide during organic decay.

The observations of circular shapes with concentric growth lamella (Figure 42) of possible cyanobacteria on bedding surface 6 may represent microstromatolites, possibly growing vertically on the seafloor, in contrast to the microstromatolites inhabiting truncated trilobite tunnels. Dark coloured, inner rims of the objects could represent staining of phosphate. The observation of microstromatolites growing on a cephalopod conch could indicate that the organisms needed a firm place to settle and/or benefitted from the rotting organic tissue in the conch.

The observations of microstromatolites strengthens the hypothesis of bedding surface 6 as a hardground, since microstromatolites occur in the same stratigraphic level inside and outside the tunnels, based on the fact that microstromatolites can not grow in buried sediments. Flügel (2004) characterizes microstromatolites as indicators of hardgrounds, being a substrate to both ferrigenous and phosphatic microstromatolites. Compared to the study of Chacón & Martín-Chivelet (2008), where the stromatolites were larger and formed in a pelagic seafloor environment, the microstromatolites in the Svartodden Mbr. were most likely to represent a shallow marine environment, due to the abundant bioturbation and the shallow water fauna.

The scouring effect made by current transported cemented material during the final stage of the hardground, may have removed much of the microstromatolites, leaving only a few specimens left.

5.3.3 Brachiopods

Acrotretid inarticulated brachiopods are present in the Svartodden Mbr., and the group is abundant in eastern faunas in Baltoscandia, including Sweden and Estonia (Holmer, 1989). The recorded acrotretid brachiopods are present in the unit continously from bed 3. The possibly identified genera *Conotreta*, *Myotreta* and *Biernata* are also present in the equivalent Holen Limestone in Sweden (Holmer, 1989). Although little is known about their relationship to lithofacies/confacies and depth, the observed genera in the Svartodden Mbr. could witness a time equivalent similar environmental setting in the Oslo Belt as in the Scanian Belt. The

acrotretid brachiopods belonged to the benthic epifauna, however no reported modes of attachment to substrates are known from the recorded genera.

Thin section studies of brachiopods in the Svartodden Mbr., eg. PMO 221.485 (bed 6) shows an impunctate brachiopod where pores are absent, most likely due to abrasion before final burial. This could indicate a shallow environment with high enough energy to promote abrasion of shells. The group is present through the complete unit. Brachiopods were also likely to be abundant during periods when the seafloor was moderately soft, inhabiting seafloors rich in carbonate mud (Wilson & Palmer, 1992). Burrowing lingulacean brachiopods with an infaunal life habit are known from the Ordovician (Holmer, 1989), and although the group has not been identified in the unit, they may have produced some of the observed trace fossils.

5.3.4 Bryozoans

Cryptostome, cystoporate and trepostome bryozoans have been observed in the Svartodden Mbr. Bryozoans represent <1% of the skeletal grains in the unit, having a low abundance in the thin sections. The bryozoan fauna is fragmented, showing minor roundness, indicating a short transportation of the fragments. Concentrations of bryozoa in the vicinity of hardgrounds have not been recognized, although this could represent a sampling bias since few thin sections cover the potential hardground intervals.

5.3.5 Cephalopods

The former name of the Svartodden Mbr., "Endoceras Limestone" (Etage 3cγ), was erected according to its rich content of endoceratids such as the genera *Vaginoceras* and *Cycloendoceras*, although the genus *Endoceras* was not remarkably abundant (Størmer, 1953). The overwhelming abundance of orthoconic nautiloids at the Slemmestad IF arena locality, possibly several millions of specimens, makes it possible to infer that cephalopods were a remarkably dominant group, and that the environmental conditions during the period were optimal to cephalopods.

The nautiloid cephalopods are believed to have been the largest group of predators in the sea

covering the Baltic platform during the Middle Ordovician. They may have lived on a diet that included trilobites, being vulnerable and easy preys when they were in the process of molting.

The great dominance of *Proterovaginoceras incognitum* is remarkable, constituting 100 % percent of the counted specimens at the studied locality. Higher presence of other species from the order Endocerida at the Baltoscandic shelf, e.g. *Anthoceraas buchi* in the equivalent limestones in Sweden (Kröger, 2012), may indicate different environmental preferences among the cephalopods. A low number of coiled representatives of the order Tarphycerida are present in bed 6 of the Svartodden Mbr., and apparently absent in the underlying beds (bed 1-5). Limiting factors for their low abundance may include depth and predation.

After sinking through the water column and reaching the seafloor, the cephalopod conchs were likely to be filled with sediment. The siphuncle alignment in the 270° position, points towards a seafloor environment devoid of strong currents, where only the back and forth movement by swash currents affected the empty cephalopod shells (cf. Reyment, 1970). Random siphuncle alignments have previously been thought to represent rolling of the shells on algal mats, reported from the Orthoceratite Limestone in Sweden (Reyment, 1968).

The horizontally embedded cephalopod shells appear to have a preferred orientation on bedding surface 4 and 6 of the Svartodden Mbr. On the bedding surface of bed 4, the cephalopod apex direction points towards north-east, suggesting palaeo currents directed south-west. On bedding surface 6 on the other hand, the apex directions indicate a palaeo current direction to the north-east.

Intense corrosion of the upper halves of cephalopod conchs is believed to have resulted from a slow sedimentation rate. This phenomenon is common on conchs through the entire unit, and can be associated with several hardground- or firmground surfaces. Based on the lack of fragments observed in thin sections, it is believed that chemical abrasion of the conchs occurred, rather than fragmentation by physical processes. This could indicate that most of the conchs got deposited in a somewhat low energy environment below normal wave base. However, thin section studies of selected conchs show borings on the seafloor-facing side of the shell (Figure 62), indicating minor rolling of the shell on the seafloor. A probable explanation is that shells were exposed on the seafloor for different lengths of time before

final burial. In some periods, the sedimentation rate might have been higher, protecting the shells from rolling and from boring organisms. Variations in energy levels on the seafloor might also have been affected by storms, causing a disturbing effect on the skeletons on the seafloor down to storm wave base.

The calcite mineralized circles described as a common feature on bedding surface 6, resemble very much vertical oriented orthoconic conchs. Although vertical nautiloid conchs have been reported elsewhere in Baltoscandia (Reyment, 1968), a more thorough explanation for the occurrence of vertical orthoconic nautiloids is missing in previous investigations. The gas-filled chambers in the endocerartid cephalopods may also have contributed to the vertical position of the conchs on the seafloor for a limited time period.

The possibility of having conchs from the order Endocerida, being approximately 0.3-0.5 m in length, standing upright in the substrate during deposition, seems highly unlikely. Factors substantiating this proposition are the intensity of firmgrounds, the effect of gravity, current activity and the time involved within the dissolution process. However, it is here suggested that the circles on bedding surface 6 might represent jointed parts of the living chamber of the orthoconic cephalopods, which were possibly more easily loosened and broken off from the main conch. The phenomenon is limited to the uppermost bedding surface of the Svartodden Mbr., and could indicate a change in the depositional environment or an evolutionary change in the conch strength of the cephalopods.

5.3.6 Trilobites

The observed trilobites in the Svartodden Mbr. were predominantly benthic, living in shelf environments, and may have been preyed upon by cephalopods. Molting stages in trilobites made the group an important sediment contributor in the Svartodden Mbr. Their high abundance indicates that the particular seafloor conditions were optimal to trilobites, a group known to inhabit near shore environments (Benton & Harper, 2009). Trilobites may also have used the conchs of dead cephalopods to hide in, while waiting for their new exoskeleton to mineralize.

Burrowing trilobites from the genus *Asaphus* may have produced the Type 1 *Thalassinoides* trace fossils, judging from the sizes of the burrows (< 2 cm in diameter), and the occurrence of trilobite tracemakers in time equivalent limestones in Sweden. Habitual infaunalism of the trilobites is belived to have been ecological advantageous and due to specific substrate conditions (Cherns et al., 2006). The tunnels were probably formed in a firmground cohesive substrate, in which the trilobites could dwell, hide from predators (cephalopods) breed and molt, feed on detritus or bringing food back into (Cherns et al., 2006). The formation of tunnels may indicate a well oxygenated seafloor environment.

The content of trilobite grains through the unit is high, ranging from 5-10 percent of the skeletal grains in the limestone, based on the microfacies analysis.

5.3.7 Ostracodes

Ostracodes have previously been described as a common sediment contributor to the Orthoceratite Limestones of Sweden, and in the rest of Baltoscandia (Tinn et al., 2001). The recorded ostracodes from the acid insoluble residue are putative and diagenetically altered by phosphatization. Specimens were not identified to species level, due to bad preservation. However, they are likely to be representatives from the orders Archaeocopida or Palaeocopida.

Field observations and thin section analysis indicate that ostracodes are abundant through the entire Svartodden Mbr. at Slemmestad. The group has also proved to be one of the most abundant fossil groups in the unit. In the central confacies belt of Baltoscandia, the ostracode fauna is rich and diverse, indicating a stable environment and favorable conditions (Tinn et al., 2001). Ostracode assemblage structures show a close relationship with sea level changes, hence further studies of ostracodes from the Ordovician rocks in the Oslo Region could help shed light on this subject.

5.3.8 Echinoderms

Cystoids and crinoids are regarded as the most common groups of echinoderms during the Ordovician (Jaanusson, 1984). Crinoid fragments have been identified in all of the analysed

thin sections, and the group is regarded as one of the most important contributors in the sediment buildup. Their relatively stable high-Mg calcite skeleton dissolves commonly during deposition and gets replaced by secondary calcite (Sprinkle & Guensburg, 2004). Ordovician echinoderms are abundant in thin, interbedded limestone units, which were deposited in shallow epicontinental seas (Sprinkle & Guensburg, 2004). Due to the easy disarticulation of echinoderm skeletons, no systematic identifications of the skeletal elements observed in thin sections and in the acid insoluble residue have been performed. Several of the crinoid fragments show signs of microborings, indicating that the skeletal grains were exposed on the seafloor for long periods before burial.

5.3.9 Conodont biozones and CAI

The Svartodden Mbr. shows a rich and diverse fauna of conodonts, based on the amount of elements picked from the acid resistant residue. A high amount of conodont elements often indicates a slow sedimentation rate. The genus *Drepanodus* is particularly abundant in the studied samples. It was first described by Pander in 1856, and later its type species *Drepanodus arcuatus* was described by Miller, 1889 (Löfgren & Tolmacheva, 2003). The species is thought to have been widely geographically distributed throughout the Ordovician period (Löfgren & Tolmacheva, 2003). The recorded conodont species from the dissolved samples, belong to the biozone *Eoplacognathus pseudoplanus* (Löfgren, 1995; 2000) sharing more than three characteristic species from the biozone. The particular species typical for the biozone are *Protopanderodus rectus, Drepanodus arcuatus, Drepanoistodus basiovalis, Eoplacognathus? variabilis, Scalpellodus gracilis* and *Baltonodus medius.*

The recorded conodonts show a CAI value of 4, indicating a heating of 190ºC - 300ºC, as a function of the burial depth, geothermal gradient or heat transfusion from igneous intrusions. The particular temperature interval reflects a burial depth up to 10.5 km, when the average geothermal gradient is 100ºC/3.5 km. The heating effect introduced by surrounding igneous batholiths is a more probable factor causing the CAI value of the conodonts. The batholiths in the Slemmestad area are of syenitic, porphyritic and granitic origin, and are of Permian age (Larsen et al., 2008). These are located on the western and southern borders of the Ordovician sequence in the Slemmestad area.

5.3.10 Conodont biozone correlation with meteorite events in Sweden

Meteorites in the Orthoceratite Limestone at Kinnekulle in Sweden were described by Schmitz et al. (1996). The Lower Ordovician Orthoceratite Limestone appears at the early-late Arenig boundary and ends near the early-late Llanvirn boundary. Biostratigraphically, the basal and the topmost unit of the Swedish Orthoceratite Limestone belongs to the *Baltoniodus triangularis* and the *Eoplacognathus suecicus* conodont zones, respectively (Schmitz et al., 1996). The Svartodden Mbr. of late Arenig age was deposited during the mentioned time interval of the Orthoceratite Limestone in Sweden. Hence, one could expect to find meteorites in the Svartodden Mbr., if the two units are time equivalents. At two thirds up in the Lower Ordovician Orthoceratite Limestone, 10 meteorites were found in a 1 m thick limestone bed, grey in colour and rich in marl layers. The complete 20 m thick section of the Orthoceratite Limestone is biostratigraphically spannning the *Amorphognathus variabilis-Microzarkodina flabellum* conodont subzone (Schmitz et al., 1996).

According to Löfgren (1999), the *A.* "*raniceps*" trilobite biozone spans the Svartodden Mbr. which coincides with the *Amorphognathus variabilis* biozone (Lindström, 1971 and Löfgren, 1976) *in* Löfgren (1999).

Based on these correlations, the meteorites in Sweden were deposited during the same time interval as the deposits representing the upper Hukodden Mbr., the Lysaker Mbr. and the Svartodden Mbr. Hence, there is an enhanced possibility to encounter meteorites in the Svartodden Mbr. During this period, the meteorite flux to the Earth was strongly increased, due to an asteroid disruption event in the asteroid belt (Tassinari et al., 2004). However, so far no meteorites or meteor-elements have been discovered in the Svartodden Mbr.

5.3.11 Bioclasts of uncertain biological affinity

PMO 224.360/B could represent a fragment of a brachiopod based on its morphology. Its composition is mainly calcium phosphatic. PMO 224.360/C could represent a phosphatized crinoid fragment. The high abundance of similar skeletal fragments through the unit could indicate that brachiopod shells were easily disintegrated on the seafloor. The biological affinity of the remaining specimen PMO 224.360/A could not be established.

5.3.12 Trace fossils

High numbers and high diversity of trace fossils found on bedding surface 6 of the Svartodden Mbr. make the locality intriguing to ichnological studies, as well as the abundant burrows in vertical section of the unit.

To hardground sedimentologists, trace fossil ichnofaunas are of great relevance. Patterns of ichnofabric (bioturbation and bioerosion) are closely related to sea level changes during the deposition of Lower to Middle Ordovician sections on Baltoscandia (Webby, 2004). Ichnotaxa such as *Trypanites*-like borings and "Amphora-like" borings, later redescribed by Ekdale & Bromley (2002) as *Gastrochaenolites oelandicus*, have been reported from all over Baltoscandia (Dronov et al. 2002), including the Huk Fm. (Ekdale & Bromley, 2002). Dronov et al. (2002) conclude that the ichnological record presents the best image of the interplay between sedimentation, erosion and hardening of sediment, i.e. a suitable means in the identification of hardgrounds and discontinuity surfaces.

Most trace fossils (Type 1 and Type 2) on the uppermost bedding surface of bed 6 in the Svartodden Mbr. are regarded as complex endogenic burrows, of the genus *Thalassinoides*. *Thalassinoides* is characterized by endogenic burrows and tunnel systems, as sites of dwelling and feeding activities (Ekdale & Bromley, 2003). The biological affinities of the trace makers forming *Thalassinoides* are in many cases unknown (except from the mentioned trilobites above), but modern candidates forming extensive *Thalassinoides*-like burrows are deposit-feeding crabs, lobsters and schrimps (Ekdale & Bromley, 2003).

Both *Thalassinoides* (Type 1) and *Thalassinoides bacae* (Type 2) on bedding surface 6 are interpreted to have been formed in a firm substrate which later became stained with iron minerals such as pyrite and dolomite (described in Chapter 6). The trace fossil *Thalassinoides* (trace fossil Type 1), appears in extensive tunnel networks with a positive epirelief, possibly due to the mineral staining and hence the lower susceptibility to weathering compared with the limestone. In a later stage of the hardground setting, most of the tunnels were likely to be filled with silty material, which is probably why some of the tunnels appear as shaly tunnel networks. It is suggested that the truncated tunnels of *Thalassinoides* traces which contain microstromatolites (Type 1), were closed off from further infilling of silty material,

preserving the microstromatolites. No borings into the two types of *Thalassinoides* traces have been identified, a feature to expect in cases of hardground settings (Wilson & Palmer, 1992).

As previously mentioned, the trace makers of the *Thalassinoides* (Type 1) were most likely trilobites committing to an infaunal life mode, a feature for the first time to be reported from the Huk Fm. This interpretation is based on the similar *Thalassinoides* trace fossils observed in time equivalent limestones in Sweden, which contained *in situ* trilobites (Cherns et al., 2006). The tunnel walls excavated in the semi-lithified substrate are composed of dark linings standing approximately 1 mm above the surface. Hence, it is suggested that the *Thalassinoides* producers, the trilobites, were secreting a sticky substance which was glued onto the tunnel walls, stabilizing the tunnels. Such wall linings of trace fossils are mentioned in Pollard et al. (1993). The organic linings may in turn have promoted the growth of microstromatolites. It has been attempted to find recordings of animals producing wall-linings in more recent *Thalassinoides* trace fossils, but no literature describing such features were found.

Thalassinoides bacae was described by Ekdale & Bromley (2003) from Lower Ordovician limestones in southern Sweden. Their paleoethologic interpretation of the tunnels is that they represent agrichnial traces, in which microbial organisms grew and were preyed upon by the organism inhabiting the burrow. The biological affinity of the trace maker is unknown, but the organism is believed to have been a deposit feeder. Environmental factors such as a low oxygenated sea bottom, low energy environment and a low supply of detrital organic matter are thought to have promoted bacterial growth on the seafloor and in the sediments. Suggested biological affinities of the *Thalassinoides bacae* trace makers are trilobites, ceranthid sea anemones, enteropneust acorn worms and/or burrowing crustaceans (Ekdale & Bromley, 2003). Although the authors state that trilobites rarely produce burrows of an anastomosing fashion, this hypothesis can most likely be abandoned due to the *Thalassinoides* tunnel-forming trilobites reported by Cherns et al. (2006).

The many vertical shafts observed on the bedding surface 6 of the Svartodden Mbr. are comparable to the observations in Ekdale & Bromley (2003), and have been interpreted to have optimized the water circulation system in the *Thalassinoides bacae* burrow systems. Based on polished slabs of the vertical shafts seen in bed 6 of the Svartodden Mbr., the

tunnels are thought to have been kept open while the organisms moved back and forth through the tunnel networks. A later infilling of laminated silty material is related to environmental changes possibly brought about by the subsequent hardground environment of bedding surface 6.

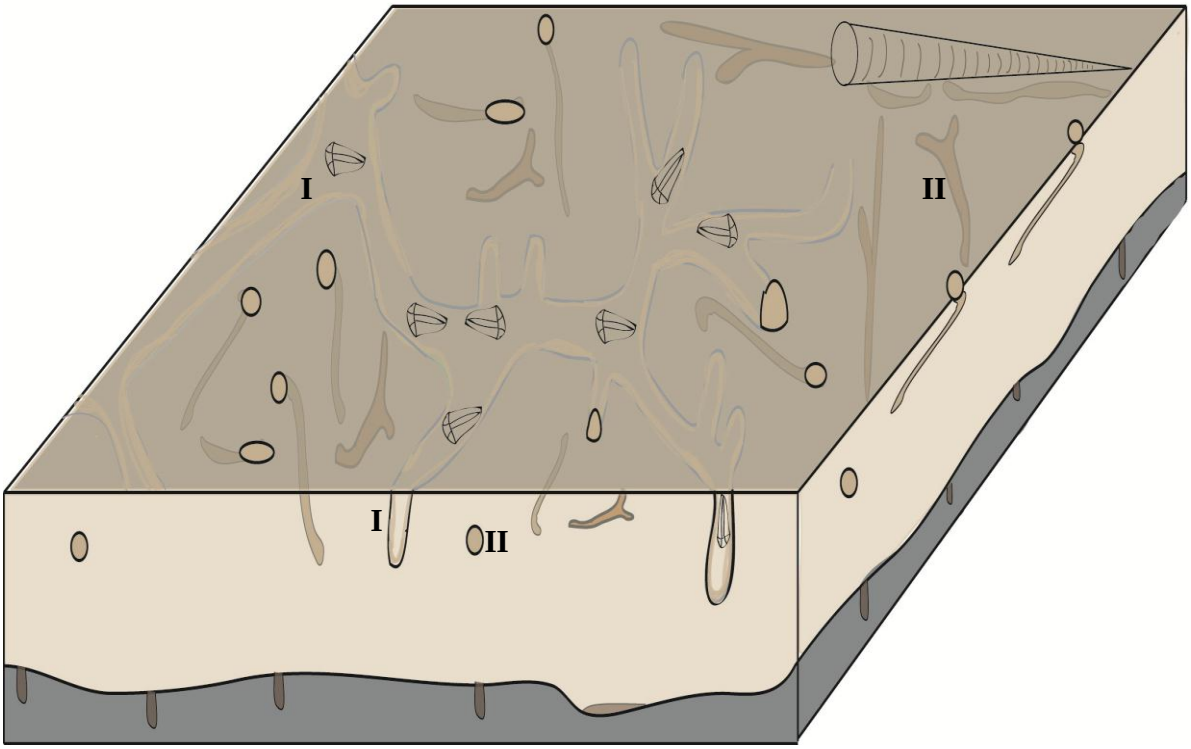

Figure 66: Illustration of the firmground trace fossil fauna of the Svartodden Mbr. The tunnels marked by I represent the *Thalassinoides* tunnels excavated by trilobites, while the tunnel-tubes marked by II represent the *Thalassinoides bacae* of unknown biological affinity.

The formation of trace fossils in the Svartodden Mbr. is connected to hardgrounds. Pre-omission vertical burrows, identified as *Skolithos*, are easiest to identify in vertical sections (Figure 57). These burrows were formed in an initial firm seafloor. During hardground formation, cementation occurred in the sediment surrounding the burrows, preserving them with hardened walls and cemented crust. The hardened burrows might have protruded all the way down to the uncemented zone, consisting of unconsolidated sediment (Wilson & Palmer, 1992). The brown coloured crusts of the trace fossils observed in weathered surfaces and sections (Figure 57), are most likely limonitic, due to the oxidization of the pyrite. The crusts may also contain phosphate. The seafloor, probably being starved in sediment input, was subject to large scale pyritization, as indicated from the pyritized walls of the *Thalassinoides*

bacae burrows as seen in Figure 55. According to Ekdale & Bromley (2003), mineralization of the burrow walls formed during the microbial growth inside the burrows while the trace makers were present.

The tiering positions of the studied trace fossils indicate trace fossil activity near the sediment-water interface, and in the sediment immediately below the sediment-water interface

5.3.13 Palaeoecology

Paleontological data obtained from the Svartodden Mbr. at the Slemmestad IF arena locality are indicative of a diverse and rich fauna, consisting of the groups presented in the sub-chapters above. According to Wilson & Palmer (1992), the groups abundant during the formation and burial sequence of a typical Ordovician hardground were initially a soft bottom community, represented by strophomenid brachiopods, trilobites and infaunal burrowers. In a subsequent hardground environment, boring and encrusting organisms in the need of solid hold-fasts were likely to dominate, including bryozoans and echinoderms. Recent documentations of trilobites as tracemakers of *Thalassinoides* tunnel-like burrows bring several aspects into light regarding the ecological conditions in- and on the seafloor substrate. The endogenic tunnels formed in firmgrounds, are common in beds 3-6 of the unit. The lack of evident firmgrounds below this level may have reduced the trilobite's ability to excavate the sediments, being soft instead of firm.

Hardground reconstructions such as those presented by Brett & Liddel (1978) show marked similarity to what is observed within the Svartodden Mbr. Characteristics of a hard ground environment witnessed in the Svartodden Mbr. are the pre-omission burrows, the firmground fauna, and the hardground fauna. *Trypanites* borings into the hard seafloor is however an important feature of hardgrounds, but has not yet been identified in the unit. This supports the idea that the Svartodden Mbr. is dominated by firmgrounds, which rarely turned into true hardgrounds. According to Flügel 2004, hardgrounds are typical of micrite-filled microborings covered by microstromatolites with impregnations of iron and/or manganese. These characteristics fit well with the observations presented above, and strengthen the theory of bedding surface 6 as to represent a hardground.

Evaluation of fossils with known ecological preferences, are relevant to the assemblages of conodonts and brachiopods, as well as trilobites and cephalopods in the present study. Field observations of common trilobite coquinas and trilobite tunnel systems, strengthen the assumption of a shallow marine depositional environment. According to McKerrow (1978), crinoids and bryozoans are abundant in shallow water environments. These groups are present in relatively high portions of the skeletal grains observed in the Svartodden Mbr. hence this also supports a shallow depositional environment.

Trilobite associations of the shallow marine limestone facies of the Svartodden Mbr. have not been defined, due to the difficulties of species identification in the unit. In the Helskjer Mbr. on the other hand, trilobite associations are reflected by a low diversity and a deeper water fauna (Hansen, 2009).

Rasmussen & Stouge (1995) combined conodont faunas with sedimentological analysis from from the late Arenig-early Llanvrin Stein Fm. in Norway (Mjøsa area), and found five conodont biofacies representing distinct shelf settings. The species assemblages in the different biofacies consisted of several of the observed species in the present study. However, due to the low amount of identified taxa in this study, an identification of conodont biofacies in the unit could not be established.

Trace fossils used as palaeoecological proxies are discussed in Buatois & Mángano (2011), where a *Thalassinoides* dominated trace fossil fauna is thought to indicate aerobic bottom waters and shallow tiering of the sediments. The abundant *Thalassinoides* traces in the Svartodden Mbr. are typical in a wide variety of environments (Buatois & Mángano, 2011) hence they are poor as palaeoenvironmental indicators.

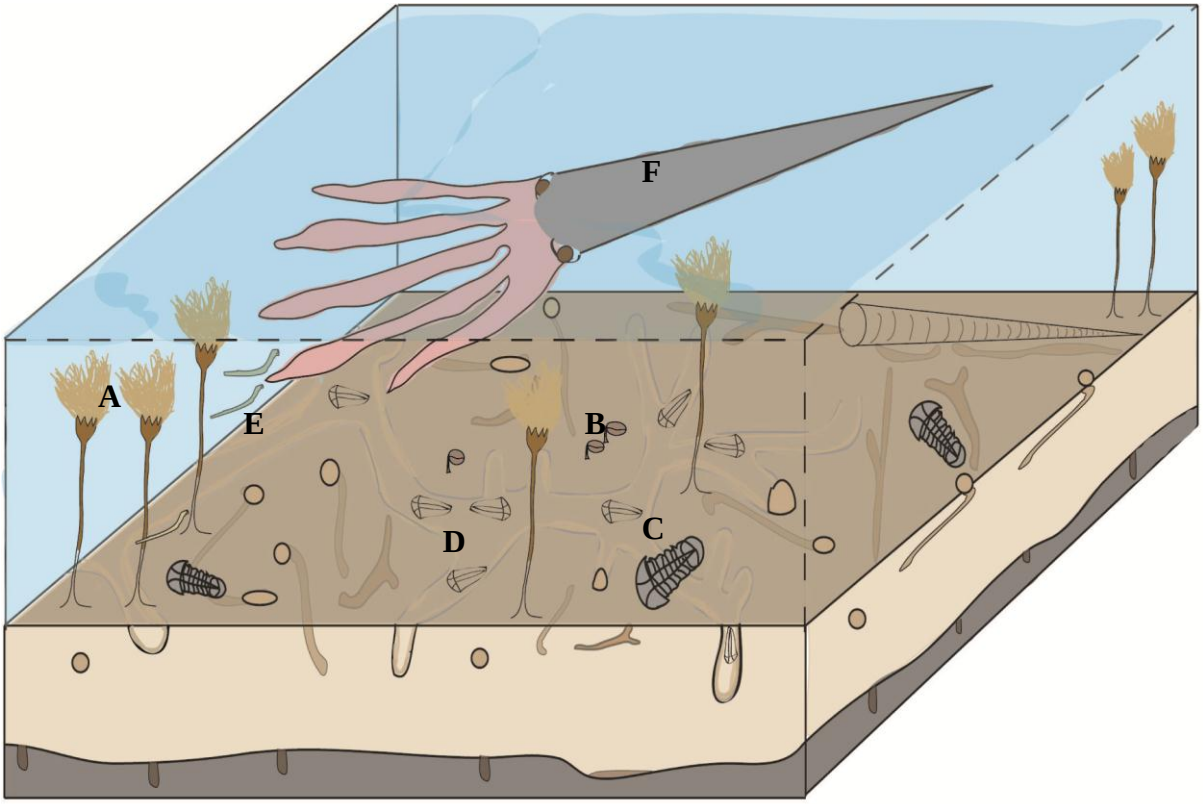

Figure 67. Illustration of a potential firmground community in the Svartodden Mbr. and some of its associated endogenic, benthic and nektonic macrofauna. Crinoids (A), brachiopods (B), trilobites (C) above and below (D) the sediment surface, nektonic conodonts (E) and endoceratid cephalopods (F).

6 Sedimentology

This chapter will mainly cover the sedimentary aspects, and some of the diagenetic processes occurring in the Svartodden Mbr., based on field observations and analysis of the unit. Several authors have mentioned the condensation and omission surfaces present in the Svartodden Mbr. (Hansen et al., 2009; Owen et al., 1990; Nielsen, 1995; Skaar, 1972). No research on the Svartodden Mbr. has until the present study presented geochemical data in context with the depositional history of the unit, with the aim of identifying possible hardgrounds or events.

6.1 Previous work

The Svartodden Mbr. has formerly received little scientific attention, despite its great abundance of fossils and peculiarity of being a "pure" limestone in the otherwise shale dominated Ordovician succession of the Oslo Region. Most studies of Lower Palaeozoic rocks are based on large intervals between analysed samples, and have focused on greater trends than detailed descriptions of faunas and depositional histories of the different Ordovician sediments. Bjørlykke (1974) presents the mineralogical and geochemical composition of the clastic sediments of the Oslo region, although only one sample is analysed for the whole of the Huk Fm. in the Oslo-Asker area. Further south-west from the Oslo-Asker area, Klemm (1982) describes the Ordovician succession at Vestfossen and Krekling, while Svendsby (1987) mapped and described the Eikeren to Mjøndalen area.

Apart from being logged and described in field by several authors, only Skaar (1972) analyses the Huk Fm. in detail by means of geochemistry and petrographic microscopy. Sedimentological features such as bed thicknesses, current directions, content of trace fossils and body fossils from several localities of the Huk Fm. across the Oslo Region were described. The study presented a short microfacies summary, the mineral content and the diagenetic history of the members in the Huk Fm. Field observations, XRD analysis and thin section microscopy were the foundation on which the study was based on. Main results from the study of Skaar (1972) are presented in Figure 68.

Primary features	Bioclastic material: cephalopods, ostracods, brachiopods, bryozoans, crinoids and trilobites			Primary calcite	Trace fossils: *Chondrites* and *Planolites*	Peloids (faecal pellets)	Ooids
Diagenetic alterations	Phosphorite	Dolomite	Stylolites	Secondary precipitation of calcite		Pyrite	Glauconite

Figure 68: Previous sedimentary recordings in the Svartodden Mbr. (modified from Skaar, 1972).

Skaar (1972) suggests a eustatic lowering of the sealevel in the Middle Ordovician, and a low sediment input from a shallow Telemark area to the west. With respects to the Svartodden Mbr. in the Oslo-Asker area, the deposition is believed to have occurred during uplift of the area, in a shallow environment with a depth of 20-40 meters or shallower due to observations of ooids. The Huk Fm. is believed to have been deposited during a timeinterval of 1-2 million years (Skaar, 1972). The diagenetic history of the Huk Fm. was also described by Skaar (1972), and is summarized below, with emphasis on the Svartodden Mbr. (3cγ):

1. Accumulation of calcite derived from the breakdown of organic components, as well as transporeted clastic material
2. Formation of dolomite crystals just beneath the sediment surface, probably formed by calcite and pore water saturated with respects to Mg-ions from chlorite in solution
3. Bioturbation causing mixing of dolomite crystals with the sediments
4. Recrystallization of calcite in porespace
5. Formation of pyrite, together with crystals of dolomite, formed alongside stylolites
6. Compaction
7. Formation of stylolites
8. Lithification of the complete unit
9. Folding and fracturing of the complete unit

6.2 Results

This section presents the combined information regarding field studies and studies of polished slabs, thin sections and acid insoluble residue. In addition, geochemical data from XRF, magnetic susceptibility and isotopes has been collected, to further shed new light on the depositional setting of the Svartodden Mbr. In addition to field studies, cathodoluminescence microscopy and staining of thin sections has been performed, with the aim of revealing the diagenetic history of the unit.

Figure 69: The main locality at the Slemmestad IF arena Photo:Ragnar Husum

6.2.1 Field observations

Lithology, texture and rock colour

Differentiating the Svartodden Mbr. as a limestone was performed by using dilute 10 % hydrochloric acid, in which the limestone was reacting strongly. Grading of grain size is present in bed 4 and 6 and on the bedding surfaces, where corroded cephalopod conchs in some areas are covered by a thin layer of slightly coarser grains (packstone). Elsewhere, no particular grading is visible. Textural observations of grains from the thin section analysis are presented in Chapter 5.

Impurities and grain size are key factors in the colour of most limestones. In fresh surfaces, the observed colour of the Svartodden Mbr. is dark to light grey. Weathered surfaces are light grey to yellow, and some areas have an orange-brownish coloured hue.

Bedding and stratification

The measured thickness of the complete limestone unit is 2.0 m, while the logged section of under- and overlying units make up 2.4 m. The thickly bedded unit was divided in six beds based on lithology and clear boundary planes between the beds. Bed 3, 4 and 6 are distinguished by having exposed bedding surfaces, as indicated in Figure 17. The divided beds from bed 3 to 6 consist of several thinner, less pronounced sub-beds, marked by stylolites and clay seams, as well as possible firmgrounds. Bed one starts at the boundary to the underlying Lysaker Mbr., where the lithology is dominated by the intercalation of nodular limestone and shale beds. Bed 1 is approximately 15 cm thick, and has a higher content of clastic material than the overlying beds.

The boundary between bed 1 and 2, is marked by a one cm thick clay lamina, visible due to its less weathered nature than that of the surrounding rock. The bed has a rich content of sub horizontal clay seams, which could be pressure solution seams. No firm- or hardgrounds could be identified. Cephalopods and trilobites are abundant. The transition from bed 2 to bed 3 is marked by a 1 mm thick shale lamination with a wavy habit, with cephalopod conchs resting on top of the surface. The bed contains a few shaly laminae, possibly stylolites. Approximately 6 m^2 of bedding surface 3 is shown at the locality. Here, the surface is covered by a 2 mm thin clay lamina, possibly clay seams.

The boundary between bed 3 and 4, is distinguished by the 2 mm thick clay lamina mentioned above. Bed 4 is rich in clay laminae, or possible stylolites. Few cephalopods are recorded in the lower and middle section, but the number increases towards the upper 15 cm of the bed. Several possible firmgrounds are also more abundant near the top of the bed. The bedding surface of bed 4 covers an area of some 60 m^2, rich in cephalopods, some showing peculiar patterns (Figure 47). The surface has a more orange weathering colour than that of the main bedding surface of bed 6 (topmost bed).

There is a sharp boundary between bed 4 and bed 5, marked by an incision forming an open space, and infilling of palaeosoil between the two limestone beds. The gap measures 3 cm in thickness, and is traceable in vertical section in the complete area. In bed 5, sub-horizontal thin lines of brown-orange colour, are often seen in combination with burrows which sometimes are filled with weathered, brown coloured, crusty material. The bed also contains many shale laminae, especially in the middle part of the bed. These possible firm- or hardground structures appear frequently throughout the bed. A 1 cm thick zone of several brown coloured, crusty laminae marks the transition from bed 5 to bed 6. High intensities of lithified burrows, seen as irregular surfaces shown in brown outline in vertical sections are observed. Lithological contrasts between these surfaces suggest the presence of several firm- or hardgrounds in bed 6. Most cephalopod conchs show corroded tops, apart from a few within the sub-beds of bed 6. The corroded cephalopod conchs of bedding surface 6 are often covered by coarser carbonate grains, of a coarser packstone texture. Some areas of bedding surface 6 show thin, shaly laminae, possibly representing stylolites or clay seams.

The high abundance of trace fossils is remarkable on the bedding surface of bed 6, described in Chapter 5. Conjugated fracture patterns (120°/60°) are present of high intensities in the unit (Figure 69), often seen as vegetated. The fractures are filled with calcite cement (reacts when exposed to 10 % hydrochloric acid) and are cutting each other, visible in Figure 69. Fracture thicknesses range from approximately 0.1 cm to 1 cm. Some of the fractures have caused minor vertical displacement of the vein-divided units in the outcrop, especially evident on the bedding surface of bed 4. Veins showing vertical displacement have an average slip of 0.5 cm. The studied section of the Svartodden Mbr. at the Slemmestad IF arena, has a dip of 30°, and an average strike of 227°.

Field logs

The Galgeberg Mbr. of the Tøyen Fm. and the Huk Fm. were logged at the Bjerkåsholmen locality in Slemmestad (Figure 70). The Svartodden Mbr. of the Huk Fm. and the Helskjer Mbr. of the Elnes Fm. were logged at the Slemmestad IF arena, as shown in Figure 71.
The abbreviates used during the logging; M, W and P are reffering to the classification of mudstone, wackestone or packstone, respectively. The mud-content in the units is only visually estimated.

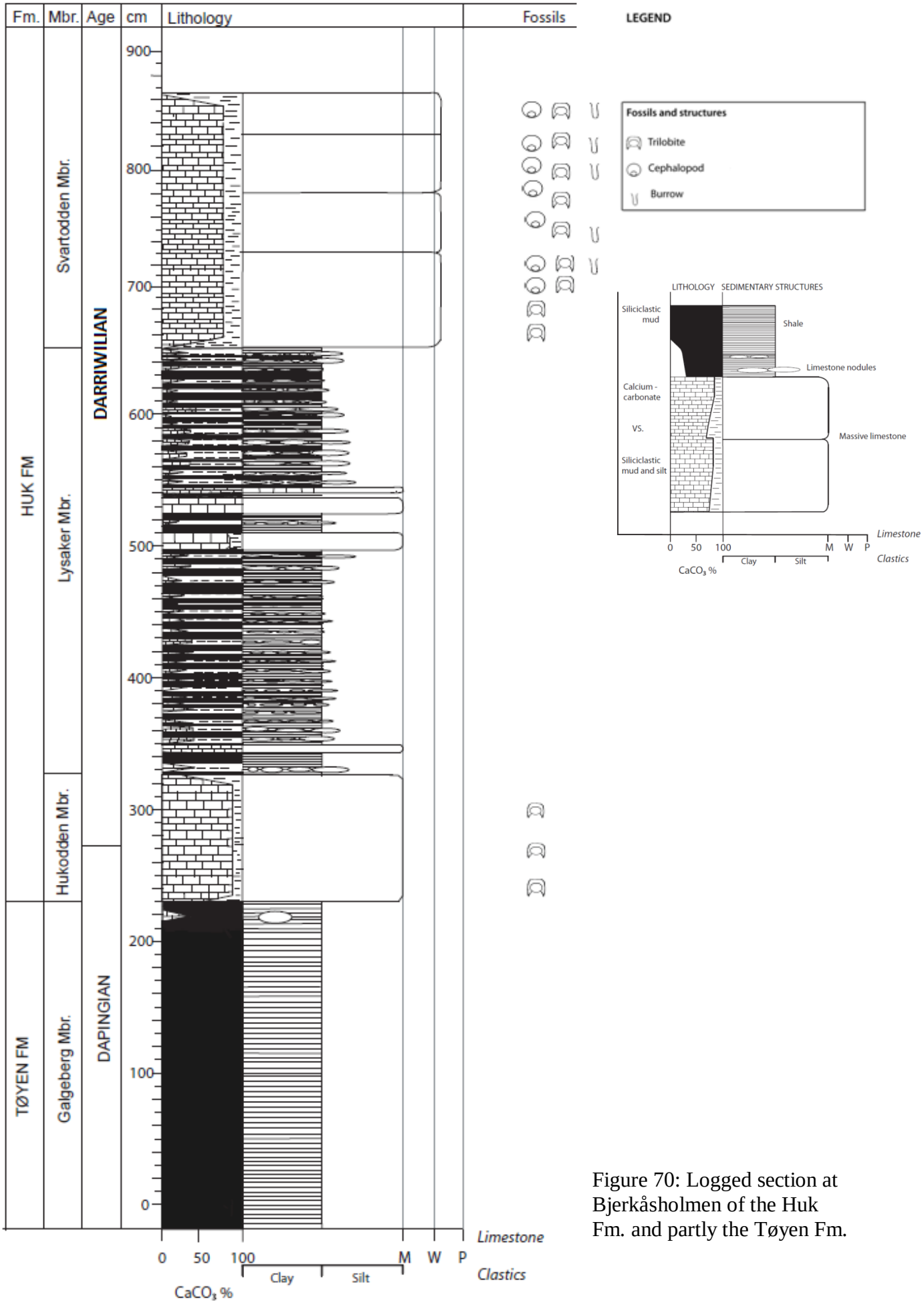

Figure 70: Logged section at Bjerkåsholmen of the Huk Fm. and partly the Tøyen Fm.

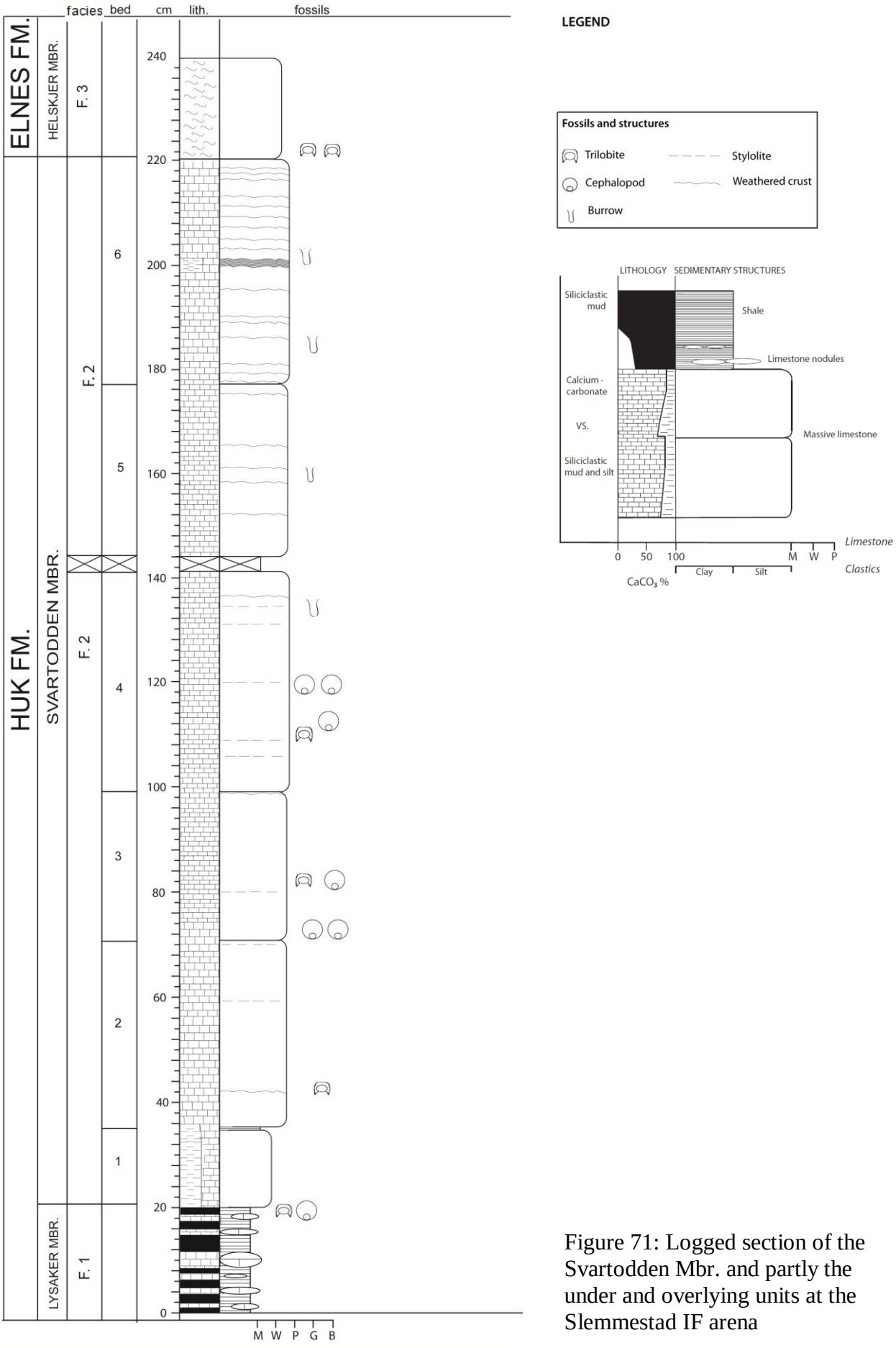

LEGEND

Figure 71: Logged section of the Svartodden Mbr. and partly the under and overlying units at the Slemmestad IF arena

Observations of sub-beds in bed 3-6

Certain levels from bed 3 to bed 6 in the artificial core show clear lithological boundaries, often marked by burrows where the overlying sediments fill the cavities of the burrows. The sub-beds in beds 3-6 are often thinner than 5 cm, and are differentiated from bedding parallel stylolites by colour contrasts. The upper surfaces of the sub-beds are often draped by bedding parallel stylolitization. No burrows have been seen to protrude the sub-bed boundaries in field studies or in the core. Differentiating between stylolites and sub-beds is difficult in field studies, but the different features are more evident in the artificial core. Cephalopod conchs showing half of the conch missing (Figure 72) is a commom feature in the Svartodden Mbr., and are ofte witnessed in context with bed boundaries, stylolites and clay laminations (see logged section, Figure 71). Conchs which are not dissolved are never present at bed-boundaries, but located within the deposits.

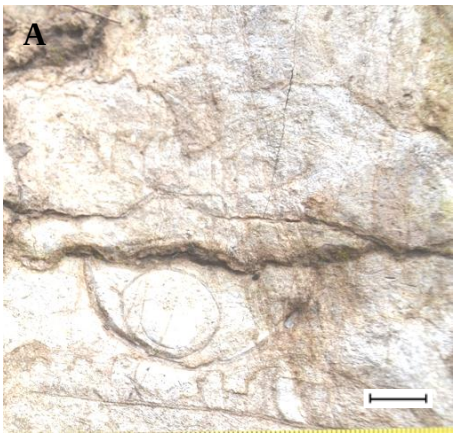

Figure 72: A. Truncated cephalopod conch in a sub-bed of bed 5. Scale bar = 1 cm.

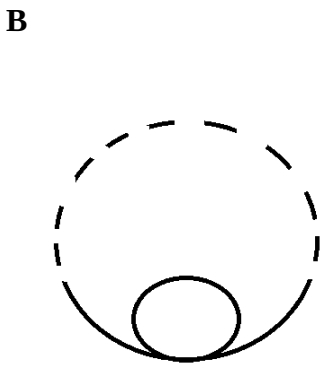

Figure B. Illustration of the amount of dissolution of conchs (stippled line).

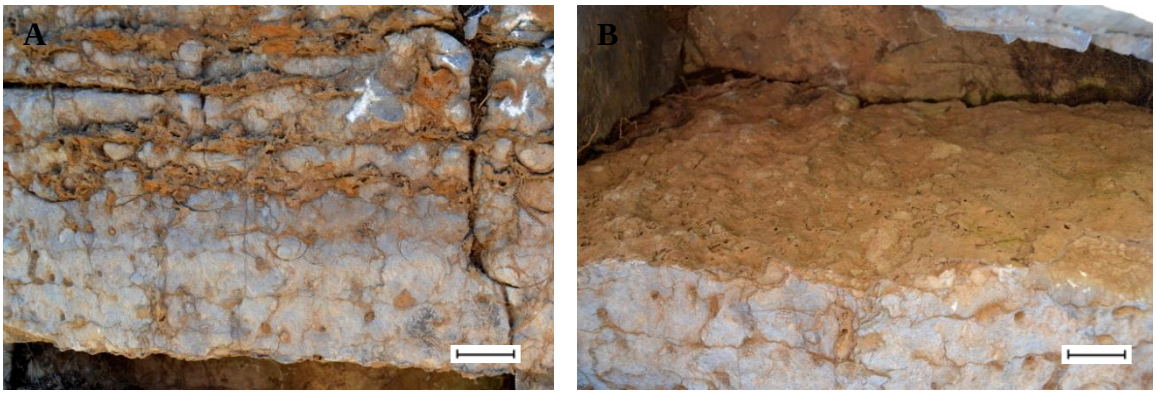

Figure 73: Boundary between bed 5 and bed 6. A. Vertical section showing an irregular boundary. B. Horizontal view, showing a bedding horizontal dark lamina. Scale bars = 3 cm.

Stylolites and clay seams

Pressure dissolution seams, also known as stylolites are common in the Svartodden Mbr. both horizontally and vertically aligned. However, stylolites are in certain cases hard to discriminate from primary deposited sub-beds and clay seams (Figure 74).

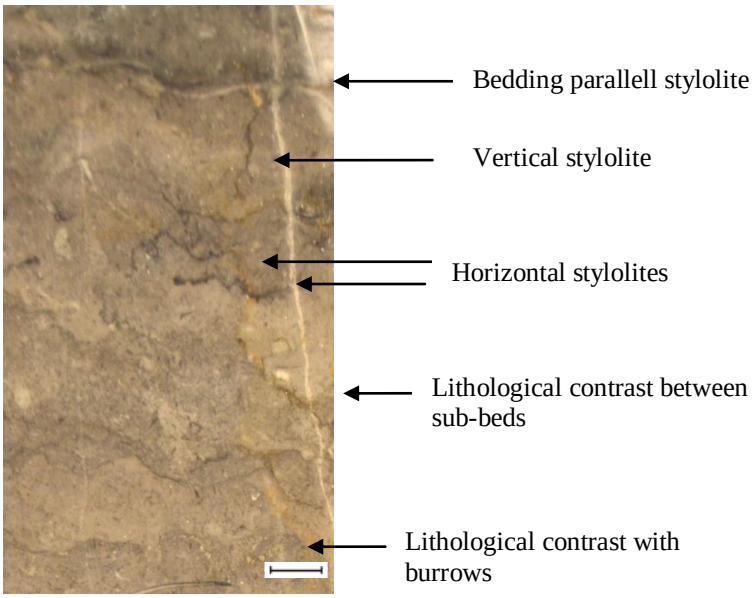

Figure 74: Photo from the cut and polished core, showing sub-beds differentiated from stylolites by contrasts in over- and underlying lithologies, from bed 6. Scale bar = 1 cm.

The exposed bedding surfaces of bed 3, 4 and 5 all show areas with laminae of stylolites, dark grey in colour and approximately 0,5 cm in thickness. The horizontal stylolites or clay seams are approximately 0.1- 1.0 cm thick, running bedding parallel with the beds or sub-beds. They have minor amplitudes (<0.5 cm). The abundant stylolites on the bedding surfaces and in vertical sections occur with high frequency and at low spacing intervals. Junction points where vertical stylolites meet horizontal stylolites are often marked by areas of silty material.

Vertical stylolites are thinner, 0.1-0.5 cm thick, cutting primary features of the bedding surfaces as well as bedding parallell stylolites. Skeletal fragments are often cut by horizontal stylolites or clay seams (Figure 78), which in turn are cut by vertical stylolites, which are cut by the calcite filled fractures (Figure 75).

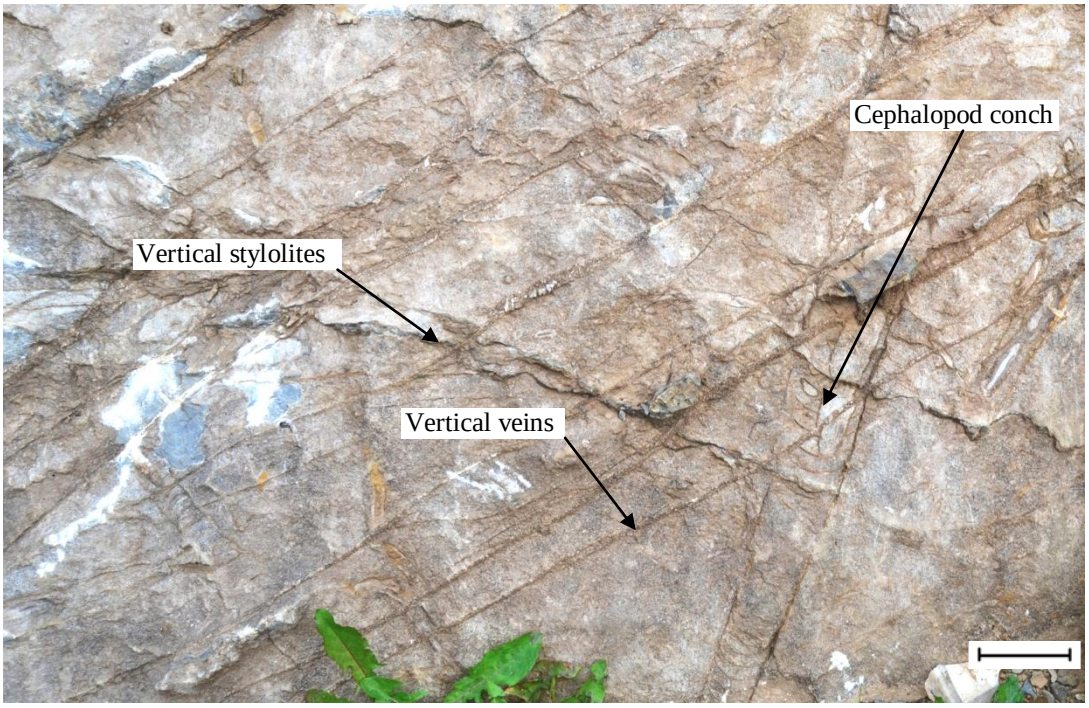

Figure 75: Bedding surface of bed 4: Vertical pressure solution seams that truncate cephalopod conchs. Calcite veins cut primary structures and pressure solution seams. Scale bar = 5 cm.

One cephalopod specimen with possible pyrobitumen infill was observed on the bedding surface of bed 6. The chamber infill from the border shows white cement, followed by a black coloured rim, and towards the center a brown coloured cement. The incorporated material with the black colour could be the remains of pyrobitumen or possibly phosphate (Figure 76). The cement was stained with Alizarin Red S, and stained pink, hence it consists of calcite.

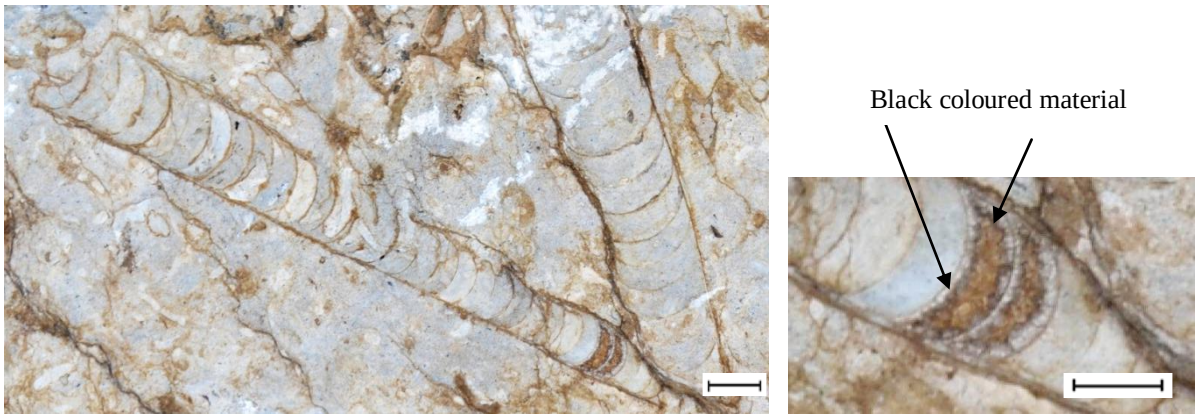

Figure 76: Chambers containing possible pyrobitumen or phosphate. Scale bars = 1 cm.

6.2.2 Sediment composition

Based on petrographical microscopy studies of thin sections, cores and acid insoluble residue, the composition of the Svartodden Mbr. will hereby be presented. The primary deposited components of the unit are considered as skeletal debris and micrite. The main aspects of the microfacies analysis is presented in Chapter 5, however a summary of the skeletal groups is presented in Figure 77. Detailed observations from the thin section analysis are presented in Appendix 7. A description of the core, stratigraphic levels of thin sections and their content of fossil groups are presented in Figure 77 below.

Synsedimentary authigenic minerals, such as pyrite and dolomite have precipitated *in situ* after burial, and will be further described. Dissolution of matrix followed by the replacement of e.g. dolomite will also be illustrated.

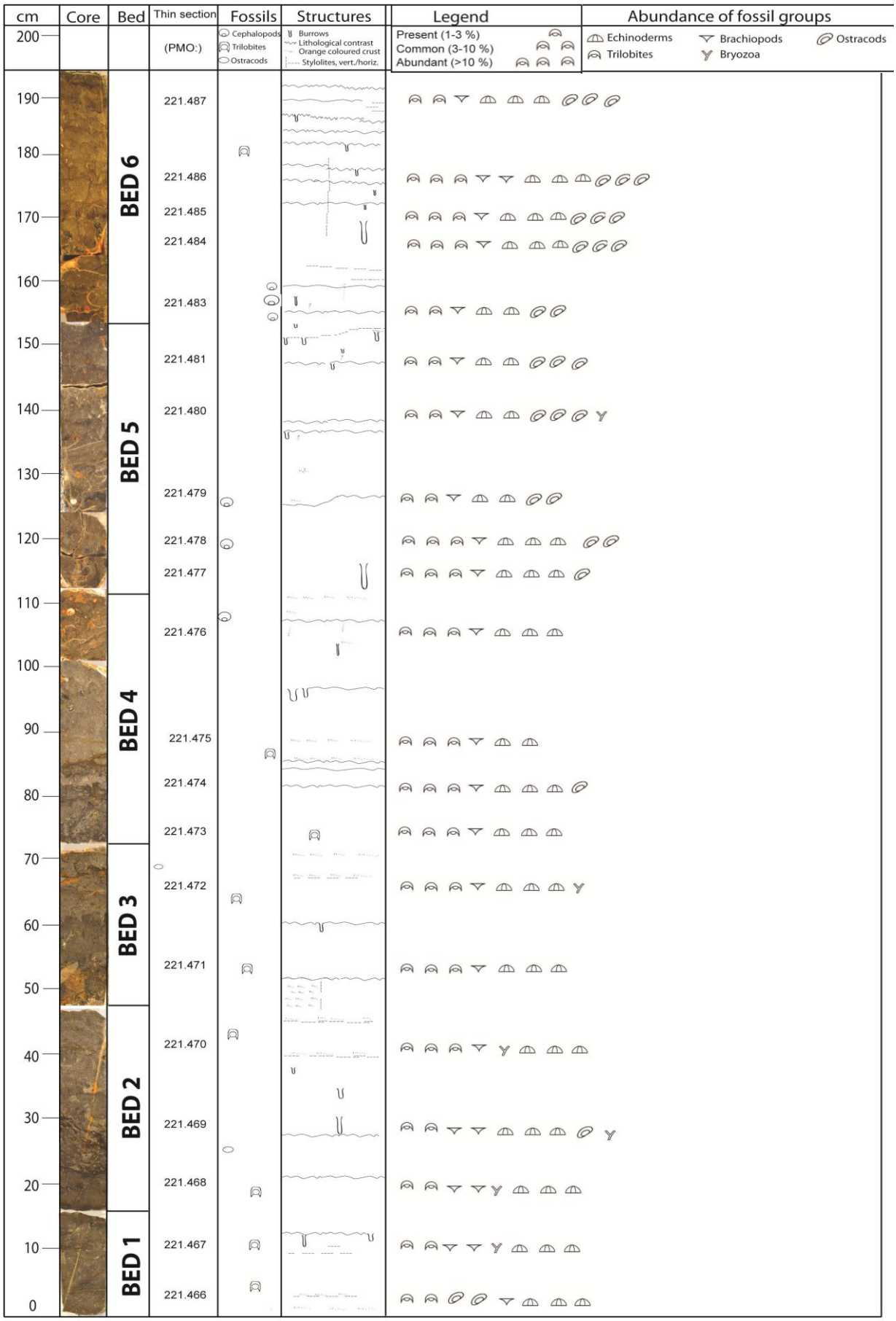

Figure 77: Core images, thin section positions, sedimentary structures and fossil content.

Grain sizes of the unit reflect the size of the bioclastic grains which are mainly of packstone texture. A detailed scheme of the grain size textures observed from the thin section analysis is presented in Appendix 7. No siliciclastic grains larger than the fraction silt have been identified in the acid insoluble residue, including quartz grains.
The syndepositional authigenic minerals have grain sizes from clay to fine sand. Non-bioclastic material identified from the three samples of acid insoluble residue is listed below in Table 3, together with relative abundance in the samples. There is a higher content of quartz grains, dolomite and pyrite in bed 5 and 6 than in bed 1-4, based on observations from the acid insoluble residue. Quartz grains are present in all samples.

Table 3: Relative abundance or presence of minerals in the acid insoluble residue.

Sample	Quartz grains	Pyrite	Dolomite	Mica
SL 5+6	Present	Abundant	High abundance	Not observed
SL 3+4	Present	Low abundance	Low abundance	Present
SL1+2	Present	Present	Low abundance	Present

The presence of clay seams in the boundaries between sub-beds is shown in Figure 78. The zones have variable thicknesses up to 500 µm. No fractured dolomite crystals have been identified in the vicinity of the horizontal clay seams.

Figure 78: Bedding parallel clay seam at the sub-bed boundary below bedding surface 6. Scale bar = 100 µm.

Euhedral pyrite crystals are particular abundant in the periphery of burrows (Figure 55), as well as in the matrix and on fossil skeletal material. As previously mentioned in Chapter 5, pyrite was highly abundant in the acid insoluble residue.
Petrographic studies of veins in thin section showed no content of pyrobitumen. Skeletal fragments in the vicinity of the veins are sharply cut.

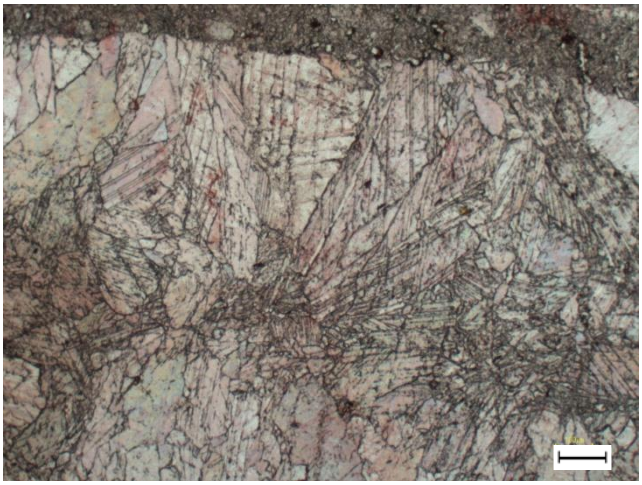

Figure 79: Alizarin Red stained thin section showing pink staining of calcite cement in the vein (PMO 221.516). Scale bar = 100 µm.

Thin sections stained with Alizarin Red solution shows dolomitization from bed 3 to bed 6, by its characteristic habit of not being stained by the solution. The dolomite in bed 3 is characterized as patchy dolomitized micrite filling the space between grains in packstone. The dolomite crystals are subhedral, and contain a core of calcitic micrite. Crystal sizes are smaller than 20 µm in diameter.

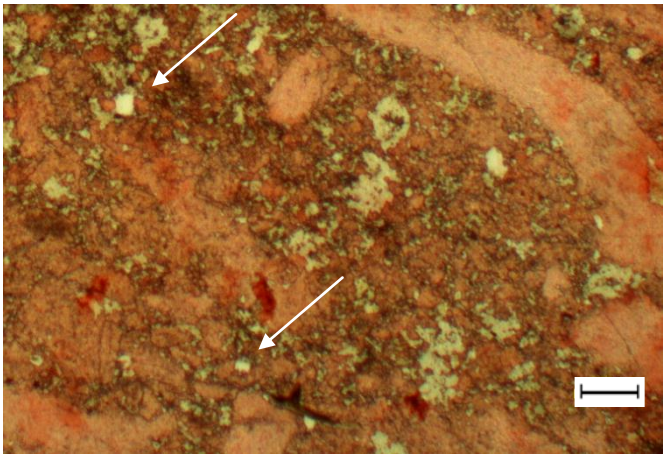

Figure 80: Thin section stained with Alizarin Red. Dolomite crystals (appear white) are indicated by the arrows (PMO 221.476). Scale bar = 100 µm.

Increasing dolomitization is observed in PMO 221.480 (bed 4), and the lithology is characterized as dolomitized micrite in packstone. The overall crystal shape is still subhedral, and most crystals appear with a calcitic micrite core.

In bed 6, the dolomitization appears more strongly, as indicated in Figure 81. Crystals are euhedral-subhedral, micrite cores are less common and certain skeletal grains have dissolved and been replaced by dolomite. Sizes of the dolomite crystals are approximately 60 µm in diameter or less.

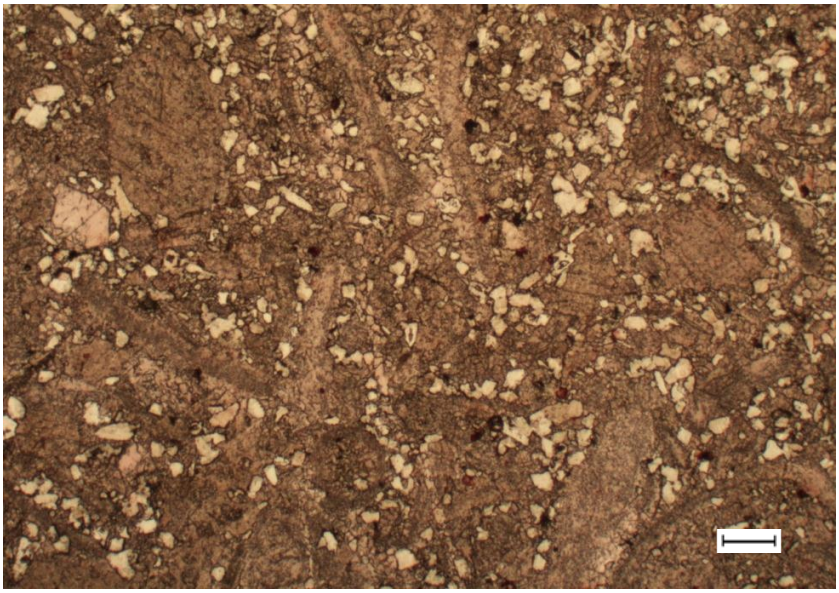

Figure 81: Thin section from the upper part of bed 6 showing abundant, rhombohedral dolomite (PMO 221.626). Scale bar = 100 µm.

Thin sections of some burrows show a higher abundance of dolomitization than in the surrounding areas, e.g. PMO 221.626 (Figure 82).

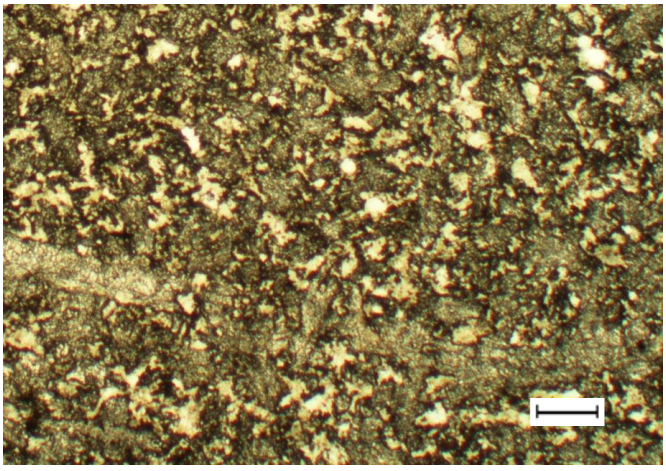

Figure 82: Matrix in burrow which is replaced by dolomite (PMO 221.626). Scale bar = 100 µm.

Investigated, stained thin sections of cemented cephalopod conchs show no signs of dolomitization.

Observations of dolomite in context with stylolites is present in PMO 221.485 where vertical dissolution seams cut dolomite crystals, while unfractured dolomite crystals are concentrated in horizontal dissolution seams.

6.2.3 XRF core data

Enrichment of the elements manganese (Mn), iron (Fe), phosphorous (P) and sulphur (S), is used as indicators of hardground horizons (Flügel, 2004). The following gives a short evaluation of important trends of the relevant elements through the analysed core (Figure 84).

Trends of P

A high phosphorous content of 150-250 ppm can be observed from the XRF plot in the interval 30-60 cm from the base of the core. Particularly bed 2 and 3 seem to have an overall higher content of phosphorous compared to the remaining beds. Close up to the upper boundary of bed 4, a 3 cm thick dark stain in the core corresponds to closely spaced peaks of phosphorous. Burrows can also be identified in the specific interval. Several of the phosphorous-peaks in the graph occur where the sediments imaged in the core appear as dark colured or in the proximity of lithological contrasts and burrows.

Trends of S

The sulphur content through the core fluctuates in the interval between 0-100 ppm, only with a few exceptions of higher enrichments. In the lower part of bed 1, a peak of approximately 120 ppm occurs, and can also be correlated by a moderate enrichment of phosphorous of 60 ppm. At approximately 85 cm from base, another 120 ppm peak occurs, and can be associated with a lithological contrast on the imaged core. At 92 cm from base, a 200 ppm peak appears, and traces of burrowing are evident in the core image. A new sulphur-peak at 142 cm from base can also be associated with burrows. A minor peak, reaching 100 ppm is evident in the upper part of bed 5. High amounts of S of 200-330 ppm occurs in the upper 20 cm of bed 6, again when the amount of burrows is high.

Trends of Mn

The amount of manganese thorugh the core seems to increase steady towards the top of the unit. A few deviations of higher intensities are present in bed 5 and in the lower part of bed 6. An intense manganese-peak is observed at the upper boundary of bed 5.

Trends of Fe

The content of iron fluctuates between 0-2000 ppm, except from at 85 cm from base, at the top of bed 6 (190 cm from base), and at the top of bed 5 (163 cm). In the latter case, the concentration is 60 000 ppm. Any correlative structures imaged in the core reflecting the iron-peaks have not been identified, apart from the two enrichments near the upper parts of bed 5 and 6.

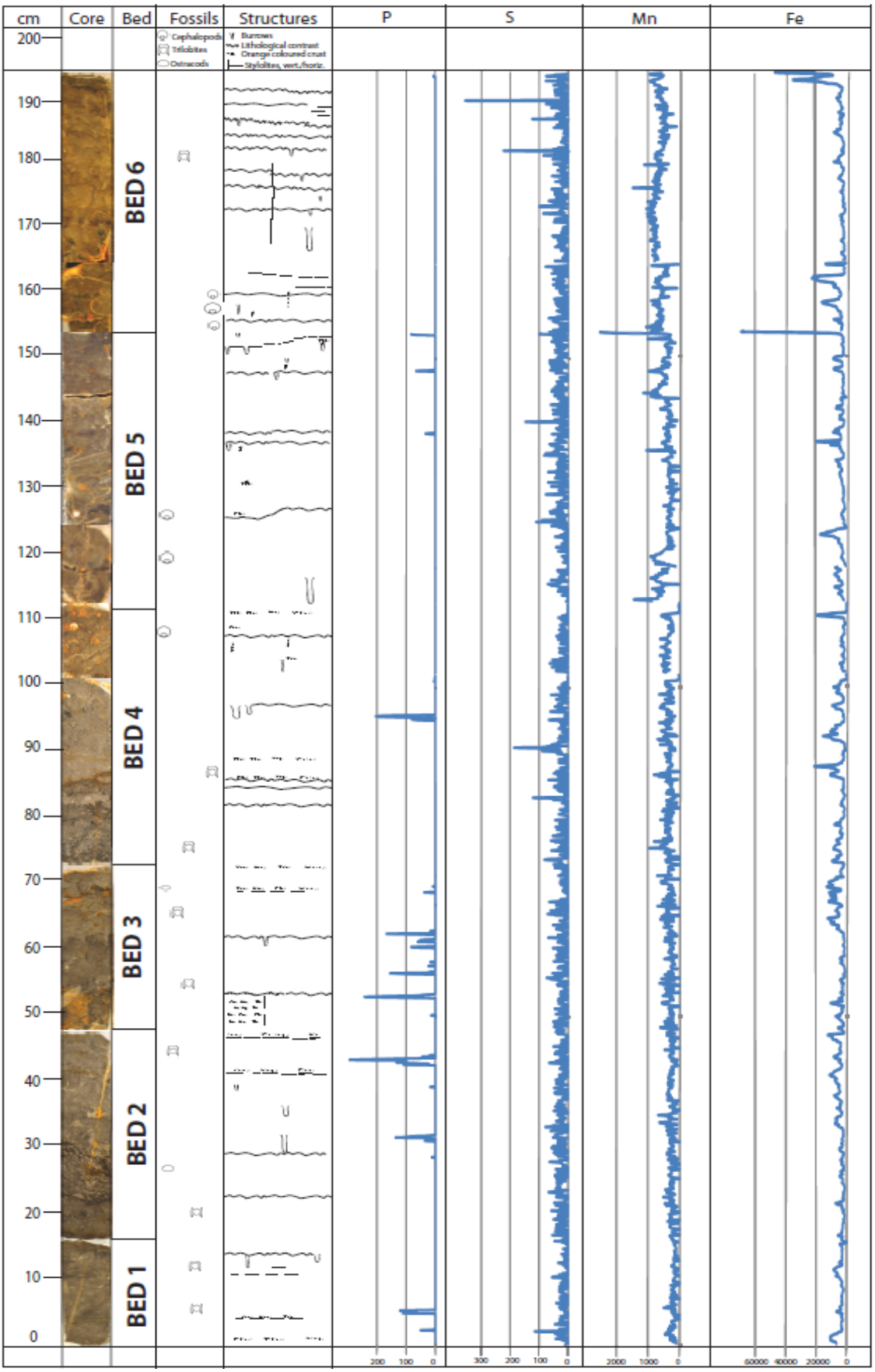

Figure 84: Core image, fossils and structures in core, and XRF plot of P, Mn, S and Fe.

6.2.4 Isotopes

12 samples with approximately 15 cm spacing was extracted from the artifical core, avoiding cemented areas. The ratios $\delta\ ^{13}C\ /^{12}C$ and $\delta\ ^{18}O/^{16}O$, are plotted below.

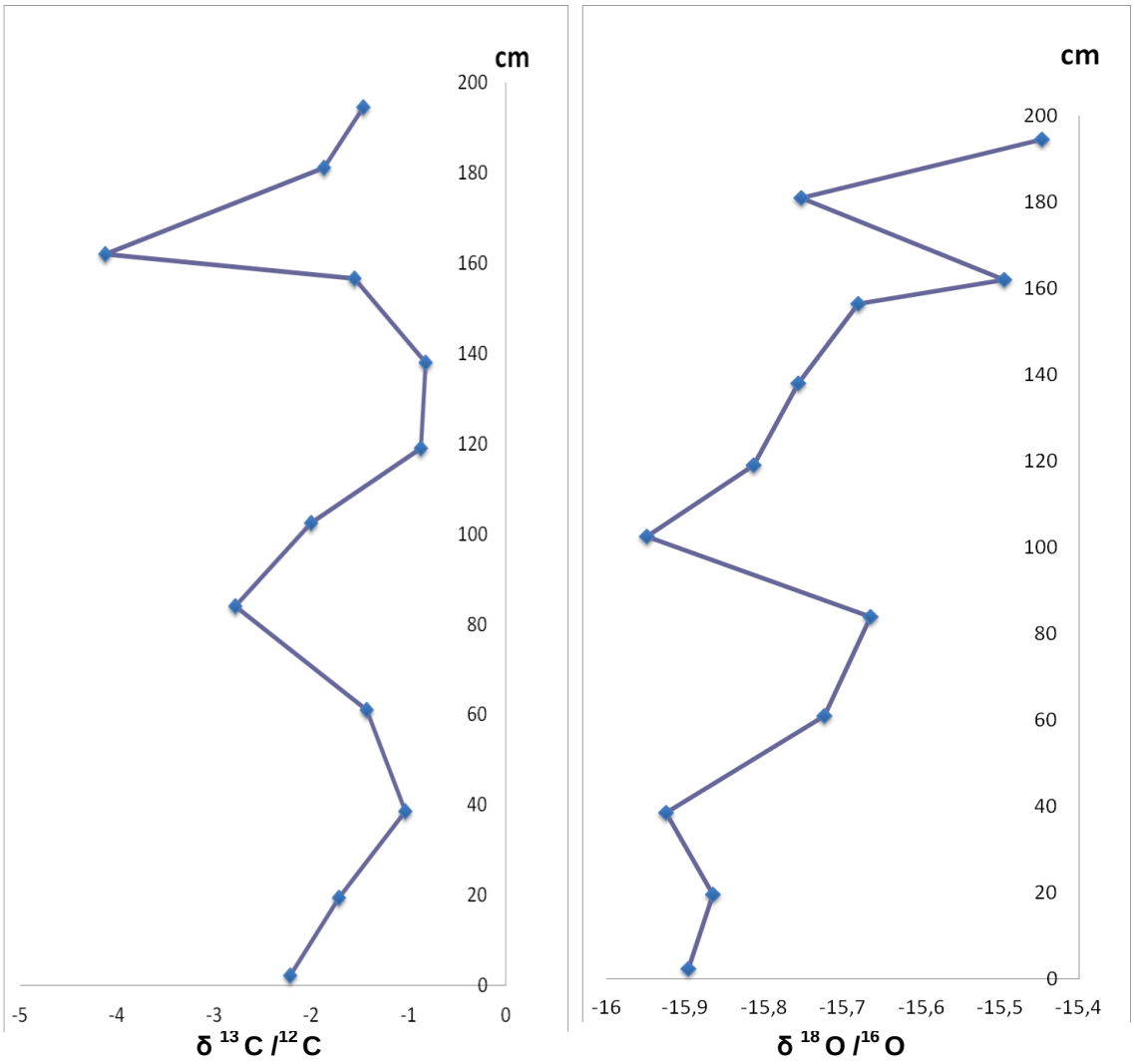

Figure 85: Plotted values of $\delta\ ^{13}C\ /^{12}C$ and $\delta\ ^{18}O/^{16}O$ from the artificial core.

Since oxygen isotopes are prone to be re-set by circulating hydrothermal circulation, a calculation of palaeotemperatures was performed on the O-values, in order to check if the isotopes have been modified. An apparent covariation between the two isotopes seems to take place, shown by the negative increase in the magnitude of ^{13}C and the positive increase of ^{18}O (e.g. at 0.80 m from base).

6.2.5 Magnetic susceptibility

Magnetic susceptibility of the artificial core was measured every fifth cm.

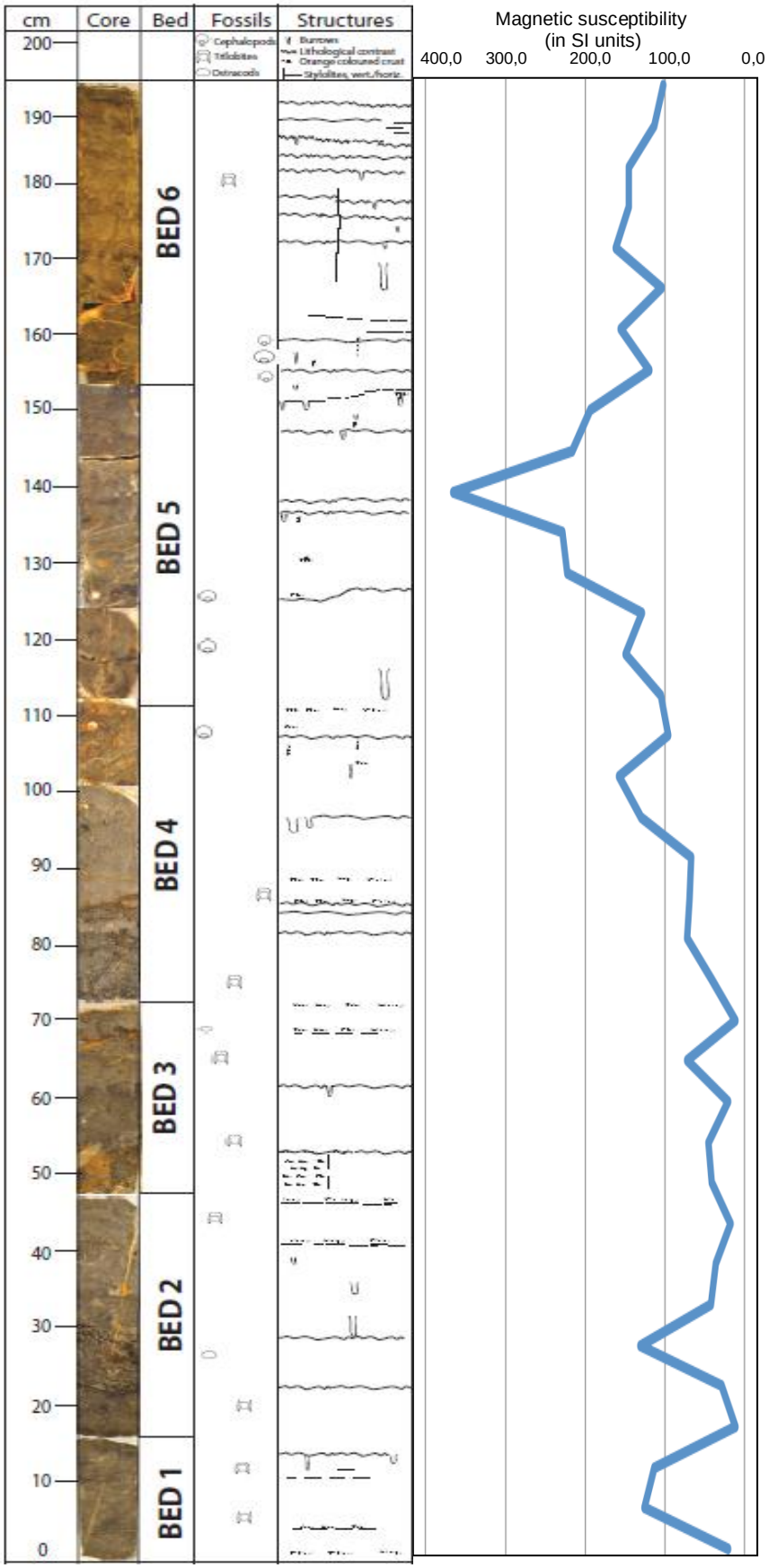

Figure 86: Variations in the magnetic susceptibility through the Svartodden Mbr.

6.2.6 Cathodoluminescence microscopy

Variations of cement generations are visible through CL microscopy, and can indicate a shift from oxidizing porewater to reducing porewater, with a luminescence change from light orange (favouring Mn^{2+}) to non-luminescent (favouring Fe^{2+}). The pore water-filled siphuncles in cephalopods were prone to become cemented due to the open space in which mineral growth could occur. The cement generations are identified based on Tucker (2001).

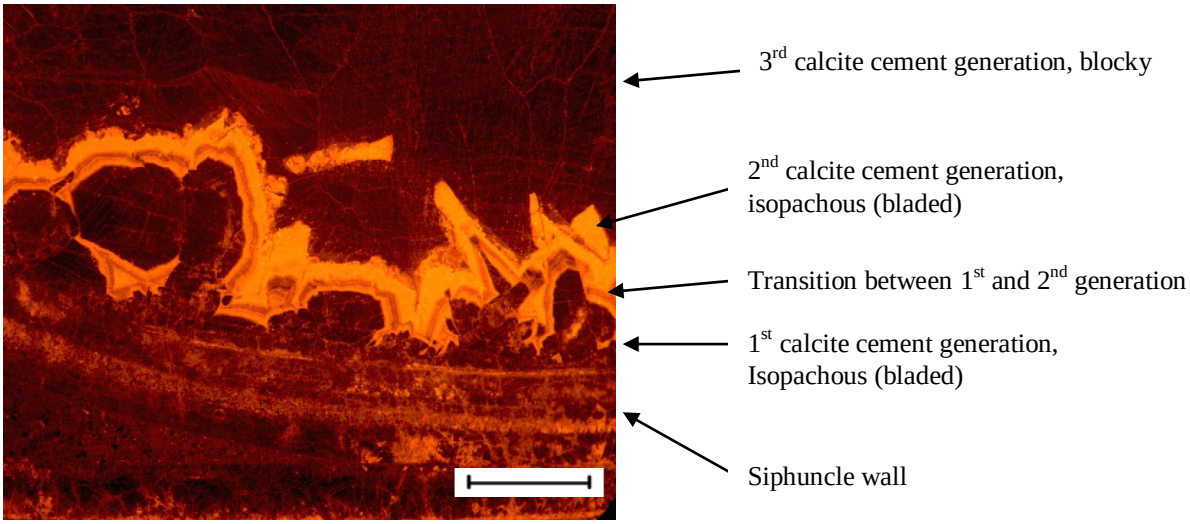

Figure 87: CL-photo showing 3 cement generations (PMO 221.482). Scale bar = 500 µm.

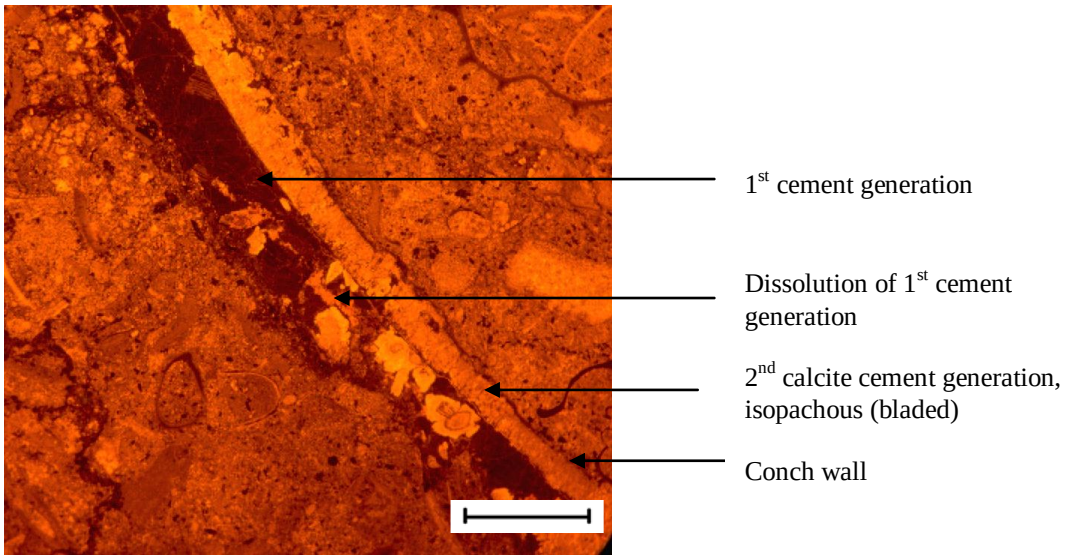

Figure 88: CL-photo showing 2 calcite generations and a missing 3rd generation cement (PMO 221.483). Scale bar = 500 µm.

The CL study of the cemented cephalopod siphuncles in PMO 221.482 showed two different generations of cement precipitation (illustrated above in Figure 87), and two phases of cement dissolution. The first stage of cement precipitation is shown by a non-luminescent cement, in the wall of the siphuncle. The second generation cement shows continous growth with transition bands from the non-luminescent primary cement. The second cement is orange in colour. Dissolution of the first generation cement is evident in the siphuncle within the boundaries of the secondary cement. The second generated cement shows also signs of dissolution near the top beneath the overlying vadose-silt, which has being transported with the porewater. The third generation of cement occurs above the vadose silt, and fills the remaining space of the siphuncle. Three types of cements are identified; bladed prismatic cements, blocky cement and coarse mosaic cements.

PMO 221.483 showed two generations of cementation, and one episode of cement dissolution. The cementation history of the conch began with dissolution of the aragonitic test, followed by the 1st cement generation with a non-luminescent colour in oxic porewaters. The 1st cement generation was then partly dissolved, and the 2nd generation, orange luminescent cement was formed. Compared to PMO 221.482, a third generation of cement is missing.

6.3 Facies descriptions

Sedimentological facies can be described as a specific sediment-body which has formed in a restricted area having a specific depositional setting (Boggs, 2006). In addition, the concept of facies was described by Moore (1949 *in* Boggs, 2006), as ”any areally restricted part of a designated stratigraphical unit which exhibits characters significantly different from those of other parts of the unit.”

In the case of the studied members of the Huk Fm. and the Elnes Fm., facies are recognized based on evidence from their depositional texture, field logs and observations, structures and characteristics seen in thin section samples. Facies boundaries are based on the occurrence of abrupt changes in characteristic features of the rocks, representing shifts in the depositional environment, e.g. the transition from limestone to mudstone facies. The observed facies in this

study have been categorized into three distinct facies associations, presented in Table 4 as F1, F2 and F3. The thicknesses of the facies and facies associations are based on field measurements from the logged section at the Slemmestad IF arena locality. Baseline is set 20 cm below the boundary between the Lysaker Mbr. and the Svartodden Mbr.

Table 4: Summary of the 3 associated facies related to the Svartodden Mbr.

Facies No.	Facies	Texture	Biological / physical structures	Height above base
1	Nodular limestone	Shales, mudstone and wackestone	Bioturbation, body fossils, lamination, calcite nodules,	0-0.20 m
2	Massive limestone	Wacke- and packstone	Highly bioturbated, poor sorting, bodyfossils, flame structures, pyrite and dolomite rich	20-1.41 m 1.44-2.23 m
3	Calcareous mudstone	Shales, carbonate mudstone	Good sorting, body fossils	2.23-2.43 m

Facies 1: Nodular limestone

Figure 89: Nodular limestone facies (F1); intercalations of carbonate nodules and shale. Scale bar = 10 cm.

The nodular limestone facies is characterized by the intercalations of marl and limestone laminae, where the limestone nodules have a slightly more brownish colour than the shales

which are light grey coloured. The limestone shows a mudstone to wackestone texture, and appears as isolated elongated nodules. The unit is traceable as the lowermost lithology which outcrops at the Slemmestad IF arena locality, with a prominent bedding surface, predominantly of shales. The bedding surface shows several complete trilobite specimens, imprints of endocerid cephalopods, brachiopods and bioturbation. In vertical section, most of the limestone nodules are easily weathered probably due to diagenetic alterations (Figure 89).

Facies 2: Massive limestone

Apart from bedding, very few primary sedimentary structures have been observed in the unit during field studies. The absence is most likely caused by the high amount of bioturbation, diagenetic alterations and weathering. The limestone is regarded as thick bedded consisting of several thin-bedded sub-beds. The lowermost part of the unit, bed 1, is characterized by a higher amount of argillaceous limestone, and shows a transition from mud dominated to a more carbonate dominated deposition. The deposits appear condensed, witnessed by truncated cephalopod conchs, irregular bedding boundaries marked by lithified *Skolithos* burrows.

Figure 90: Weathered (yellow and brown coloured) and fresh (grey) surfaces of the upper part of F2 (the Svartodden Mbr.). Scale bar = 4 cm.

Facies 3: Calcareous mudstone

The lower boundary of this lithology is distinguished by a sharp lithologic contrast from yellow limestone (F2) to brown-grey coloured, fine grained marl, which is rich in calcium carbonate. Observable features in the unit are large and abundant trilobite fragments.

Figure 91: A. F3 with its lower contact resting on F2. Scale bar = 5 cm.

6.4 Facies associations

Based on the observed features in the distinct facies descriptions, the process-response relationships in question will be discussed. Based on the deductions obtained from the active processes responsible for the different sedimentological features of each facies, one can infer the depositional environment (James & Dalrymple, 2010). The distinct facies and their characteristics facies associations are presented in Table 4, as well as their occurrence in the simplified stratigraphical column. Thicknesses of facies and facies associations are based on the stratigraphical thicknesses observed during field logging of the rock sections.

The depositional environment causing formation of nodular limestone facies, as observed in Facies 1, was discussed by Möller & Kvingan (1988). Two main factors in the genesis of nodular limestone facies were reported. The first was large scale cyclicity caused by sea-level changes, in combination with bed variations due to changes in water agitation and organic surface productivity. The second proposal was an early diagenetic formation of the nodules by

calcium carbonate cementation. The light grey colour of the enclosing shale, opposed to black shale, indicates well-oxygenated conditions.

The presence of the nodular limestone facies (F1) presented above, may indicate that the deposition took place in a neritic environment below storm-wave base, due to the observed neritic fauna (brachiopods, trilobites), and apparently the lack of primary sedimentary structures. The observed fauna in the massive limestone units (F2) consists of cephalopods, bryozoans, trilobites, ostracodes, brachiopods, echinoderms, conodont animals and ichnofossils, suggesting a shallow neritic and well-oxygenated shelf environment, possibly between normal wave base and storm wave base, in the photic zone (< 150 m). The main current direction was probably running NE-SW. The sub-beds of bed 3-6 probably became early semi-lithified, forming firmgrounds. Eroded upper halves of cephalopod conchs are a common feature in the unit, and can be related to bioerosion, erosion and dissolution on the seafloor. It is believed that the sedimentation rate in the area was very low, based on the abundant microborings on skeletal grains, as seen in Figure 63, Chapter 5.

Abundant excavating *Asaphus* trilobites formed horizontal burrows and tunnels in bed 6. Observations of microstromatolites on bedding surface 6 further strengthen the assumption of a hardground setting marking the transition to the overlying facies F3. The limestone facies F2 corresponds to the Svartodden Mbr. The depositional setting of the Svartodden Mbr. is believed to have taken place on an extensive widespread carbonate platform, based on the resemblance in fauna associations northwards towards the Mjøsa area, westward to the Eiker-Sandsvær area and eastwards into Sweden.

The limestone dominated marl facies (F3) shows a rich trilobite fauna and no cephalopods or hardgrounds. Hansen et al. (2010) assumed the facies to represent a somewhat deeper marine setting with less energetic bottom conditions compared to the overlying limestone facies. The unit corresponds to the lowermost part of the Helskjer Mbr. and is belived to mark a drowning event, known as the Helskjer drowning (Hansen et al., 2010).

6.5 Discussion

6.5.1 Environmental conditions and regional setting

In contrast to modern conditions, the precipitation of calcite in Lower Palaeozoic seas was dominated by preferred precipitation of low-Mg calcite, due to the lower concentrations of Mg^{2+} ions in the seawater (Stanley & Hardie, 1998). This can be related to the precipitation of calcite mud, which most probably was dominated by low-Mg calcite.

The epicontinental sea covering most of Norway and the rest of Baltoscandia during the early Middle Ordovician (465 Ma), was a site of extensive deposition of limestone-, marl- and shale-facies sediments. The input of terrestrial material was variable, but generally low. As previously mentioned, Baltica was positioned approximately 30 º S during the Darriwilian, and the corresponding climate is believed to have been temperate-subtropic, with a sea water temperature of approximately 20 ºC. The climatic conditions during the period are believed to have been stable, based on the consistant faunal assemblage. Sea levels during the deposition of the Huk Fm. in the Oslo-Asker area fluctuated from a regression mirrored by the deposits in the Hukodden Mbr. to several regressions and transgressions during the Lysaker Mbr. and to a highstand level observed in the Svartodden Mbr. (Nielsen, 2004).

The regional extent of the Svartodden Mbr. can be traced eastwards to the Eiker-Kreklingen area, thinning southwards to the Skien-area, thickening northwards to the Mjøsa area (Skaar, 1972), and eastwards into the equivalent Holen Fm. in Sweden, where the unit is considered as more condensed than in the Oslo-Asker area. It has been suggested that the Svartodden Mbr. was deposited in a shallow marine environment well above maximum storm wave base, but below fair weather wave base (Hansen et al., 2010). Until the onset of the deposition of black shales, a land area positioned on the western margin of Baltica, called the Telemark land (Hansen et al., 2010) is believed to have been subaerially exposed. Conglomeratic sandstone facies on the edge of this shallow exposed land is thought to have been deposited in a beach environment on the epicontinental platform.

During the Cambrian period, the extensive deposition of the organic rich black mud is believed to have covered most of Baltoscandia, including the Telemark land on the western margin of Baltica, onlapping on the basal conglomerate deposited on the eastern margin of the Telemark land. A continued global transgression during the Lower and Middle Ordovician

(Nielsen, 2004) and limited input of siliciclastic material on the shallow shelf (Owen et al., 1990) promoted a widespread deposition of carbonate sediment on the extensive epicontinental platform on Baltica.

Based on previous interpretations of the depositional setting on the western margin of Baltoscandia, a model is presented in Figure 92. The model illustrates the regional depositional environment as a shallow and widespread seafloor covering the continent from west to east. Telemark land and Trondheim land are believed to have been shoals, with low reliefs above the sea level, based on the low siliciclastic input during the deposition of the Huk Fm. The land areas may have been significantly more important as sources of siliciclastic material during the onset of the Caledonian compressional deformation, possibly from the Sandbian (Late Ordovician) and onwards. It should be noted that Bjørlykke (1974) and Schovsbo (2003), among others, have suggested that obduction of island arcs on the western flank of Baltica, contributed with the main part of siliciclastic material in Baltoscandia.

On a more detailed level, the deposition of the Huk Fm. in the Oslo-Asker district was marked by the change from a deep to a shallow shelf environment, shown by the graptolitic shale facies of the Tøyen Fm. to the trilobite rich limestone facies observed in the Hukodden Mbr. The continuing deposition of the nodular limestone facies witnessed in the Lysaker Mbr. reflects interchanging deposition of muds and more calcium carbonate rich material.

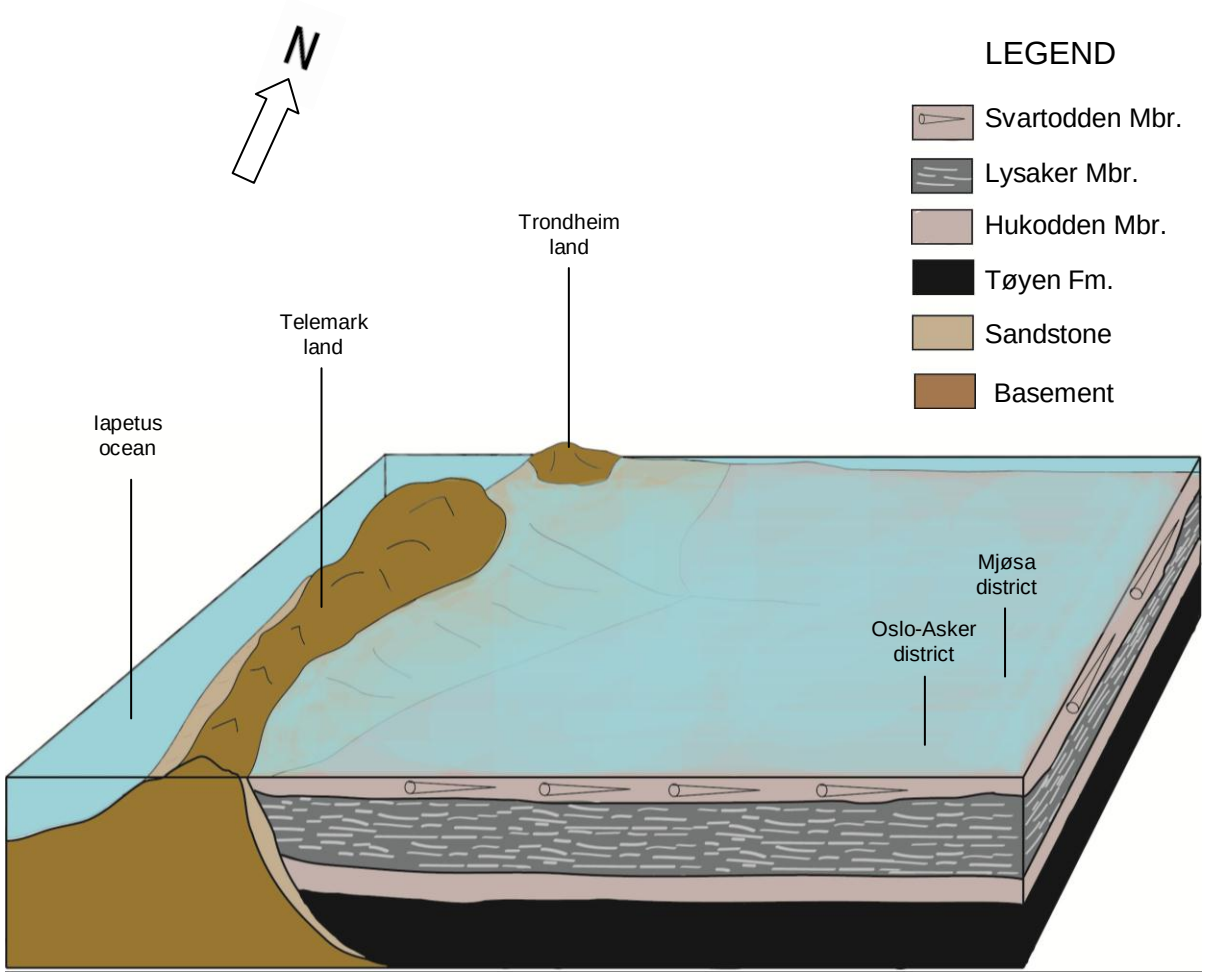

Figure 92: A shallow depositional setting on the western border of the epicontinental shelf of Baltoscandia (based on the interpretation by Hansen et al., 2010).

6.5.2 Classification of the Svartodden Mbr.

After Dunham's classification of limestones according to depositional textures, the Svartodden Mbr. is classified as a *partly dolomitized packstone*. The sediments are portrayed by a grain-supported calcium carbonate contributing fauna, rich in endoceratid cephalopods, trilobites, echinoderms, acrotretid brachiopods, ostracodes and bryozoans. The matrix is mostly made up of microcrystalline micrite with grain size < 0.03 mm. The further details of the microfacies analysis is presented in the Appendix 7.

6.5.3 Depositional environment

Net sedimentation rates of the Svartodden Mbr. is considered as low, compared to the more shale rich Lysaker Mbr. Based on chronostratigraphy (Nielsen, 2004) and the stratigraphic thickness of the unit (2.0 m), the net sedimentation rate during the deposition of the Svartodden Mbr. is believed to have been approximately 0.4 cm/1000 years after compaction, although significant amounts of sediment may have been removed during firmground events.

The facies association interpreted from the limestone deposits of the Svartodden Mbr. suggests a shallow, continental shelf, with a very low gradient and wide lateral extension. According to Boggs (2006), the presence of micrite in ancient limestones indicates a deposition in quiet water conditions, meaning that the winnowing was low and did not remove the mud.

The quartz grains present in the acid insoluble residue samples ranging through the complete Svartodden Mbr. were most likely transported and primary deposited. Regarding the latitudinal position of Baltica, subaerially exposed land areas may have been sources of desert sands, and during storms, particles might have been transported long distances, and eventually been deposited in the area.

Based on the presence of microstromatolites and hence microbial mats, the seafloor was probably in the photic zone, and the sea level is believed to have been shallower than 150 m, some place between the inner and neritic shelf setting. Although Skaar (1972) observed ooids in the unit and suggested a sea level of 20 to 40 m, the missing observation of ooids in this study makes the interpretation of a precise sea level depth difficult.

The thin bedded stratigraphic units composing the more thick bedded segments of the Svartodden Mbr. (bed 1-6) is characteristic of condensed sections. The repetitive occurrence of thin beds (approximately 5 cm in thickness) in beds 3-6 may reflect a stable shelf environment. Observations support the interpretation of an environment with periods of higher carbonate production followed by periods of no net deposition and condensation, forming firmgrounds or possibly hardgrounds.

Based on star shaped patterns of cephalopod conchs on bedding surface 4 (Figure 47), a polymodal current direction seem to have been dominating. On bedding surface 6, the current

direction was running from the N-E direction, possibly suggesting incoming currents from the Iapetus Ocean in between the Telemark land and the Trondheim land to the north-west. The large amount of benthic and endogenic activities witnessed from burrows and tunnels indicate that the seafloor was oxic. Based on varying amounts of corrosion on cephalopod conchs through the unit, the sediment influx to the seafloor was variable, with periods of high productivity and low productivity of the calcium carbonate secreting organisms. The conchs, which were up to 10 cm in diameter, were probably exposed to bioeroding agents for long periods of time, experiencing massive dissolution.

The minor burrow production observed in bed 1-2 may represent higher sedimentation rates in these beds, due to a higher input of terrestrial material and/or a higher productivity on the shelf. The observation of flame structures, representing water escaping from clay into carbonate sands, in bed 2 also indicate a higher content of siliciclastic material at this level.

Analysis of the weathered, logged section in field and the artificial polished core shows when combined, a better data set regarding interpretations of bedding and sub-beds. Frequent *Skolithos* burrows observed in the core from bed 3 and upwards, are easier to characterize than the same trace fossils in vertical outcrops. *Skolithos* are believed to have been produced during periods when the sediment was semi-consolidated, and later became partly cemented into firmgrounds. Hence, the burrows became preserved as open galleries while new, increased sedimentation filled the pre-omission burrows. This can explain the occurrence of several episodes of firmground formation in the Svartodden Mbr., described more in detail below. Based on the collected data, it is proposed that bedding surface 6 evolved into a hardground, in which several of the hardground characteristics have been identified. It is possible that other distinct hardgrounds occur in the unit, but restricted information gained from outcropping bedding surfaces complicates the identification.

The following evidences for hardground formation from bedding surface 6 are summarized below:

I. Lithologic contrasts causing the formation of a separate bedding surface
II. > 50 % of the cephalopod conchs in vertical section have been truncated by bioerosion, erosion and dissolution.

III. Deposition of shale infilling in the *Thalassinoides* traces marking a possible regional sea level highstand event
IV. Limonitic impregnations of iron and possibly phosphate
V. Microstromatolites

The variable concentrations of the elements Fe, S, P and Mn through the artificial core has also provided further information about possible hardgrounds in the unit. All of the elements above show higher concentrations near the upper boundary of bed 5, possibly indicating formation of a hardground. Enrichment of iron is apparent just below the top of bed 5 and bed 6, and could be seen in context with the mineral staining of bedding surface 6 and in the vertical section of the uppermost part of bed 5. However, no additional data supporting a hardground has been obtained due to a missing bedding surface of bed 5.

The abundant pyritization in the peripheries of the burrows can be associated with the enrichment of sulphur at same levels. Increased phosphate levels in the XRF-data are often witnessed in context with burrows and sub-bed boundaries which most likely represent condensed surfaces, based on the formerly described pre-omission *Skolithos* burrows. The depositional environments causing enrichment of phosphate in the epicontinental sediments of Baltica, has been discussed by several authors. Trela (2005) reported seasonal changes in upwelling-currents caused by Ekman transport, witnessed by phosphate enrichment in sediments from Ordovician limestones in Poland. The accumulation of phosphates was believed to have evolved in combination with low sedimentation rates due to a slow carbonate production by a temperate water biota (Trela, 2005).

Nordlund (1989) described phosphatic hardgrounds from Öland in Sweden from the Volkhov/Kunda boundary, the same time interval as when the deposition of the Svartodden Mbr. took place. The phosphatic surfaces in vertical section observed in the limestone in Öland, shows similar characteristic phosphate-features as those recorded in the Svartodden Mbr., e.g. a soft- and hard- bottom fauna, pyrite, and eroded siphuncle tubes. However, certain observations in the current study are not shared, e.g. ooids, glauconite and intraclasts. The depositional setting causing the accumulations of phosphatic surfaces was explained by Nordlund (1989) as to have formed while blankets of organic material was deposited on a semi-emergent to emergent seafloor. During diagenetic processes, the breakdown of organic material was likely to have caused the release and precipitation of phosphates. The

depositional conditions were likely to reflect periodical fluctuations in depth, fluctuating between submergent, semi-emergence and emergence of the seafloor (Nordlund, 1989).

Phosphorite beds in the Svartodden Mbr. were reported by Skaar (1972), and the enrichment was explaned in terms of accumulated fossil residue and excrements on the seafloor, during periods of condensed sedimentation. The idea of upwelling as an additional trigger of phosphorite beds on the shelf in the Oslo area was regarded as less likely by Skaar (1972).

If the upwelling should have played a significant role in the concentration of phosphorite, one should assume that the upwelling occurred on the western margin of Baltica. Nutrient rich water may have been transported between the Telemark land and the Trondheim land, and in the ocean between Telemark land and Avalonia to the south-west. These suggestions are based on the directions of the surface ocean currents in the Iapetus Ocean during the period, reported by Cocks & Fortey (1990), Finney & Xu (1990), Wilde (1991) and Barnes (2004), which could promote Ekman currents from deeper sea levels, as suggested by Trela (2005). In addition, genesis of phosphatic hardgrounds in time-equivalent limestones in Sweden is related to sea level fluctuations forming periods of submergence, semi-emergence and emergence of the seafloor. Phosphatic hardgrounds are related to periods when the seafloor was semi-emerged or emerged (Nordlund, 1989). Based on this hypothesis, it is suggested that the sub-bed boundaries observed in the Svartodden Mbr. reflect periods of higher accumulation of organic material, during periods of lowered relative sea level. The accumulated organic matter on the firmgrounds would eventually lead to the enrichment of phosphate during burial and diagenesis.

The following lists and illustrates interpretations of incipient firmgrounds on the sea bottom, and the subsequent formation of a hardground, based on the results presented above.

Firmground evolution

I. During periods of semi-submergence of the seafloor and a very low sediment input (carbonate mud, skeletal debris and terrestial material), an upper layer of sediments on the seafloor became semi-lithified by an early cementation of the carbonate mud, seen as pre-omission burrows of *Skolithos*.

II. A fauna typical of firmgrounds, consisting of possibly two species (or more) of tunneling trilobites, ostracodes, bryozoans, crinoids and brachiopods colonized the seafloor. Abundant trilobites formed one (or two) type(s) of complex tunnel systems below the sediment surface.

III. Accumulated organic material covered the firmground and filled the burrows.

IV. Pyritization of the open burrows is believed to have taken place while animals were still using the tunnel systems in a slikely reducing environment.

V. Organic decay of the organic matter during burial and diagenesis released phosphate, which appears today together with pyrite on the firmground sub-bed boundaries as weathered brown, crusty laminae.

After the events presented above, it is believed that the firmground either became buried due to enhanced sediment input, or the condensation continued.

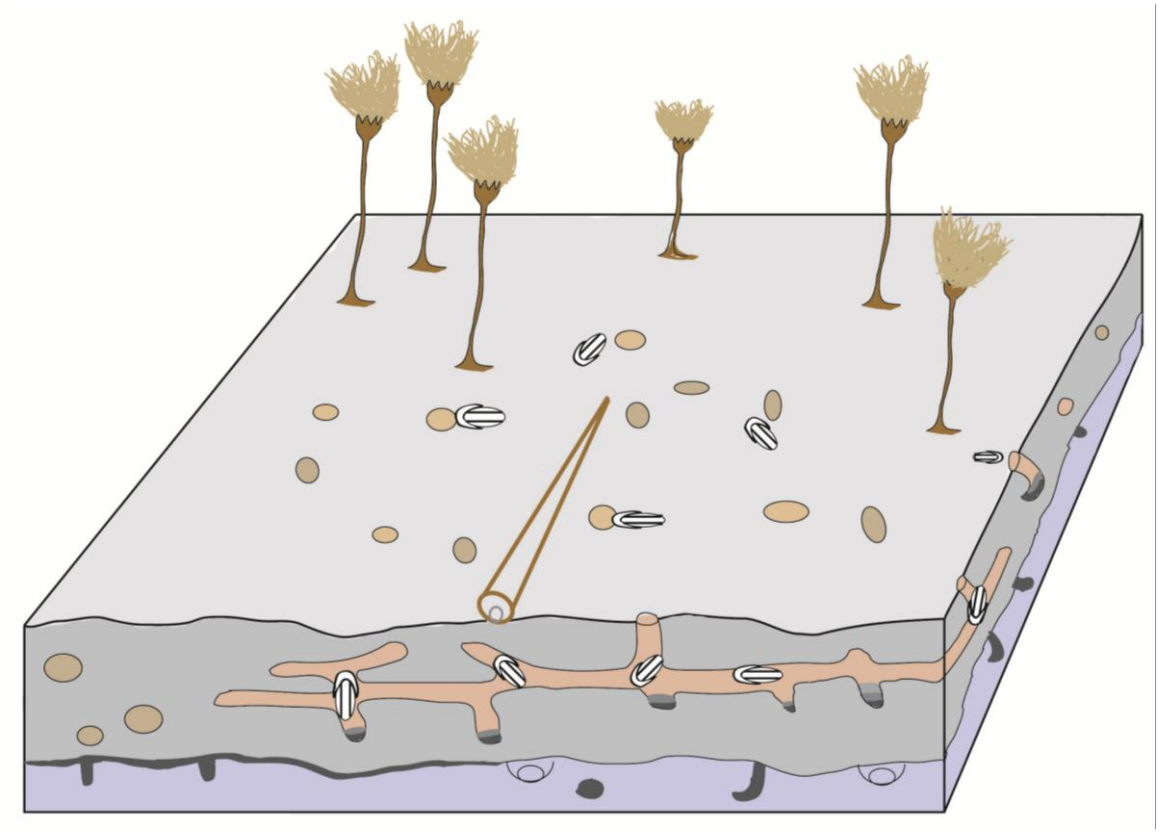

Figure 93: Illustration of firmground environment in bed 6 with high activity of burrowing trilobites and a low, steady input of skeletal debris. The firmground fauna is presented in Chapter 5.

I. A low sealevel during semi-emergence of the seafloor continued, in addition to a very low sediment input.

II. During continued condensation of the firmground, erosive agents such as bioerosional organisms such as algae, bacteria and fungi became more abundant, causing borings and fragmentation of skeletal grains.

III. Several semi-lithified burrows and tunnels of *Thalassinoides* were filled by silty material.

IV. Mobile grains of lithified sediments did most likely scour and winnow the seabottom, truncating trilobite tunnels and cephalopod conchs, possibly removing a considerable amount of the pre-existing bed.

V. Microbial mats as present microstromatolites and possibly oncolites, colonized the hardground.

VI. The final stage of the hardground was marked by an increase in the sediment input, providing a new basis for a firmground or a new depositional cyclus.

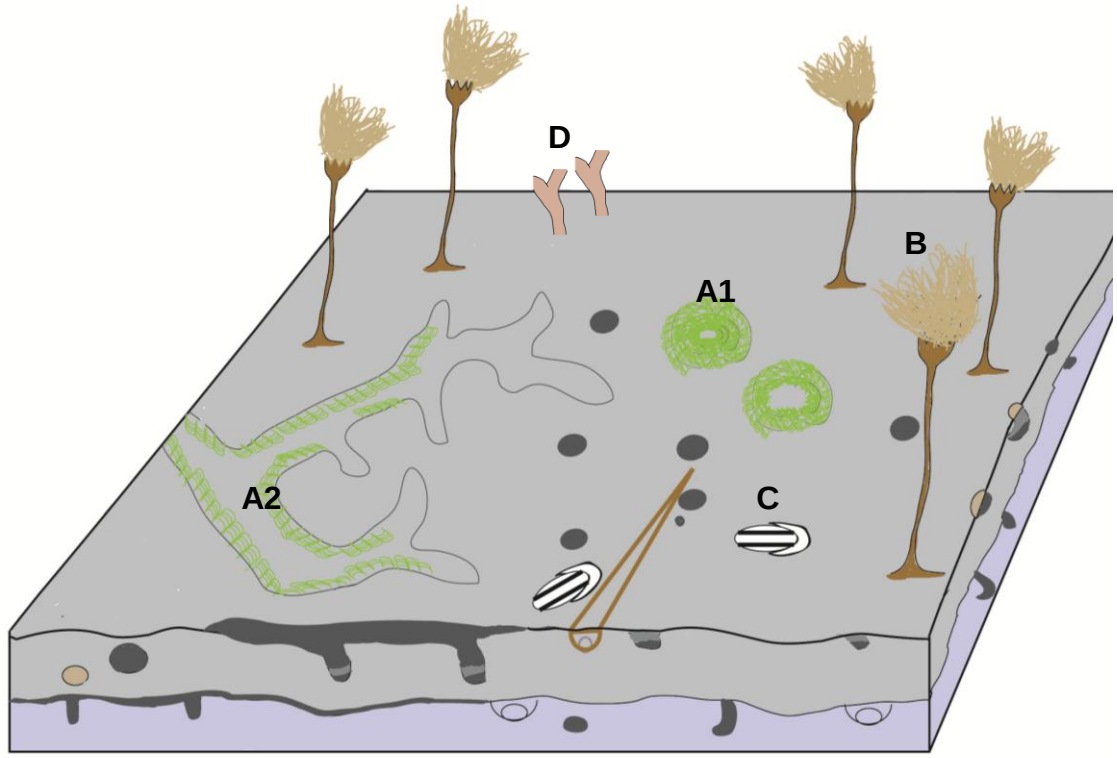

Figure 94: Illustration of the hardground setting and hardground fauna on bedding surface 6 of the Svartodden Mbr., containing microstromatolites (A1), microstromatolites in burrows (A2), crinoids (B), trilobites (C) and possibly bryozoans (D). The complete fauna is illustrated in Figure 67 in Chapter 5.

In the specific case of the hardground evolved on bedding surface 6, it is suggested that the relative sea level was lowered, based on the sea level reconstruction curve by Nielsen (2004). A hiatus between the Svartodden Mbr. and the Helskjer Mbr. has also been reported by Nielsen (2004) and Bruton (2010), before the deposition of the marly limestone dominated Helskjer Mbr. continued during a rising sea level and eventually drowing (Nielsen, 2004).

Magnetic susceptibility of the artificial core shows fluctuating levels in the unit, however, no particular cyclicities have been observed. The sample-frequency of 5 cm may have been too low to detect any trends.

6.5.4 Isotopes

Until the present study, no studies of carbon and oxygen stable isotopes have been performed on sediments from the Huk Fm. Isotopic signatures of Ordovician seawater from marine authigenic precipitates, such as carbonates, are well suited for chemostratigraphical and palaeoenvironmental studies, and can reveal isotopic events in different lithologies across a continent or several continents. Interpretations based on isotopic data still remains a controversal subject, although several studies point to confident environmental scenarios during the Ordovician (Shields & Veizer, 2003).

Fluctuating levels of dissolved inorganic carbon (DIC) recorded in the oceanic stable isotope composition of $\delta\ ^{13}C$, can be used to interpret environmental changes such as changes in the carbon circulation system of ancient oceans. Positive excursions in organic carbon are believed to represent increased biological activity and enhanced burial in epeiric seas, possibly caused by nutrient upwelling (Ainsaar et al., 2010).
Isotopic values of $\delta\ ^{18}O$ are known to be useful in Ordovician paleoenvironmental interpretations of seawater levels, temperature, salinity, pH and diagenetic alteration (Shields & Veizer, 2003). However, the quality of the isotope signals obtained from carbonate rocks depends on the degree of alteration of primary mineralogy, as well as diagenetic changes of the rock (Flügel, 2004).

Isotopes from altered rocks can lead to erroneous conclusions and hence the data should be tested. $^{18}O/^{16}O$ isotopic ratios are used in palaeo-seawater temperature calculations, and can

be used as a tool in revealing the preservation of the primary mineralogy of the host rock. If the obtained palaeo-temperature of the seawater gives a realistic value, one could assume that the isotopes obtained from the host rock are unaltered and present true signals.
The oxygen isotopic data from the Svartodden Mbr. can be tested accordingly by calculating palaeo-seawater temperature, as presented below.The temperature was calculated assuming $\delta^{18}O$ seawater = 0 ‰V-SMOW (dw).

The formula used in the calculation is the following:

$$T\ ^{o}C = 16.9 - 4.38\ (d_c - d_w) + 0.1\ (d_c - d_w)^2, \text{ where}$$

$$d_w = 0$$

$$d_c = -15{,}495$$

$$T\ (^{o}C) = 16.9 - 4.38\ (-15.495 - 0) + 0.1\ (-15.495 - 0)^2 = \underline{109\ ^{o}C}$$

The calculated palaeo seawater temperature of 109 ^{o}C indicates that the O-isotopes recorded from the Svartodden Mbr. are affected by warm hydrothermal water which circulated through the unit during deep burial depths. The obtained temperature might reflect the temperature of the hydrothermal solution, in addition to the original temperature when the calcium carbonate was precipitated.

The oxygen isotope graph shows a positive trend of the $\delta^{18}O$ content through the unit, which can represent an interval between a glacial/greenhouse transition. A partly climatic interpretation for the Ordovician trend of increasing $\delta^{18}O$ is supported by the observation that, once the long term trend with increasing calcite $\delta^{18}O$ through the phanerozoic is removed, four icehouse-greenhouse cycles, which have been independently confirmed by paleoclimatic studies, can be recognized in the $\delta^{18}O$ record (Veizer et al., 2000).

A composite carbon isotope curve for the Huk Fm. equivalent Holen limestone in Sweden (Ainsaar et al., 2010) presented below (Figure 95) is suitable in the correlation of the obtained isotopic data from the Svartodden Mbr. The Holen Limestone is an equivalent to the Lysaker Mbr., the Svartodden Mbr. and the Helskjer Mbr. of the succession in Norway. Hence, only the middle part of the Holen Limestone isotope graphs are possible to correlate with the one from the Svartodden Mbr. Compared with the Holen limestone which has an average $\delta^{13}C$ content of 0-1‰, the isotopic trend of the Svartodden Mbr. is more negative with 3 peaks

measuring a $\delta^{13}C$ content of -2,5 ‰or less. The question why the isotopic data from the Svartodden Mbr. are so substantially more negative compared to isotopic values from the Holen limestone, remains unanswered.

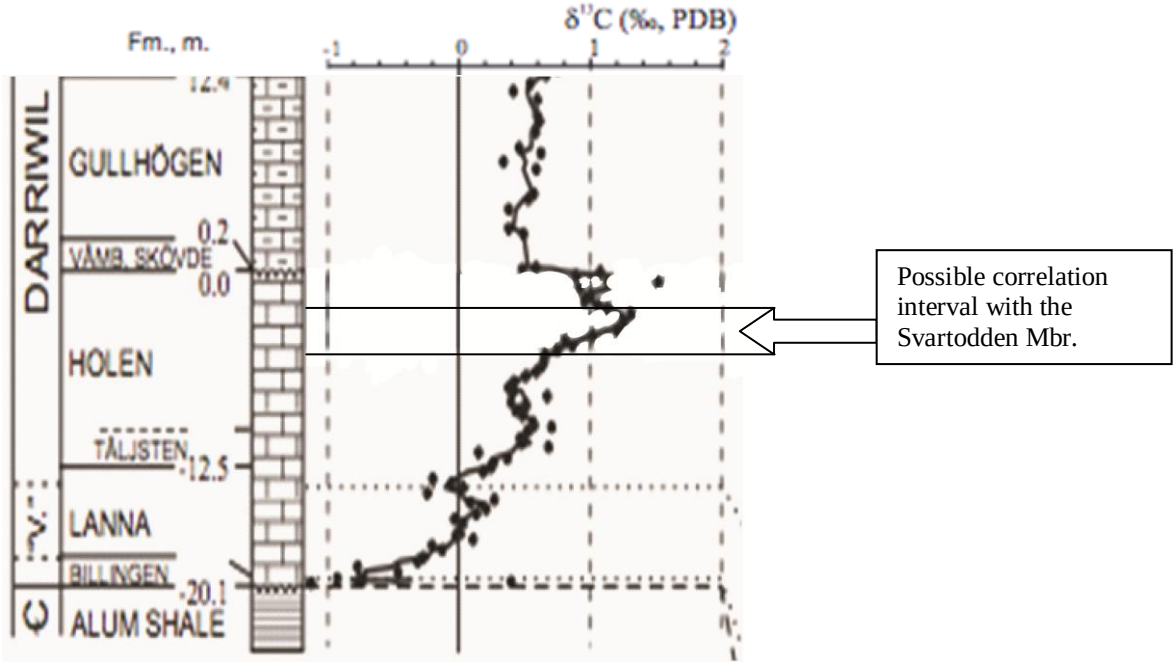

Figure 95: Middle–Upper Ordovician carbon isotopic record from Västergötland (Sweden). The arrow on right hand side indicates the section of the Holen limestone which is correlated with the Huk Fm. Modified from Ainsaar et al, (2010).

A gradual positive increase of $\delta^{13}C$ in Baltoscandic successions during the Middle-Ordovician is seen in context with a cooling of equatorial sea surface temperatures into modern day-like conditions (Ainsaar et al., 2010). Neither a positive nor a negative trend of $\delta^{13}C$ is possible to detect through the Svartodden Mbr. The more negative excursions of $\delta^{13}C$ through the Svartodden Mbr. compared to the rest of Baltoscandia could indicate a lower primary activity in this region during the Darriwilian.

Upper Ordovician $\delta^{13}C$ chemostratigraphy from the Oslo Region shows great similarities to time equivalent recordings from south-eastern and southern Estonia (Bergström et al., 2011), which might also be the case for Middle Ordovician rocks in the two regions. The $\delta^{13}C$ chemostratigraphy has proven useful to correlation of sea-level changes, recognition of Baltic stage boundaries and also with the correlation of rocks from North America and eastern Asia (Bergström et al., 2011).

6.5.5 Diagenesis

The interpretation of changes that occurred during the lithification of the Svartodden Mbr. is based on studies of thin sections and cemented conchs, as well as field studies.

Compared to siliciclastic rocks, carbonate minerals are more susceptible to dissolution, replacement and recrystallization processes (Boggs, 2006). During studies of diagenesis, one analyses and integrates depositional and diagenetic microfacies; depositional-processes acting during sedimentation, as well as diagenetic-processes acting after initial deposition until after lithification. Main features representing these diagenetic processes include pore-filling cementation, compaction and pressure solution, recrystallization and dolomitization (Flügel, 2004).

The diagenetic alterations observed in the Svartodden Mbr. are evident from changes in the rocks original depositional texture, such as porosity loss, chemical and mineralogical changes. A few diagenetic observations are discussed below, followed by an interpretation of the diagenetic history of the Svartodden Mbr.

Dolomitization

Dolomite, $CaMg(CO_3)_2$ may form by the replacement (dolomitization) of micrite or aragonitic/low-Mg calcite grains. The process depends on high amounts of Mg-rich circulating pore water, and is believed to have happened much later, possibly millions to hundreds of millions of years, after deposition took place (Boggs, 2006).

By analysis of the 21 stained thin sections comprising the unit, a gradual change in the degree of dolomitization was encountered. In bed 2, subhedral crystals with micrite cores are evident. The crystals measure approximately 20 µm or less, and have selectively replaced areas with calcitic micrite. A gradual increase of dolomite content is visible through the unit. In bed 6, dissolution of skeletal grains and calcitic micrite by the replacement by dolomite is present. The dolomite crystals are well developed, several showing euhedral surfaces, and measure approximately 50 µm or less. The concentration of dolomite in context with the highly oxidized nature of the unit in exposures does not seem to be related, unless the dolomite contains high amounts of iron.

Skaar (1972) suggested that dolomite in the Svartodden Mbr. was formed while the unit was shallow buried, and that dolomite crystals were redeposited around by the activities of trace fossils. Modern experiments indicate that precipitation of dolomite does not occur below a temperature of 60ºC and normal pressure, although geologic evidence have suggested that dolomite formed naturally at or in near-surface temperatures (Boggs, 2006). However, it seems questionable that the dolomitization in the Svartodden Mbr. occurred in the marine realm of diagenesis (shallow depths), when the previously suggested seawater temperature was approximately 20ºC. In addition, since the dolomite has replaced micrite and skeletal grains, dissolution of the low-Mg calcite original components would have had to occur before the dolomite replacement.

Conditions in which dissolution takes place are in chemically aggressive CO_2-charged porewaters in the meteoric realm, and also with an unstable mineralogy, low pH porewater undersaturated with calcium carbonate and low temperatures (Boggs, 2006). Considering dissolution occurring in the meteoric realm in relation to the distance to any subaerially exposed area (Telemark land), this process seems unlikely, unless the rock itself became subaerially exposed, a suggestion which is unsupported based on the character of the present studies. Hence, the origin of the dolomitization in the Svartodden Mbr. remains unresolved.

Bjørlykke (1974) and Skaar (1972) reported two events of dolomitization in the Huk Fm., one generation that formed early and one late.

Cementation histories

Neomorphism of calcium carbonate includes the transformation of aragonite to calcite (inversion), as well as recrystallization. During recrystallization which may take place near the seafloor, in the meteoric realm or in the subsurface burial realm, the size and shape of a crystal changes, with minor change in its mineralogy (Boggs, 2006). Cements have different kinds of crystal habits as well as CL optical characteristics, which may reflect the environment in which they were formed.

Based on the observations from the CL-microscopy, two different cementation histories were observed in the siphuncles and conchs. However, due to the limited amount of cephalopod

conchs seen in thin sections, it is possible that several other distinct cementation events took place.

Type I cementation (Seen in Figure 87, PMO 221.482)

1. Early formation of first generation calcite cementation (primary cement). Appears in CL as black with thin, light bands of bladed crystals. Precipitates within the conch above matrix infill. Suggested depth: < 2.0 km.
2. No cementation. Partial dissolution of the first generation cement, visible through vertical orange bands that are cutting the primary cement.
3. The aragonitic conch is dissolved (late) causing secondary porosity. Visible laminations of organic material from the conchs may be preserved. Suggested depth: approximately down to 2.0 km.
4. Second generation of calcite cementation (secondary cement) is light orange, precipitates in the former aragonitic conch, in the voids from the dissolved primary cement and in the remaining void in the center of the conch. Remains of organic tissue from the conchs may cause lamination with the secondary cement, crystallizing as smaller calcite crystals instead of regular sized ones. Suggested depth: 2.5-3.0 km.

Type II cementation (Seen in Figure 88, PMO 221.483)

1. Precipitation of light orange luminescent cement as a primary cement, Mg^{2+} - rich and at shallow depth, possibly < 2.0 km.
2. Dissolution of the aragonite conchs and aragonitic skeletal material, causing secondary porosity.
3. Partial dissolution of the primary cement.
4. Second generation of cement, dark in colour and coarse mosaic. Filling in the voids from the aragonite dissolved conchs. Possibly oxidizing conditions. This can represent a break in the cementation sequence, and possibly uplift. Approximate depth may be 2.0-3.0 km.

Since the process of dissolution and the process of cementation takes place under opposite conditions, the pore water composition is believed to have fluctuated with periods of high and low CO_2-content, high and low temperature, variations in Mg^{2+} and Fe^{2+} -content and pH, as well as the influence of pressure variations. Two factors causing dissolution of primary cements is karst formation or the release of CO_2 due to increased maturation of organic material causing increased acidity of porewater by generation of H_2CO_3 acid. In the first case, formation of karst seems unlikely since the sediments are believed to have been buried deep. In the latter case, the lowered pH of the pore water may have corroded the primary cement and left open voids, a process which seems more likely than formation of karst.

Possible pyrobitumen observed in cemented conchs

Figure 76 shows possible pyrobitumen inside the cemented chambers of a cephalopod conch, visible as a black, thin rim. No sample of the specimen was possible to collect, but the observation could indicate an active source rock beneath the Svartodden Mbr. In addition, the pyrobitumen in the conch is a good indication of the particular burial depth in which the final cemententation of the unit took place.

Similar oil stains in cephalopod conchs have been reported from Sweden, although in a much higher abundance. Pyrobitumen has previously been sampled from Lower Ordovician carbonates in Slemmestad (Pedersen et al., 2007), establishing its presence in the area. Petroleum occurring in Lower Palaeozoic sediments is known from Scandinavia and the Baltic states, and the source rock producing this petroleum was the organic-rich mud, deposited during the Cambrian, Ordovician and Silurian (Pedersen et al., 2007). In the case of the Oslo Region, these muds are likely to be the Alunskifer Fm. and the Tøyen Fm., stratigraphically in the vicinity to the Huk Fm. Based on geochemical analysis of bitumen and oils from Norway and Sweden, Pedersen et al. (2007) suggested that the generation, migration and accumulation of petroleum in Lower Palaeozoic sediments took place during a time interval from the Late Silurian to the Early Devonian, and during the Lower Permian and the Upper Triassic. During the Silurian to the Devonian, the Oslo Region received considerable amounts of sediments due to the formation of the Caledonides while the foreland structural deformation influenced the sedimentation pattern of the area.

Based on normal geothermal gradients, it is here estimated that the burial depth of the Svartodden Mbr. was approximately at 5-7 km (200 ºC) when the rock experienced its final major cementation stage, with the incorporation of pyrobitumen in cephalopod conchs. The process is believed to have taken place during the Middle Devonian (approximately 300 Ma).

Stylolites and clay seams

Chemical compaction forming dissolution at grain to grain contact, seen as stylolites and clay seams on a larger scale, is highly evident in the Svartodden Mbr., in outcrop, the artificial core and in thin sections. According to Boggs (2006) chemical compaction in limestones occur at depths from 200 to 1500 m, accompanying physical compaction which efficiently decreases porosity. Two distinct stylolite generations have formed in the Svartodden Mbr; bedding parallel stylolites and vertical stylolites. The studied bedding parallell stylolites are believed to have formed along existing bedding boundaries of main beds and sub-beds, based on their appearance in the artifical core and thin sections (Figure 74), due to vertical compression. The vertical stylolites cut horizontal stylolites, and must have formed at some time after the formation of the bedding parallel stylolites, due to horizontal compression by the Caledonian Orogeny.

Buried by sediments, the Svartodden Mbr. may have been buried approximately 400 m by the beginning of the Silurian with the onset of the foreland basin setting of the Oslo Region, due to the Caledonides. This deformation probably induced the formation of bedding parallell stylolites.

Diagenetic history

Diagenesis can be divided in three stages; shallow burial (eogenesis), deep burial (mesogenesis) and uplift and unroofing (telogenesis) (Boggs, 2006). Based on the results and discussion above, an interpretation of the major diagenetic alterations in the Svartodden Mbr. is hereby presented.

Early stage; shallow burial

- In the marine realm and in close vicinity of the seafloor, bioerosion of carbonate grains seen as microborings took place, with followed precipitation of micrite in the open borings.
- Below the sediment-water interface, neomorphism of the calcium carbonate grains took place, as well as primary dissolution of aragonite, e.g. in cephalopod conchs, and in micrite. Precipitation of Mg^{2+}-rich calcium carbonate cement in dissolved voids took place in the oxidized zone, but the composition of the pore water was variable, causing different cementation histories in this environment.
- Rotting of organic material resulting in phosphate precipitation.
- Early formation of dolomite by the replacement of micrite.
- Formation of pyrite which was concentrated around burrows in reducing pore water.
- Chemical dissolution at grain boundaries forming bedding parallel stylolites.

Late stage (deep) diagenesis

- Continued physical and chemical compaction, reducing remaining porosity and increased formation of horizontal stylolites.
- Dissolution of shallow formed cements, caused by increased acidic porewater with a high CO_2 content.
- Uptake of possible pyrobitumen in cephalopod conchs (possibly during Silurian-Devonian times).
- Cementation of Fe^{2+}- rich, mosaic cements, formed in reduced pore water, possibly at depths between 5 to7 km.
- Dissolution of skeletal grains and matrix by the replacement of secondary dolomite.
- Continued burial and compression.
- Folding and thrusting caused by the foreland basin development during the Silurian (possible fracturing and cement infill).
- Formation of vertical stylolites due to the enhanced horizontal compression from the rising Caledonides.

- Extensional deformation during the Late Carboniferous to Triassic rifting in the Oslo Region (possible fracturing and cement infill).
- Continued burial and compression.

Uplift and unroofing

- Major uplift and possible re-cementation stages from the deep subsurface to the shallow subsurface.
- Weathering and erosion from the last glacial periods.
- Continued weathering and oxidation of the unit at the surface (present state).

7 Conclusions

The uppermost limestone unit in the Huk Fm., the 2.0 m thick Svartodden Mbr. at the Slemmestad IF arena locality has been analysed for its content of fossils, firmgrounds and hardgrounds, as well as its diagenetic alterations. The many shell-bearing fossil cephalopods recorded in the Svartodden Mbr. are known from the Middle Ordovician epicontinental deposits on Baltica, deposited during a time interval when the relative sea level was at its highest. Regarding palaeontology, the most abundant body fossil in the unit is by far the orthoconic endoceratid cephalopod, *Proterovaginoceras incognitum*. Other identified species of the order endoceratida is *Anthoceraas buchi*, while coiled cephalopods recorded from the order Tarphycerida are mostly from the genera *Estoniceras* and *Holmiceras.*
Different groups of organisms recorded in the unit includes trilobites, brachiopods, bryozans, conodonts, ostracodes and echinoderms, contributing as skeletal grains in a calcitic micritic framework. The Svartodden Mbr. has been identified as a partly dolomitized packstone.

Samples of acid resistant material contained conodonts, ostracodes and acrotretid brachiopods. The conodonts were used for biozone detection, as well as indicators of burial temperature. Two recorded species from the *Eoplacognathus? variabilis* conodont biozone, *Drepanodus arcuatus* and *Baltoniodus medius*, have been identified in the Svartodden Mbr. The colour of the conodonts indicated a colour alteration index of 4, representing a burial temperature of 190ºC - 300ºC, introduced by intrusive batholiths in the area during the late Carboniferous to Triassic crust extension of the Oslo Region.

Two types of trace fossils on the upper bedding surface of the studied unit consist of horizontal tunnels identified as *Thalassinoides*, as well as trilobite formed tunnels and shafts, identified as *Thalassinoides bacae*. The tunnels were formed in semi-lithified sediments, and were kept open while trilobites used them for shelter from the carnivorous cephalopods or simply for feeding strategies. *Skolithos* trace fossils in vertical sections of the unit appear characteristically due to their colour contrast with the surrounding rock, caused by the weathering habit of the burrow-infill, which is rich in pyrite, phosphate and possibly dolomite.

Regarding the depositional environment, it is believed that the calcium carbonate deposits accumulated on an extensive, shallow shelf with very low gradients. The lowermost 20 cm of

the unit is marked by a higher content of clay, marking a transition from the more shale-rich underlying Lysaker Mbr. Few indicators of low sedimentation rates, such as micro borings, are also missing from this level. Firmground characteristics such as corroded cephalopod conchs, pre-omission burrows of the *Skolithos* trace fossil, and increased bioerosion of skeletal grains becomes abundant in the upper 1.7 meters of the unit. In addition, clay seams and stylolites seem to mark possible firmgrounds, where pre-omission burrows were formed before the sediment became firm and later filled with the overlying deposits which often show a colour contrast. A ten-fold of such repetitions of firmgrounds are present within the upper 1.7 meters of the unit. Recognition of hardgrounds was based on several techniques, in which field observations, thin section microscopy and XRF analysis were important. Only one hardground was identified in the Svartodden Mbr., being the uppermost bedding surface of the unit. The hardground characteristics of the surface includes features such as pre-omission burrows, winnowing and scouring by loose sediment on the surface, truncated cephalopod conchs and siphuncles. Microstromatolites observed in truncated trilobite burrows, in the vicinity of cephalopod conchs and on the seafloor, are also regarded as features typical of a hardground environment. Mineral encrustations of iron are also abundant on the hardground surface, based on the XRF-analysis.

High accumulation of organic matter on firmgrounds produced precipitation of phosphate during shallow burial depths, observed in the samples as phosphatized crinoid fragments and ostracodes, as well as dark-stained sediment. Diagenetic alteration of the unit includes (in succeeding order) compression, pyritization, horizontal compression resulting in bedding parallell stylolites and clay seams, 2 generations of dolomitization, up to 3 cement generations, vertical pressure solution resulting in vertical stylolites and clay seams. Late stage diagenesis includes fracturing and infilling of cement. Uplift, unroofing and erosion of the unit took place during a relatively short time interval.

Sources of previously published work on the faunas in the Svartodden Mbr. have been consulted during the current study. The literature review has revealed a need for more systematic studies of the groups representing hardground and firmground communities in the Middle Ordovician sedimentary sequence in Norway, such as brachiopods, trilobites, ostracodes, bryozoans, and last but not least, trace fossils and microstromatolites.

8 References

Aguado, E. & Burt, J. E. 2007: *Understanding Weather & Climate, (4th ed)*. Pearson Prentice Hall, 562 pp.

Ainsaar, L. & Meidla, T. 2004: Stop 4. Paekna quarry. *In*: Hints, O. & Ainsaar, L. (*Eds*). *WOGOGOB-2004 Conference Materials*, 125.

Ainsaar, L., Meidla, T. & Martma, T. 2004: The Middle Caradoc Facies and Faunal Turnover in the Late Ordovician Baltoscandian palaeobasin. *Palaeogeography, Palaeoclimatology, Palaeoecology 210*, 119 – 133.

Ainsaar, L., Kaljo, D., Martma, T., Meidla, T., Männik, P., Nõlvak, J. & Tinn, O. 2010: Middle and Upper Ordovician carbon isotope chemostratigraphy in Baltoscandia: a correlation standard and clues to environmental history. *Palaeogeography, Palaeoclimatology, Palaeoecology 294*, 189–201.

Andersen, T. B. 1998: Extensional tectonics in the Caledonides of southNorway, an overview. *Tectonophysics 285*, 333-351.

Barnes, C.R. 2004: Ordovician Oceans and Climate. *In:* Webby, B.D., Paris, F., Droser, M.L. & Percival, I.G. (*Eds*.) *The great Ordovician biodiversification event*. Columbia University Press, 72-76.

Benton, M. J. & Harper, D. A. T. 2009: *Introduction to Paleobiology and the Fossil Record*. Wiley-Blackwell, 592 pp.

Berner, R.A. 1994: 3 Geocarb II: A revised model of atmospheric CO_2 over Phanerozoic time. *American Journal of Science 294*, 56-91.

Bergström, S. M. 1980: Conodonts as palaeotemperature tools in Ordovician rocks of the Caledonides and adjacent areas in Scandinavia and the British Isles. *GFF 102*, 377-392.

Bergström, S. M., Schmitz, B., Young, S. A. & Bruton, D.L. 2011: Lower Katian (Upper Ordovician) $\delta^{13}C$ chemostratigraphy, global correlation and sea-level changes in Baltoscandia. *GFF 133*, 31-47.

Bjørlykke, K. 1974a: Depositional history and geochemical composition of Lower Palaeozoic epicontinental sediments from the Oslo Region. *Norges geologiske undersøkelse 305*, 1-81.

Bjørlykke, K. 1974b: Geochemical and mineralogical influence of Ordovician island arcs on epicontinental clastic sedimentation. A study of Lower Palaeozoic sedimentation in the Oslo Region, Norway. *Sedimentology 21*, 251-272.

Bjørlykke, K. 1978: The eastern marginal zone of the Caledonide orogen in Norway. *In*: Caledonian – Appalachian Orogen of the North Atlantic region, IGCP Project 27, Geological Survey of Canada, Paper 78-13, 49-55.

Bjørlykke, K. 2010: *Petroleum Geoscience: from Sedimentary Environments to Rock Physics.* Springer-Verlag, 508 pp.

Bockelie, J.F. 1982: The Ordovician of Oslo-Asker. *In* Bruton, D. L. and Williams, S. H. (*Eds.*): *Field excursion guide. IV Int. Symp. Ordovician System. Palaeontological Contributions from the University of Oslo 279*, 106-108.

Bockelie, J. F. 1984: The diploporita of the Oslo Region, Norway. *Palaeontology 27*, 1-68.

Boardman, R.S., Cheetham, A.H. & Rowell, A.J. 1987: *Fossil Invertebrates*. Blackwell scientific publications, 713 pp.

Bockelie, J. F. & Nystuen, J. P. 1985: The southeastern part of the Scandinavian Caledonides. *In* Gee, D. G. & Sturt, B. A. (*Eds.*), T*he Caledonide Orogen – Scandinavia and Related areas*. 69-88.

Boggs, S. Jr. 2006: *Principles of Sedimentology and Stratigraphy (4th ed).* Pearson Prentice Hall, 662 pp.

Brett, C. E. & Liddell, W. D. 1978: Preservation and paleoecology of a Middle Ordovician hardground community. *Paleobiology, 4*, 329-348.

Bromley, R.G., Hanken, N-M. & Asgaard, U. 1990: Shallow marine bioerosion: preliminary results of an experimental study. *Bulletin of the Geological Society of Denmark 38*, 85-99.

Brögger, W. C. 1882: Die silurischen Etagen 2 und 3 im Kristianiagebiet und auf Eiker, ihre Gliederung, Fossilien, Schichtenstörungen and Contactmetamorphosen. Universitätsprogramm für 2. Semester, 375 pp.

Bruton, D.L., Gabrielsen, R. H. & Larsen, B.T. 2010: The Caledonides of the Oslo Region - stratigraphy and structural elements. *Norwegian Journal of Geology 90*, 93-121.

Bruton, D. L. & Owen, A. W. 1982: The Ordovician of Norway. *In* Bruton, D. L. and Williams, S. H. (*Eds.*): *Field excursion guide. IV Int. Symp. Ordovician System. Palaeontological Contributions from the University of Oslo 279*, 10-14.

Buatois, L. & Gabriela Mángano, M. 2011: *Ichnology Organism-Substrate Interactions in Space and Time.* Cambridge University Press, 358 pp.

Candela, Y. & Hansen, T. 2009: Brachiopod associations from the Middle Ordovician of the Oslo Region, Norway. *Palaeontology 53*, 833-867.

Chacon, B. & Martin-Chivelet, J. 2008: Stratigraphy of Palaeocene phosphate pelagic stromatolites. *Facies 54*, 361-376.

Cherns, L., Wheeley, J.R. & Karis, L. 2006: Tunneling trilobites: Habitual infaunalism in an Ordovician carbonate seafloor. *Geology 34*, 657–660.

Cocks, L.R.M. & Torsvik, T.H. 2002: Earth geography from 500 to 400 million years ago: a faunal and palaeomagnetic review. *Journal of the Geological Society 159*, 631-644.

Cocks, L.R. & Fortey, R.A. 1990: Biostratigraphy of Ordovician and Silurian faunas. *In* McKerrow, W.S. & Scotese, C.F. (*Eds*.) *Palaeozoic Palaeogeography and Biogeography. Mem. Geological Society, London 12*. 97-104.

Dickson, J. A. D. 1966: Carbonate identification and genesis as revealed by staining. *Journal of Sedimentary Petrology 36*, 491-505.

Doyle, P. 1996: *Understanding fossils: an introduction to invertebrate palaeontology*. Wiley, 490 pp.

Dronov, A.V., Milulas, R. & Logvinova, M. 2002: Trace fossils and ichnofabrics across the Volkhov depositional sequence (Ordovician, Arenigian of St. Petersburg region, Russia). *Journal of the Czech Geological Society 47*, 133-146.

Dronov A., Ainsaar L., Kaljo D., Meidla T., Saadre T., & Einasto R. 2011: Ordovician of Baltoscandia: Facies, sequences and sea-level changes. *In* Gutiérrez-Marco J. C., Rábano I., & García-Bellido D. (*Eds.*) *Ordovician of the world Madrid: Instituto Geológico y Minero de Espanã*. 143–150.

Dunham, R.J. 1962: Classification of carbonate rocks accrording to depositional texture. *Mem. Am. Assoc. Pet. Geol. 1*, 108-121.

Ebbestad, J. O. R. & Isakar, M. 2004: Microgastropods in the Ordovician of Baltoscandia: potentials and prospects. *In*: Hints, O. & Ainsaar, L. (*Eds*). *WOGOGOB-2004 Conference Materials*, 27-140.

Ekdale, A.A. & Bromley, R.G. 2003: Paleoethologic interpretation of complex Thalassinoides in shallow-marine limestones, Lower Ordovician, southern Sweden. *Palaeogeography, Palaeoclimatology, Palaeoecology 192*, 221-227.

Ekdale, A.A., Benner, J.S., Bromley, R.G. & de Gibert, J.M. 2002: Bioerosion of Lower Ordovician Hardgrounds in Southern Scandinavia and Western North America. *Acta geologica hispanica 37*, 9-13.

Eniro Norge AS (Figure 16, Map source)
Available at:
http://kart.gulesider.no/, "search: Slemmestad"
(Accessed March 2012)

Epstein A.G., Epstein J.B. & Hams L.D. 1977: Conodont colour alteration-an index to organic metamorphism. *US Geological Survey Professional paper 995*, 27 pp.

Fitch, F.J., Forster, S.C. & Miller, J. A.1974: The dating of the Ordovician. *In* Basset, M. G. (*Ed*.). *The Ordovician System: proceedings of a Palaentological Assocition symposium*. Birmingham. 15-27.

Finney, S.C. & Xu, Chen, 1990: The relationship of Ordovician graptolite provincialism to palaeogeography. *In*: McKerrow, W.S. & Scotese, C.F. (*Eds*.), *Palaeozoic Palaeogeography and Biogeography. Geological Society London Memoir 12*, 123– 128.

Flügel, E. 2004: *Microfacies of Carbonate Rocks: Analysis, Interpretation and Application*. Springer Verlag, 976 pp.

Fortey, R.A, Harper, D.A.T., Ingham, J. K., Owen, A. W. & Rushton, A.W.A.1995: A revision of Ordovician series and stages from the historical type area. *Geological Magazine 132*, 15-30.

Fortey, R.A. 1984: Global earlier Ordovician transgressions and regressions and their biological implications. *In* Bruton, D. L. (*Ed*.). *Aspects of the Ordovician System. Palaeontological Contributions from the University of Oslo 295,* Universitetsforlaget. 37-50.

Frey, R.C., Beresi, M.S., Evans, D.H., King, A.H. & Percival, I.G., 2004: Nautiloid cephalopods. *In*: Webby, B.D., Droser, M.L., Paris, F., Percival, I.G. (*Eds.*). *The Great Ordovician Biodiversification Event*. Columbia University Press, 209–213.

Frýda, J. & Rohr, D.M. 2004: Gastropods. *In*: Webby, B.D., Droser, M.L., Paris, F., Percival, I.G. (*Eds.), The Great Ordovician Biodiversification Event*. Columbia University Press, 185–195.

Gradstein, F. M., Ogg, J. G., Schmitz, M. D. & Ogg, G. M. 2012: *A Geologic Time Scale 2012*. Elsevier.

Goldstein, J. I. 2003: *Scanning electron microscopy and X-ray microanalysis (3rd ed).* Kluwer Academic/Plenum Publishers, 689 pp.

Hammer, Ø., Harper, D.A.T. & Ryan, P.D. 2001: Past: Paleontological statistics software package for education and data analysis. *Paleontological Association*, 2001.

Hansen, J. & Harper, D.A.T. 2008: The late Sandbian – earliest Katian (Ordovician) brachiopod immigration and its influence on thebrachiopod fauna in the Oslo Region, Norway. *Lethaia 41*, 25–35.

Hansen, J., Nielsen, J. K. & Hanken, N-M. 2009: The relationships between Late Ordovician sea-level changes and faunal turnover in western Baltica: Geochemical evidence of oxic and dysoxic bottom-water conditions. *Palaeogeography, Palaeoclimatology, Palaeoecology 271*, 268-278.

Hansen, T. 2008: Mid to late Ordovician trilobite palaeoecology in a mud dominated epicontinental sea, southern Norway. In: Rábano, I., Gozalo, R. & Garcia-Belliodo, D. (*Eds*). *Advances in trilobite research*, 157-165.

Hansen, T. 2009: Trilobites of the Middle Ordovician Elnes Formationof the Oslo Region, Norway. *Fossils and Strata 56*, 1- 215.

Hansen, T., Nielsen, A.T. & Bruton, D. L. 2011: Palaeoecology in a mud-dominated epicontinental sea: A case study of the Ordovician Elnes Formation, southern Norway. *Palaeogeography, Palaeoclimatology, Palaeoecology 299*, 348-362.

Harper, D.A.T. 1985: Distributional trends within the Ordovician brachiopod faunas of the Oslo Region, south Norway. *In*: Racheboeuf, O.R. & Emig, C.C. (*Eds.*), *Les Brachiopodes fossils et actuels. Biostratigraphie du Paléozoïque 4*, 465-475.

Harper, D. A. T. & Mac Niocaill, C. M. 2002: Early Ordovician rhynchonelliformean brachiopod biodiversity: comparing some platforms, margins and intra-oceanic sites around the Iapetus Ocean. *Geological Society, London, Special Publications 194*, 25-34.

Heim, A. 1924: Uber submarine Denudation und chemische Sedimente. *Geologische Rundschau. 15*, 1-47.

Henningsmoen, G. 1953a: Classification of Paleozoic straight-hinged ostracods. *Norsk Geologisk Tidsskrift 31*, 185-288.

Henningsmoen, G 1953b: The Middle Ordovician of the Oslo Region. *4.* Ostracoda. *Norsk Geologisk Tidsskrift 32*, 35-56.

Henningsmoen, G. 1954*:* Upper Ordovician Ostracods from the Oslo Region, Norway. *Norsk Geologisk Tidsskrift 33*, 69-108.

Hillgärtner, H. 1998: Discontinuity surfaces on a shallow-marine carbonate platform (Berrasian, Valangian, France and Switzerland). *Journal of Sedimentary Research 68*, 1093-1108.

Hints, L., Oraspõld, H. & Pirgu, J. N. 2004: Stages in the East Baltic: lithotypes, biozonation and problems of correlation. *In*: Hints, O. & Ainsaar, L. (*Eds.*). *WOGOGOB-2004 Conference Materials*, 41-42.

Holmer, L.E. 1989: Middle Ordovician phosphatic inarticulate brachiopods from Västergötland and Dalarna, Sweden. *Fossils and Strata 26*, 1-172

Holtedahl, O. 1920: Notes on the Ordovician fossils from Bear Island collected during the Swedish expeditions of 1898 and 1899. *Norsk Geologisk Tidsskrift 5*, 79-94.

Hrouda F., Clupácová M. & Chadima M. 2009: The use of magnetic susceptibility of rocks in geological exploration (case studies only).
Available from:
http://kdjonesinstruments.com/LinkClick.aspx?fileticket=GX3dcpDkuVc%3D&tabid=5120
(Accessed March 2012)

Nielsen, A. T. 1995: Trilobite systematics, biostratigraphy and palaeoecology of the Lower Ordovician Komstad Limestone and Huk Formations, southern Scandinavia. *Fossils and Strata 38*, 1-374.

Jaanusson, V. 1961: Discontinuity surfaces in limestones. *Bulletin of the Geological Institutions of the University of Uppsala 38*, 207-288.

Jaanusson, V. 1972: Constituent analysis of an Ordovician limestone from Sweden. *Lethaia 5*, 217-237.

Jaanusson, V. 1973: Aspects of carbonate sedimentation in the Ordovician of Baltoscandia. *Lethaia 6*, 11-34.

Jaanusson, V. 1976: Faunal dynamics in the middle Ordovician (Viruan) of Balto-Scandia. *In* Bassett, M.G. (*Ed.*): *The Ordovician System: Proceedings of a Palaeontological Association Symposium*, 301–326. University of Wales Press and National Museum of Wales, Birmingham.

Jaanusson, V., 1982: The Siljan District. *In:* D.L. Bruton and S.H. Williams (eds): IV International Symposium on the Ordovician system. Field Excursion Guide. *Palaeontological Contributions from the University of Oslo 279*, 15-42.

Jaanusson, V. 1984: Ordovician benthic macrofaunal associations. *In* Bruton, D.L. (*Ed*.): Aspects of the Ordovician System. *Palaeontological Contributions from the University of Oslo 295*, 127–139. Universitetsforlaget, Oslo, Norway.

James, N.R. & Dalrymple R.W. (*Eds.*) 2010: *Facies models 4*. Geological Association of Canada, 586 pp.

Klemm, T. 1982: The Ordovician succession at Vestfossen and Krekling. *In* Bruton, D. L. and Williams, S. H. (*Eds*.): *Field excursion guide. IV Int. Symp. Ordovician System. Paleont. Contr. Univ. Oslo 279*, 139-143.

Kohut, J.J. 1972: Conodont biostratigraphy of the Lower Ordovician Orthoceras and Stein Limestones (3c), Norway. *Norsk Geologisk Tidsskrift 52*, 427 - 445.

Kröger, B. 2012: The "Vaginaten": the dominant cephalopods of the Baltoscandian Mid Ordovician endocerid limestone. *GFF 134*, 115–132.

Kröger, B. & Mutvei, H. 2004: Nautiloids with multiple paired muscle scars from Lower-Middle Ordovician of Baltoscandia. *Palaeontology 48*, 781–791.

Kröger, B., Vinther, J. & Fuchs D. 2011: Cephalopod origin and evolution: A congruent picture emerging from fossils, development and molecules. *Bioessays 33*, 602-613.

Larsen, B.T., Olaussen, S., Sundvoll, B. & Heeremans, M. 2008: The Permo-Carboniferous Oslo Rift through sixstages and 65 million years. *Episodes 31*, 52-58.

Lindström, M. 1971: Vom Anfang, Hochstand und Ende eienes Epikontinentalmeeres. *Geologische Rundschau 60*, 419-438.

Lindström, M. 1984: Baltoscandic conodont life environments in the Ordovician: Sedimentologic and paleogeographic evidence. *Geological Society of America Special Paper 196*, 33-42.

Löfgren, A. 1995: The middle Lanna/Volkhov Stage (middle Arenig) in Sweden and its conodont fauna. *Geological Magazine 132*, 693–711.

Löfgren, A. 2000: Conodont biozonation in the upper Arenig of Sweden. *Geological Magazine 137***,** 53–65.

Löfgren, A. 2003: Conodont faunas with *Lenodus variabilis* in the upper Arenigian to lower Llanvirnian of Sweden. *Acta Palaeontologica Polonica 48*, 417–436.

Löfgren, A. & Zhang J. 2003: Element association and morphology in some Middle Ordovician platform-equipped conodonts. *Journal of Paleontology 77*, 721–737.

Löfgren, A. & Tolmacheva, T. 2003: Taxonomy and distribution of the Ordovician conodont Drepanodus arcuatus PANDER, 1856, and related species. *Paläontologische Zeitschrift 77*, 203-221.

Löfgren, A. 2004: The conodont fauna in the Middle Ordovician *Eoplacognathus pseudoplanus* Zone of Baltoscandia. *Geological Magazine 141*, 505–524.

Männil, R.M. 1966: *Evolution of the Baltic Basin during the Ordovician*. 1–200. Valgus Publishers.

Marshall, D.J. 1988: *Cathodoluminiscence of geological materials*. Unwin Hyman, 146 pp.

McKerrow, W. S. (*ed*.) 1978: *The Ecology of fossils: an illustrated guide*. Duckworth, 384 pp.

Mellgren, J.I.S. & Eriksson, M.E. 2010: Untangling a Darriwilian (Middle Ordovician) palaeoecological event in Baltoscandia: conodont faunal changes across the 'Täljsten' interval (for 2009) *Transactions of the Royal Society of Edinburgh , Earth Sciences 100*, 353–370.

Moore, R.C. (*Ed*) 1964: *Treatise on invertebrate paleontology = (K) Mollusca 3*, Geological Society of America University, Kansas Press, 519 pp.

Morley, C. K. 1994: Fold-generated imbricates: examples from the Caledonides of Southern Norway. *Journal of Structural Geology 16*, 619-631.

Möller, N.K. & Kvingan, K., 1988: The genesis of nodular limestones in the Ordovician and Silurian of the Oslo Region (Norway). *Sedimentology 35*, 405–420.

Musum für naturkunde, Berlin (Figure 25 B: Tarphycerida)
Available from:
http://www.geolocation.ws/v/W/File%3ADiscoceras%20dankelmanni%2001.jpg/-/en
(Accessed October 2012)

Nagle, J. S. 1967: Wave and current orientation of shells. *Journal of Sedimentary Petrology 37*, 1124-1138.

Natural history museum, Oslo (Figure 25 A: *Nautilus*)
Available from: http://www.nhm.uio.no/fakta/geologi/fossiler/faktablader/blad_x03.htm,
(Accessed April 2012)

Nielsen, A. T. 1995: Trilobite systematics, biostratigraphy and palaeoecology of the Lower Ordovician Komstad Limestone and Huk Forrnations, southern Scandinavia, *Fossils and Strata 38*, 374 pp.

Nielsen, A. T. 2004: Ordovician Sea Level Changes: A Baltoscandian Perspective. *In* Webby, B. G., Paris, F., Droser, M. L. and Percival I.G. (*Eds.*). *The Great Ordovician Biodiversification Event*, Columbia University Press, 84-93.

Nilsen, I. R., 1985: Kartlegging av Langesundshalvøyas kambro-ordoviciske avsetningslagrekke, intrusiver og forkastningstektonikk, samt fullført lithostratigrafisk inndeling av områdets mellom-ordovicium. Unpublished Cand.scient. thesis, Palaeontological Museum, University of Oslo, Norway.

Nordlund, U. 1989: Lithostratigraphy and sedimentology of a Lower Ordovician limestone sequence at Hälludden,Öland,Sweden. *GFF 111*, 65–94.

Norges geologiske undersøkelse (Map source, Figure 9)
Available from:
http://geo.ngu.no/kart/berggrunn/
(Accessed May, 2012)

Owen, A.W., Bruton, D.L, Bockelie, J.F. & Bockelie, T. 1990: The Ordovician successions of the Oslo Region, Norway. *Norges Geologiske Undersøkelse Special Publication 4*, 3–54.

Palmer, T.J. & Wilson, M.A. 2004: Calcite precipitation and dissolution of biogenic aragonite in shallow Ordovician calcite seas. *Lethaia 37*, 417-427.

Pedersen, J.H.,. Karlsen, D.A., Spjeldnæs,N., Backer-Owe, K., Lie, J.E. & Brunstad, H. 1997: Lower Paleozoic petroleum from southern Scandinavia:Implications to a Paleozoic petroleum system offshoresouthern Norway. *AAPG Bulletin 91*, 1189–1212.

Perroud, H., Robardet, M. & Bruton, D. L. 1992: Palaeomagnetic constraints upon the palaeogeographic position of the Baltic Shield inthe Ordovician. *Tectonophysics 201*, 97-120.

Pollard, J. E., Goldring, R. & Buck, S. G. 1993: Ichnofabrics containing *Ophiomorpha:* significance in shallow-water facies interpretation. *Journal of the Geological Society 150,* 149-164.

Pratt, B. 2001: Calcification of ccyanobacterial filaments: *Girvanella* and the origin of lower Palaeozoic lime mud. *Geology 29*, 763-766.

Railsback, L.G. 1990: Influence of changing deep ocean circulation on the Phanerozoic oxygen isotopic record. *Geochimica et cosmochimica acta 54*, 1501-1509.

Ramberg, I. B., Bryhni, I., Nøttvedt, A., Solli, A., & Nordgulen, Ø. (*Eds.*) 2007: *The Making of a Land : Geology of Norway (2nd ed.).* Norsk geologisk forening, 608 pp.

Rasmussen, J. A. 1991: Conodont stratigraphy of the Lower Ordovician Huk Formation at Slemmestad, southern Norway. *Norsk Geologisk Tidsskrift 71*, 265–287.

Rasmussen, J. A. 2001: Conodont stratigraphy and taxonomy of the Ordovician shelf margin deposits in the Scandinavian Caledonides. *Fossils and Strata 48*, 1-145.

Rasmussen, J. A. & Bruton, D. L. 1995: Stratigraphy of Ordovician limestones, lower Allochthon, Scandinavian Caledonides. *Norsk Geologisk Tidsskrift 74*, 199-212 (part 4 for 1994).

Rasmussen, J. A. & Stouge, S. 1995: Late Arenig – Early Llanvirn conodont biofacies across the Iapetus ocean. *In* Cooper, J. D., Droser, M. L. & Finney, S. C. (*Eds.*) *Ordovician Odyssey: Short Papers for the Seventh International Symposium on the Ordovician System*, SEPM, Pacific Section, Book 77, 443-47.

Raup, D.M. 1973: Depth inferences from vertically imbedded cephalopods, *Lethaia 6*, 217-226.

Reyment, R.A. 1968: Orthoconic nautiloids as indicators of shoreline surface currents. *Journal of Sedimentary Petrology 38*, 1387-1389.

Reyment, R.A. 1970: Vertically inbedded cephalopod shells. Some factors in the distribution of fossil cephalopods. *Palaeogeography, Palaeoclimatology, Palaeoecology 7*, 103-111.

Reynolds, R.W. & Smith, T.M. 1995: A High-Resolution Global Sea Surface Temperature Climatology. *Journal of Climate 8*, 1571-1583.

Rozhnov, S.V. 2004: Echinoderms of the bioherms of the Baltic Ordovician basin: comparison of the coldwater (Volkhovian) and tropical (Keila) communities. *In*: Hints, O. & Ainsaar, L. (*Eds.*). *WOGOGOB-2004 Conference Materials*, 48–49

Schmitz, B., Harper, D.A.T., Peucker-Ehrenbrink, B., Stouge, S., Alwark, C.,Cronholm, A., Bergström, S.M., Tassinari, M., & Wang, X. 2007: Asteroid breakup linked to the Great Ordovician Biodiversification Event. *Nature Geoscience 1*, 49–53.

Schmitz, B., Lindström, M., & Tassinari A., M. 1996: Geochemistry of meteorite-rich marine limestone strata and fossil meteorites from the lower Ordovician at Kinnekulle, Sweden. *Earth and Planetary Science Letters 145*, 31-48.

Schvosbo, N.H. 2003: The geochemistry of Lower Palaeozoic sediments deposited on the margins of Baltica. *Bulletin Geological Society of Denmark 50*, 11–27.

Servais, T., Owen, A.W., Harper, D.A.T, Kröger, B. & Munnecke, A. 2010: The Great Ordovician Biodiversification Event (GOBE): The palaeoecological dimension. *Palaeogeography, Palaeoclimatology, Palaeoecology 294*, 99–119.

Shields, G.A., Carden, G.A.F. & Veitzer, J. 2003: Sr, C, and oxygen isotopegeochemistry of Ordovician brachiopods: a major isotopic event around the Middle–Late Ordovician transition. *Geochimica et Cosmochimica Acta 67*, 2005–2025.

Skaar, F.E. 1972: Ortocerkalksteinen (Etasje 3c) i Oslofeltet -- En undersøkelse av den mineralogiske og kjemiske sammensetning, regionalt og stratigrafisk. Unpublished Cand.scient. thesis, Palaeontological Museum, University of Oslo, Norway.

Skjeseth, S. 1952: On the Lower Didymograptus Zone (3b) at Ringsaker, and contemporaneous deposits in Scandinavia. *Norsk Geologisk Tidsskrift 30*, 138-182.

Skjeseth, S. 1953: The Middle Ordovician of the Oslo Region, Norway; The trilobite family Styginidae. *Særttrykk av Norsk geologisk tidsskrift 35*, 9-28.

Skjeseth, S. 1963: Contributions to the geology of the Mjøsa districts and the classical sparagmite area in southern Norway. *Norges Geologiske Undersøkelse 220*, 126 pp.

Spjeldnes, N. N. 1957: The Middle Ordovician of the Oslo Region, Norway. 8, Brachiopods of the Suborder Strophomenida. *Norsk Geologisk Tidsskrift 37*, 1-214.

Sprinkle, J. & Guensburg, T.E. 2004: Crinozoan, Blastozoan, Echinozoan, Asterozoan, and Homalozoan Echinoderms. *In* Webby, B.D., Droser, M. L. & Percival, I.G. (*Eds.*), 2004. *The Great Ordovician Biodiversification Event*. 226-280.

Stanley, S.M., & Hardie, L.A. 1998: Secular oscillations in the carbonate mineralogy of reefbuilding and sediment-producing organisms driven by tectonically forced shifts in seawater chemistry. *Palaeogeography, Palaeoclimatology, Palaeoecology 144*, 3–19.

Størmer, L. 1967: Some aspects of the Caledonian geosyncline and foreland west of the Baltic shield. *The quarterly Journal of the Geological Society of London 123*, 183-214.

Sturesson, U. 2003: Lower Palaeozoic iron oolites and volcanism from a Baltoscandian perspective. *Sedimentary Geology 159,* 241–256.

Størmer, L. 1953: The Middle Ordovician of the Oslo Region, Norway. 1. Introduction to Stratigraphy. *Norsk Geologisk Tidsskrift 31,* 37–141.

Sundvoll, B. & Larsen, B.T. 1994: Architecture and early evolution of the Oslo Rift. *Tectonophysics 240*, 173-189.

Svendsby, R. 1987: Et geologisk kart (målestokk 1:5000) og en beskrivelse av den kambro-ordoviciske lagrekken i området mellom Eikeren og Mjøndalen, sydvest Oslofeltet. Unpublished Cand.scient. thesis, Palaeontological Museum, University of Oslo, Norway.

Tassinari, M., Schmitz, B. & Löfgren, A. 2004: The first fossil meteorite from the mid-Ordovician of the Gullhögen quarry, Billingen, southern Sweden. *Geologiska Föreningens I Stockholm Förhandlingar 126*, 321–324.

Taylor, P.D. & Ernst, A. 2004: Bryozoans. *In* Webby, B.D., Droser, M. L. & Percival, I.G. (*Eds.*) *The Great Ordovician Biodiversification Event*. 147-156.

Tinn, O. & Meidla, T. 2001: Middle Ordovician ostracodes from the Lanna and Holen Limestones, south-central Sweden. *GFF 123*, 129-136.

Tinn, O., Meidla, T. & Ainsaar, L. 2006: Arenig (Middle Ordovician) ostracodes from Baltoscandia: fauna, assemblages and biofacies. *Palaeogeography, Palaeoclimatology, Palaeoecology 241*, 492–514.

Torsvik, T.H. 1998: Palaeozoic palaeogeography: A North Atlantic viewpoint. *GFF 120*, 109-118.

Torsvik, T. H., Trench, A., Lohmnann, K.C. & Dunn, S., 1995a: Lower Ordovician reversal assymmetry, an artefact of remagnetization or non-dipole field disturbance? *Journal of Geophysical Research 100*, 17885-17898.

Torsvik, T. H., Tait, J., Moralev, V.M., McKerrow, W.S., Sturt, B.A. & Roberts, D. 1995b: Ordovician palaeogeography of Siberia and adjacent continents. *Journal of the Geological Society, London 152*, 279-287.

Trela, W. 2005: Condensation and phosphatization of the Middle and Upper Ordovician limestones on the Malopolska Block (Poland): Response to paleoceanographic conditions. *Sedimentary Geology 178*, 219-236.

Trotter, J.A., Williams I.S., Barnes, C. R., Lécuyer, C. and Nicoll, R. S. 2008: Did Cooling Oceans Trigger Ordovician Biodiversification? Evidence from Conodont Thermometry. *Science 321*, 550-554.

Tucker, M. E. 2001: *Sedimentary petrology: An Introduction to the Origin of Sedimentary Rocks, (3rd ed)*. Blackwell Science, 262 pp.

Veizer, J., Goddéris, Y. & François, L.M. 2000: Evidence for decoupling of atmospheric CO_2 and global climate during the Phanerozoic eon. *Nature 408*, 698–701.

Webby, B.D. 2004: Introduction. *In* Webby, B.D., Droser, M. L. & Percival, I.G. (*Eds.*). *The Great Ordovician Biodiversification Event*. 1-37

Wentworth, C. K. 1922: A scale of grade and class of terms for clastic sediments. *The Journal of Geology 30*, 377-392.

Westermann, G. E. G. 1973: Strength of concave septa and depth limits of fossil cephalopods. *Lethaia 6*, 383-403.

Wilde, P. 1991: Oceanography in the Ordovician. *In*: Barnes, C.R. & Williams, S.H. (*Eds.*), *Advances in Ordovician Geology. Geological Survey of Canada Paper 90-9*, 283– 298.

Wilson, M.A & Palmer, T.J. 1992: *Hardgrounds and hardground faunas*. University of Wales, Aberystwyth, Institute of Earth Studies Publications 9, 131 pp.

9 Appendices

Appendix 1 Cephalopod key by Björn Kröger

Key to the description of cephalopods in the Huk Formation

Björn Kröger (bjoekroe@gmx.de)

if shell straight go to (A) / if shell shell curved go to (D)

(A) Straight shell:

if shell smooth go to (B)

if shell annulated/undulated o to (C)

if shell finely transversely striated, but not undulated: *Nilssonoceras kinnekullense* (Foord, 1887) see Kröger (2005) see also (1b)

shell not preserved (1)

(B) shell smooth:

siphuncle preserved, go to (1),

siphuncle not preserved, go to (2a)

(C) shell annulated:

siphuncle preserved, go to (1a),

siphuncle not preserved, go to (2b)

(1) Siphuncle preserved:

if siphuncle strongly expanded and bulbous between septa:

Adamsoceras holmi (Troedsson, 1926)

if siphuncle tubular and marginal (1a)

if siphuncle tubular and between center and conch margin (1b)

if siphuncle tubularand central (1c)

(1a) siphuncle tubular and marginal

if siphuncle diameter > 0.5 of conch cross section (1a.1),

if 0.3–0.5 of conch cross section (1a.2),

if clearly less than 0.3 of conch cross section and the specimen is small with conch diameter of less than 15 mm it is by high probability *Cochlioceras* Eichwald, 1860. Only a median section can give reliable data. Such small fragments should generally be collected.

(1a.1) siphuncle diameter > = 0.5 of conch cross section:

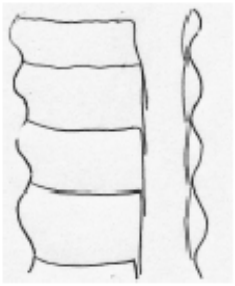

with annulated shell: *Anthoceras eichwaldi* (Balashov, 1968)

smooth shell, septal neck length = chamber length:

Cameroceras lasnamaense (Balashov, 1968)

smooth shell, septal neck length > chamber length (c. 1.5 x length of chamber):

- if siphuncle diameter >=0.7:

Proterocameroceras magnisiphonicum (Balashov, 1968)

- if siphuncle diameter c. 0.5 and apical angle of conch c. 7°-8°:

Proterovaginoceras belemnitiforme (Holm, 1885)

(1a.2) siphuncle diameter c 0.3-0.45 of conch cross section:

if siphuncular segments concave (1a.4)

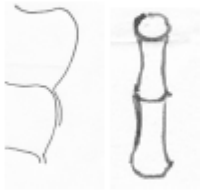

if siphuncular segments with s-shaped outline or nearly straight:

Proterocameroceras incognitum (Schröder, 1882)

(1a.4) siphuncular segments concave

if shell clearly annulated: *Anthoceras buchi* (Lesnikova, 1949)

if shell with fine transverse undulations and not perfectly smooth:
Proterocameroceras wahlenbergi (Foord, 1887)

(1b) siphuncle between center and conch margin

if siphuncle thin (less than 0.2 of conch cross section):
Nilssonoceras kinnekullense (Foord, 1887), see also (A)

(1c) siphuncle central

if siphuncle thin (less than 0.2 of conch cross section)
Holmioceras kjerulfi (Broegger, 1882); additional characters: juvenile shell curved, septal spacing narrow (typically c. 3-4 septa at distance similar to correspondent conch diameter), chambers often filled with sparite.

(2a) distance between septa

narrow (5 or more septa per distance similar to correspondent conch diameter):
Proterocameroceras sp.

medium (3-4 or more septa per distance similar to correspondent conch diameter), chambers typically, and apically always filled with sparite:
Holmioceras kjerulfi (Broegger, 1882), see also (1c)

wide (2 or less septa per distance similar to correspondent conch diameter):
Nilssonoceras kinnekullense (Foord, 1887), see also (A)

(D) shell curved:

if tightly or openly coiled go to (Da)

curved only in very small conchs (conch diameter < c. 10 mm):
Holmioceras kjerulfi (Broegger, 1882), see also (1c) and (2a)

(Da) tightly coiled

if siphuncle positioned eccentrically between conch center and margin at convex side of the shell curvature) (Da1),

else this is a taxon formerly not known from the Huk Formation

(Da1) eccentrical siphuncle position between center and conch margin at convex (outer) side of conch curvature.

if shell diameter (measured from whorl to whorl, 180°) of tightly coiled shell exceeds c. 100 mm (Da2)

else (Da3)

(Da2) tighly coiled shell exceeds c.100 mm in diameter:

if cross section of last whorl is circular:

Estonioceras perforatum Schröder, 1891 

#if cross section of last whorl is elongated :

Estonioceras imperfectum (Quenstedt, 1846) 

(Da3) shell openly coiled in diameters less than 100 mm

openly coiled shell starts with shell diameters (measured from whorl to whorl, 180°) of c. 40 mm or less: (Da4)

openly coiled shell starts with shell diameters (measured from whorl to whorl, 180°) of c. 80 mm:

- if WER <= 2: *Estonioceras kundense* Balashov, 1953

- if WER c. 2.5-3 *Estonioceras ariense* (Schmidt, 1857)

(Da4) shell openly coiled in diameters with more than 35 mm, very widely openly coiled

cross secion of whorl elliptical:

Tragoceras falcatum (Schlotheim, 1820)

cross section of whorl circular:

Tragoceras arciforme Balashov, 1953

Technical terms:

- **conch diamater:** diameter of cross section of a whorl or the cone of a straight shell
- **shell diameter:** diameter of the entire shell of the whorls of a coiled shell
- **siphuncle:** tube extending through all chambers, sometimes marginal (in endocerids), sometimes central (eg. in orthocerids)
- **septum:** partition dividing the conch into chambers
- **septal necks:** portion of the septa at opening, which is bent backward around the siphuncle
- **WER:** Worl Expansion Rate

Literature:

Balashov, Z. G., 1953. Svernutye i polisvernutye nautiloidei ordovika pribaltiki. Trudy Vsesoyuznogo Neftyanogo Nauchno-Issledovatel´skogo Geologo-Razvednoknogo Instituta, 78: 217-268, Leningrad/St. Petersburg.

Balashov, Z. G. 1968. Endoceratoidei ordovika SSSR. 170 p., Isdatjelsvo Leningradskogo Universiteta, Leningrad/St. Petersburg.

Kröger, B. 2004. Revision of Middle Ordovician orthoceratacaean nautiloids from Baltoscandia. Acta Palaeontologica Polonica 49: 57–74.

Sweet, W. 1958. The Middle Ordovician of the Oslo region, Norway. 10. Nautiloids. Norsk Geologisk Tidsskrift 38: 1-176

Troedsson, Gustaf T. 1926. On the Middle and Upper Ordovician faunas of northern Greenland. I. Cephalopods. Meddel. Gronl., 71: 1-157.

((((+ when the shell is smooth, the siphuncle is marginal and c 1/3 of shell diameter it will be by 99% P. incognitum, you can be 100% sure of the genus if the septal nacks are clearly longer than the chambers

+ when the shell is annulated it is A. buchi

+ when small and with sparitically filled chambers and high apical angle it is in almost all cases H. kjerulfi

+ when siphuncle not marginal and thin and wide chamber spacing it is in almost all cases N. nilssoni)))))


Planctoceras arciforme
Planctoceras falcatum
Estonioceras kundense
Estonioceras imperfectum
Estonioceras ariense

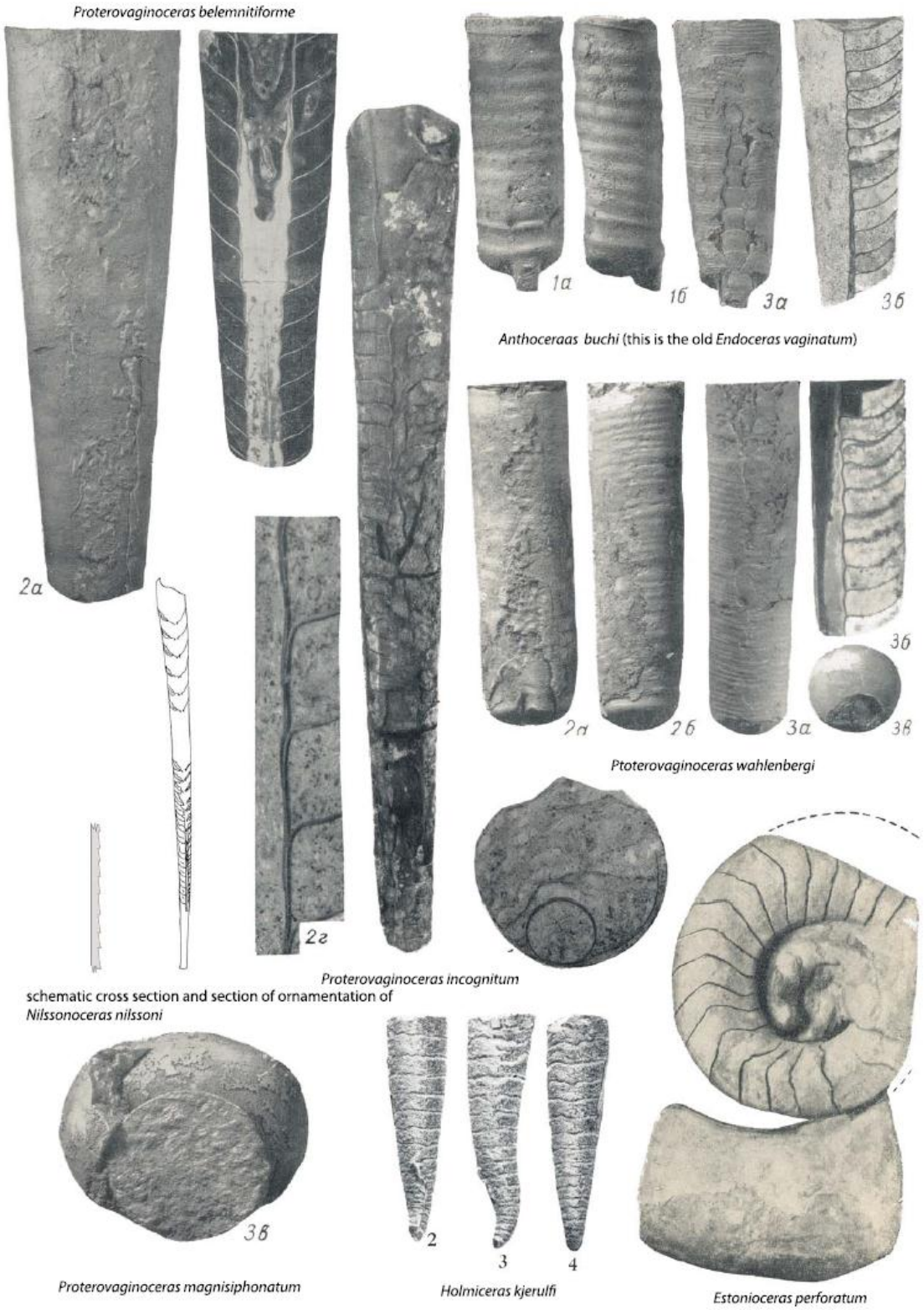
Proterovaginoceras belemnitiforme
1а
1б
3а
3б
Anthoceraas buchi (this is the old Endoceras vaginatum)
2а
2г
2а
2б
3а
3б
3в
Ptoterovaginoceras wahlenbergi
Proterovaginoceras incognitum
schematic cross section and section of ornamentation of
Nilssonoceras nilssoni
3в
2
3
4
Proterovaginoceras magnisiphonatum
Holmiceras kjerulfi
Estonioceras perforatum

Appendix 2 Conodont stubs for SEM

Sample SL1+2PMO 224.363

Sample SL3+4, PMO 224.362

Sample SL5+6, PMO 224.361

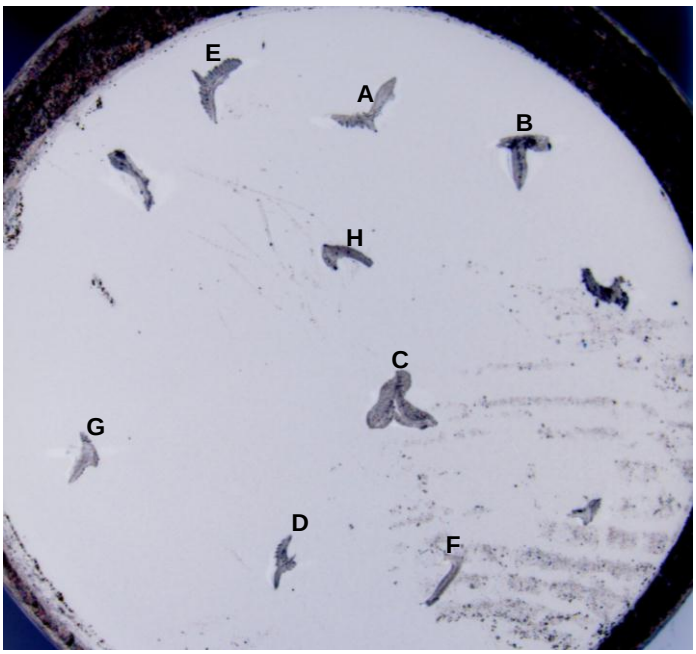

Appendix 3 Acid insoluble stub for SEM

PMO 224.360

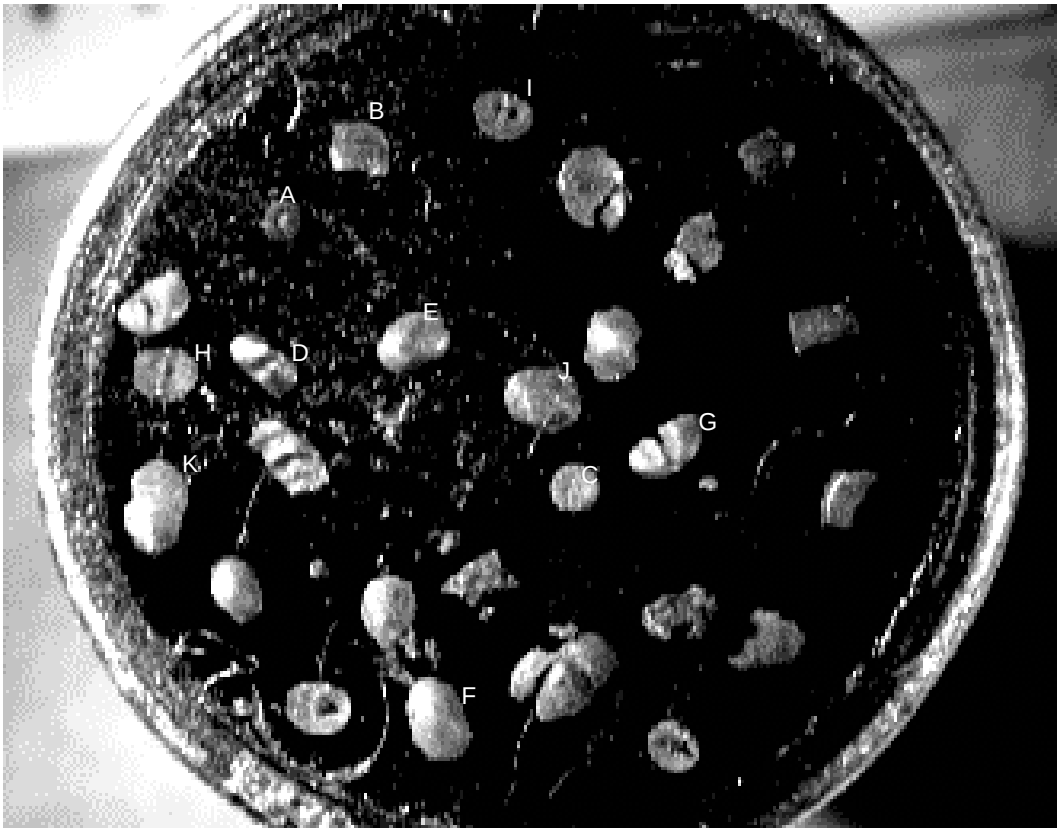

Appendix 4: SEM analysis of ostracodes

PMO 224.360/D

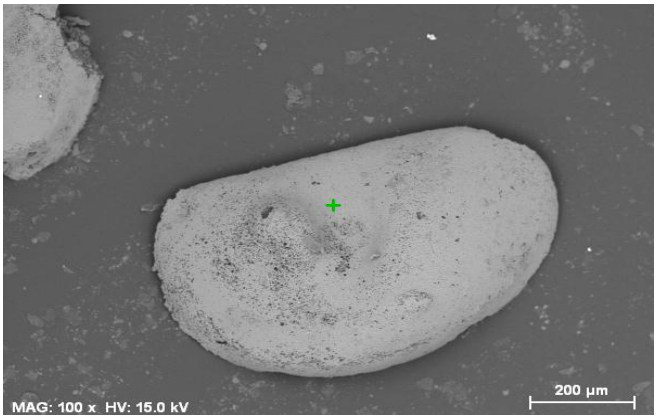

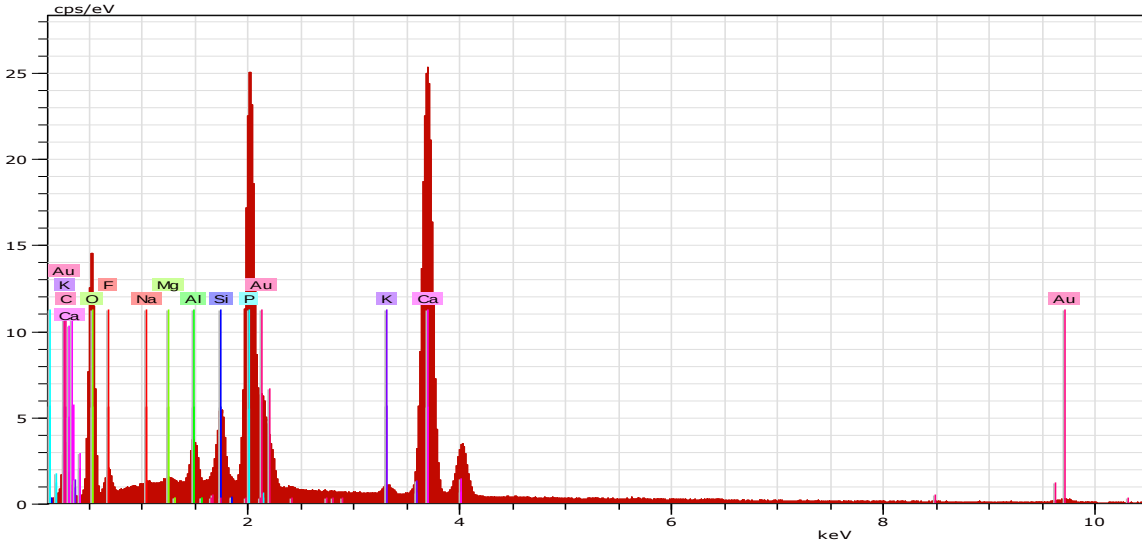

El	AN	Series	unn. C [wt.%]	norm. C [wt.%]	Atom. C [at.%]	Compound	Comp. C [wt.%]	norm. Comp. C [wt.%]	Error (1 Sigma) [wt.%]
C	6	K-series	3.69	3.33	6.48	CO2	12.22	13.53	1.20
O	8	K-series	44.66	40.33	58.87		0.00	0.00	5.21
F	9	K-series	3.33	3.01	3.69		3.01	3.33	0.49
Na	11	K-series	0.61	0.55	0.56	Na2O	0.74	0.82	0.07
Mg	12	K-series	0.01	0.01	0.01	MgO	0.01	0.01	0.03
Al	13	K-series	1.47	1.33	1.15	Al2O3	2.51	2.78	0.10
Si	14	K-series	2.44	2.21	1.83	SiO2	4.72	5.22	0.16
P	15	K-series	13.55	12.24	9.23	P2O5	28.04	31.05	0.56
K	19	K-series	0.57	0.52	0.31	K2O	0.62	0.69	0.05
Ca	20	K-series	32.32	29.18	17.00	CaO	40.83	45.22	0.99
Au	79	M-series	8.08	7.30	0.87		7.30	8.08	0.47
		Total:	110.74	100.00	100.00				

PMO 224.360/F

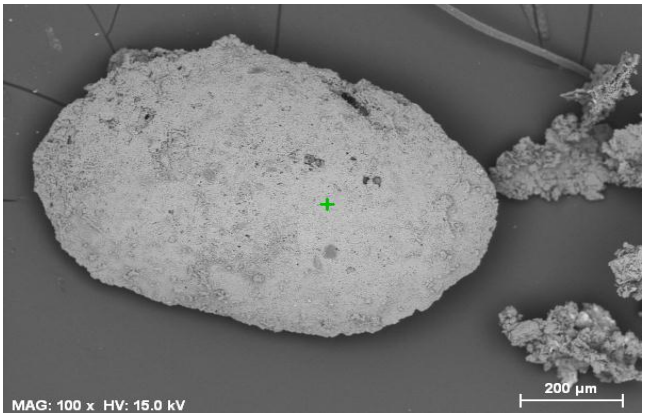

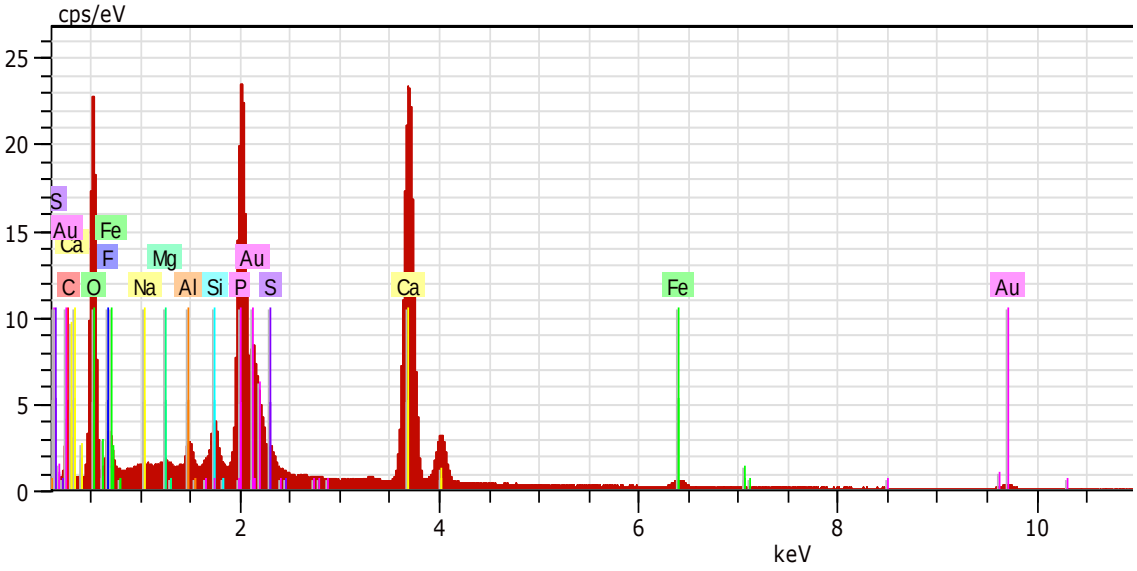

El	AN	Series	unn. C [wt.%]	norm. C [wt.%]	Atom. C [at.%]	Error (1 Sigma) [wt.%]
C	6	K-series	3.70	3.42	6.94	0.93
O	8	K-series	41.86	38.60	58.88	4.94
F	9	K-series	1.47	1.35	1.74	0.36
Na	11	K-series	1.06	0.98	1.04	0.10
Mg	12	K-series	0.01	0.01	0.01	0.03
Al	13	K-series	0.96	0.88	0.80	0.07
Si	14	K-series	1.60	1.48	1.28	0.15
P	15	K-series	12.46	11.49	9.06	0.56
S	16	K-series	1.28	1.18	0.90	0.07
Ca	20	K-series	30.86	28.46	17.33	0.95
Fe	26	K-series	1.80	1.66	0.73	0.09
Au	79	M-series	11.37	10.49	1.30	0.66
		Total:	108.44	100.00	100.00	

PMO 224.360/G

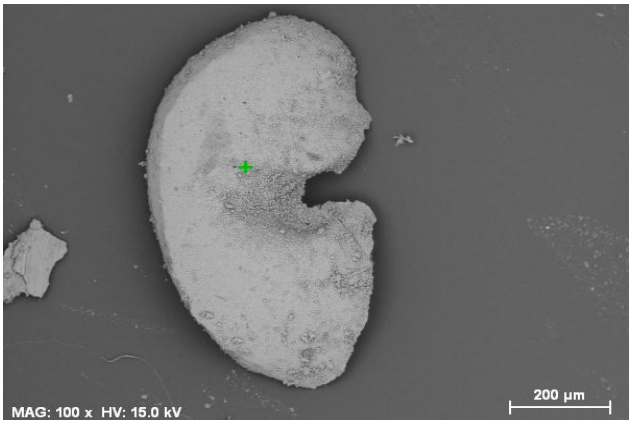

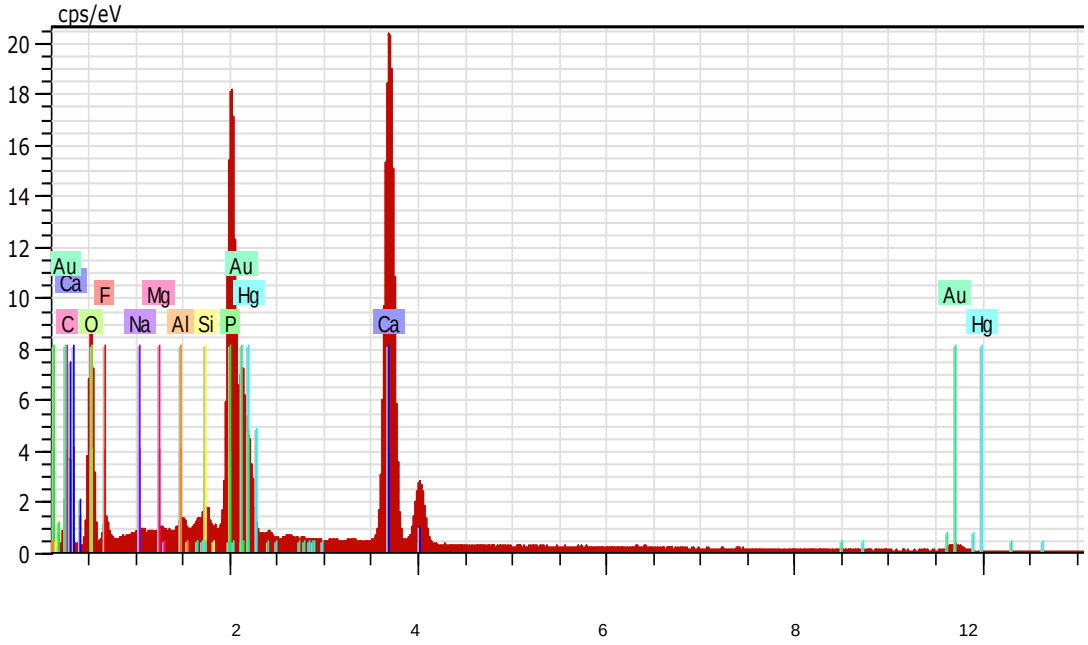

El	AN	Series	unn. C [wt.%]	norm. C [wt.%]	Atom. C [at.%]	Error (1 Sigma) [wt.%]
C	6	K-series	5.67	5.04	9.85	1.05
O	8	K-series	45.31	40.24	59.09	5.58
F	9	K-series	2.70	2.40	2.96	0.45
Na	11	K-series	0.41	0.36	0.37	0.06
Mg	12	K-series	0.00	0.00	0.00	0.03
Al	13	K-series	0.00	0.00	0.00	0.00
Si	14	K-series	0.67	0.60	0.50	0.19
P	15	K-series	12.06	10.71	8.13	0.54
Ca	20	K-series	34.35	30.50	17.88	1.05
Au	79	M-series	10.80	9.59	1.14	0.80
Hg	80	M-series	0.64	0.57	0.07	0.19
		Total:	112.60	100.00	100.00	

Appendix 5 SEM analysis of an acrotretid brachiopod

PMO 224.360/J

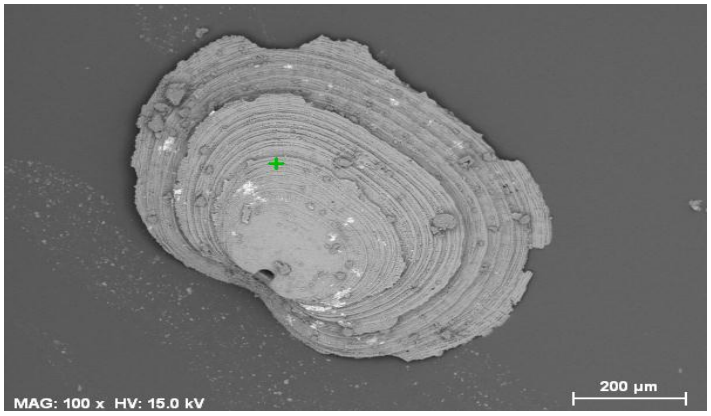

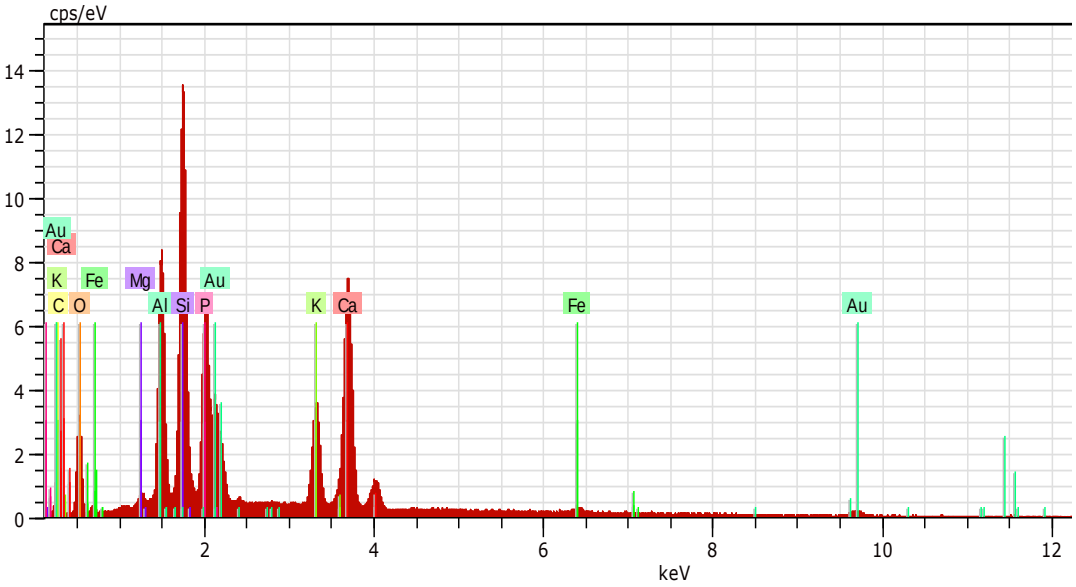

El	AN	Series	unn. C [wt.%]	norm. C [wt.%]	Atom. C [at.%]	Error (1 Sigma) [wt.%]
C	6	K-series	6.94	5.47	9.76	2.14
O	8	K-series	59.54	46.93	62.87	8.77
Mg	12	K-series	0.02	0.02	0.01	0.03
Al	13	K-series	9.80	7.72	6.14	0.49
Si	14	K-series	14.69	11.58	8.84	0.80
P	15	K-series	7.23	5.70	3.95	0.43
K	19	K-series	4.33	3.41	1.87	0.16
Ca	20	K-series	12.73	10.04	5.37	0.41
Fe	26	K-series	0.96	0.75	0.29	0.07
Au	79	M-series	10.64	8.38	0.91	0.70
		Total:	126.87	100.00	100.00	

Appendix 6 SEM analysis of unidentified specimens

PMO 224.360/A

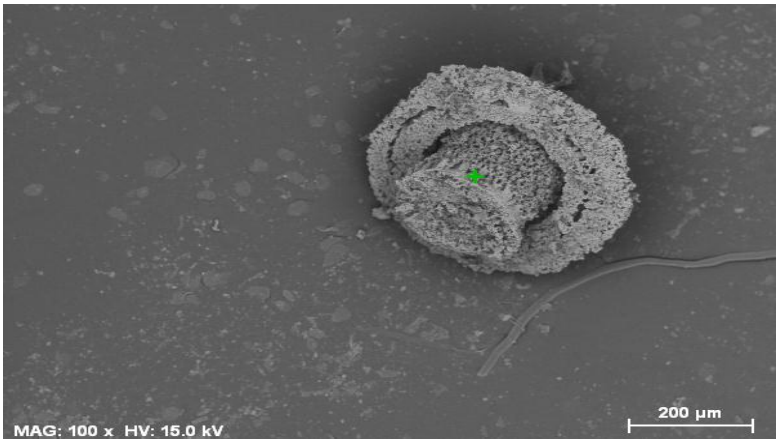

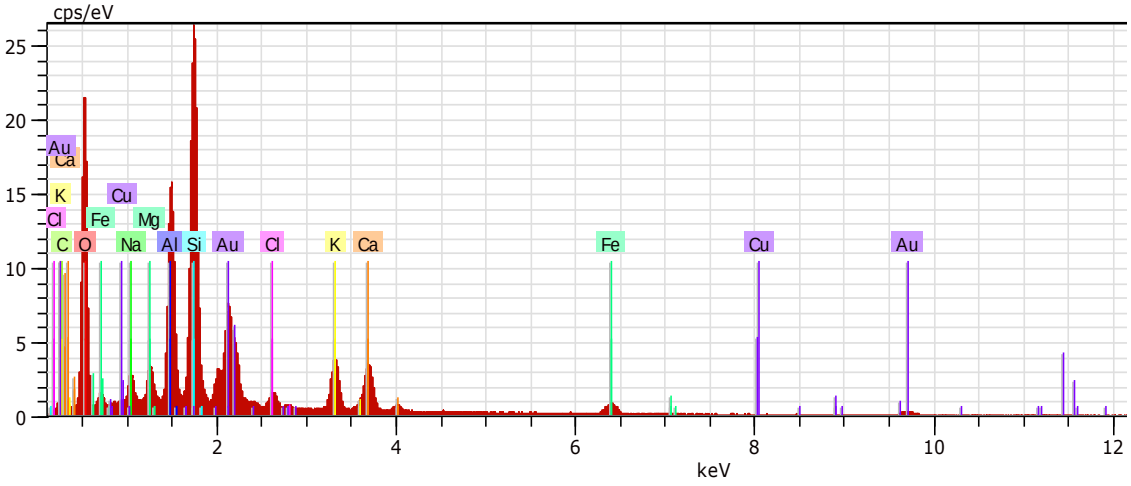

El AN Series unn. C norm. C Atom. C Error (1 Sigma)

			[wt.%]	[wt.%]	[at.%]	[wt.%]
C	6	K-series	6.66	5.60	10.89	2.94
O	8	K-series	49.10	41.34	60.29	5.77
Na	11	K-series	1.99	1.68	1.70	0.18
Mg	12	K-series	0.01	0.01	0.01	0.03
Al	13	K-series	8.92	7.51	6.50	0.44
Si	14	K-series	15.88	13.37	11.11	0.78
Cl	17	K-series	1.18	0.99	0.65	0.08
K	19	K-series	4.78	4.03	2.40	0.18
Ca	20	K-series	5.60	4.72	2.75	0.20
Fe	26	K-series	4.09	3.44	1.44	0.16
Cu	29	K-series	1.02	0.86	0.31	0.08
Au	79	M-series	19.54	16.45	1.95	0.77
		Total:	118.78	100.00	100.00	

PMO 224.360/B

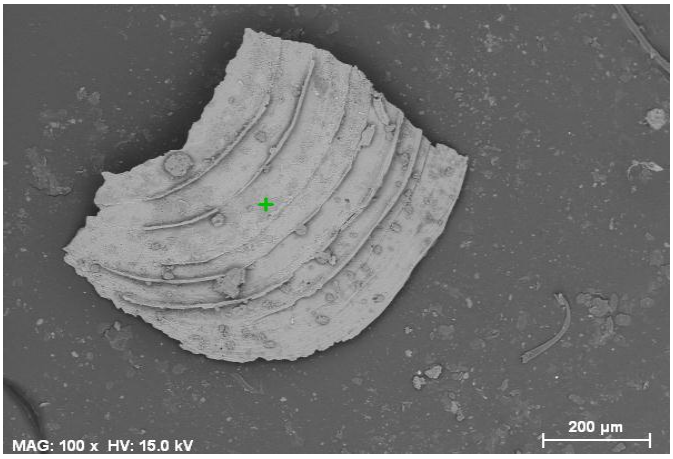

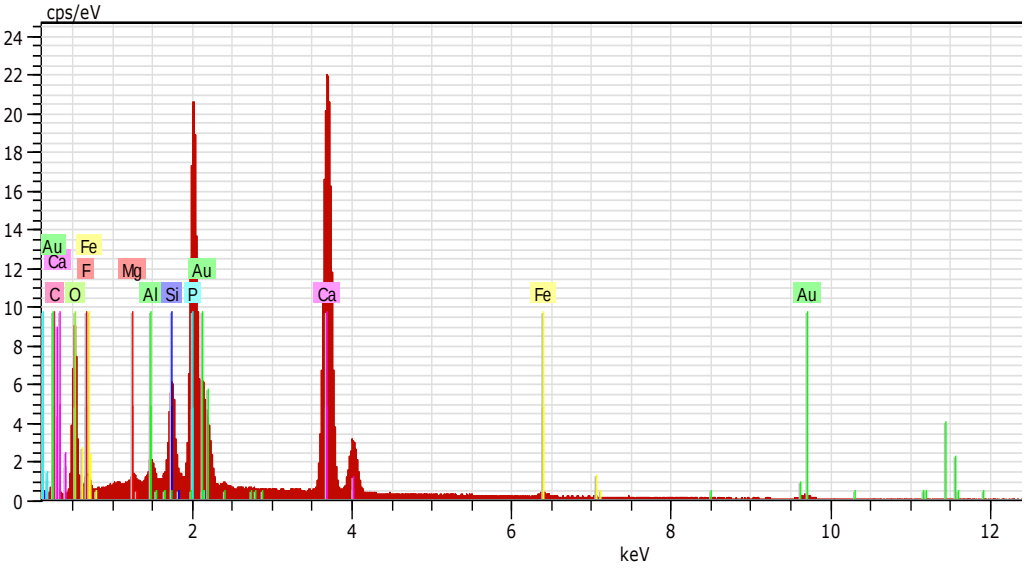

El	AN	Series	unn. C [wt.%]	norm. C [wt.%]	Atom. C [at.%]	Error (1 Sigma) [wt.%]
C	6	K-series	3.80	3.72	7.33	0.85
O	8	K-series	41.53	40.67	60.15	5.29
F	9	K-series	1.25	1.23	1.53	0.29
Mg	12	K-series	0.00	0.00	0.00	0.00
Al	13	K-series	0.52	0.51	0.44	0.05
Si	14	K-series	2.73	2.67	2.25	0.20
P	15	K-series	11.58	11.34	8.66	0.52
Ca	20	K-series	31.52	30.87	18.23	0.97
Fe	26	K-series	1.09	1.07	0.45	0.07
Au	79	M-series	8.09	7.93	0.95	0.52
		Total:	102.11	100.00	100.00	

PMO 224.360/C

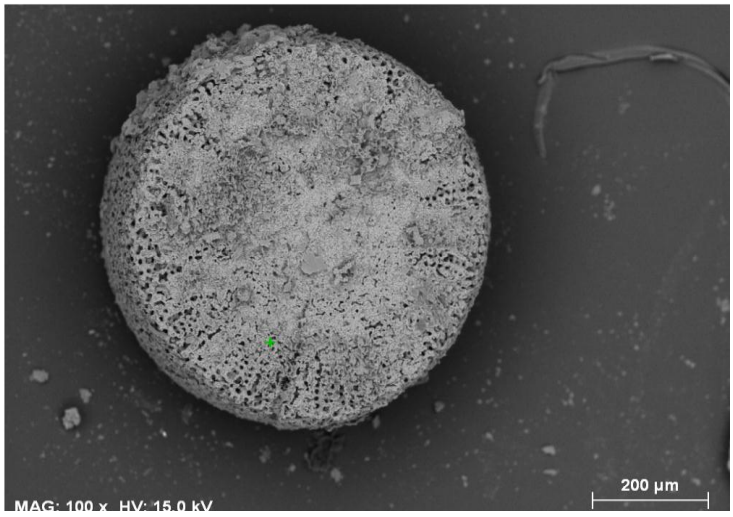

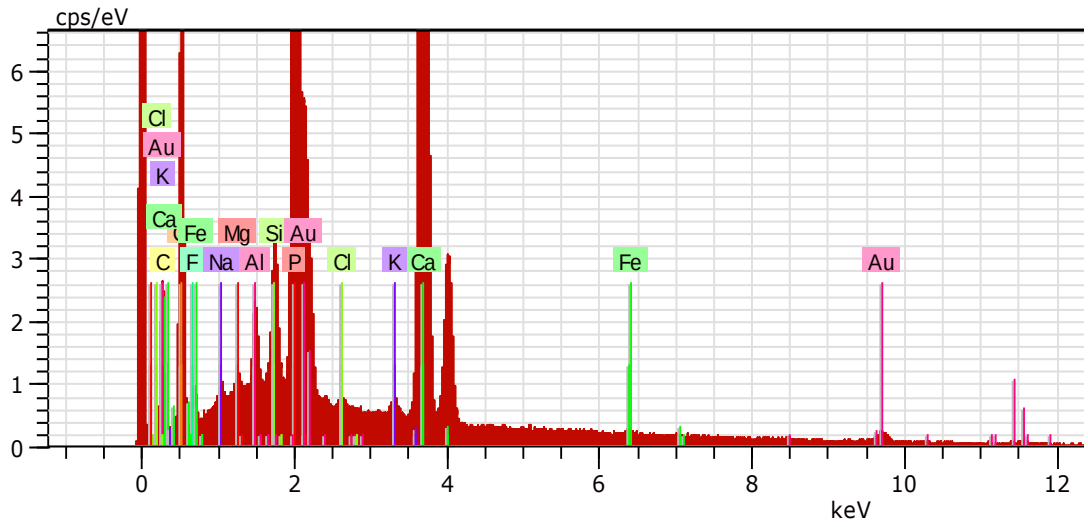

El	AN	Series	unn. C [wt.%]	norm. C [wt.%]	Atom. C [at.%]	Error (1 Sigma) [wt.%]
C	6	K-series	4.86	4.36	8.45	1.60
O	8	K-series	46.25	41.47	60.39	5.57
F	9	K-series	0.88	0.79	0.96	0.20
Na	11	K-series	0.37	0.33	0.33	0.05
Mg	12	K-series	0.00	0.00	0.00	0.03
Al	13	K-series	0.91	0.82	0.71	0.07
Si	14	K-series	1.74	1.56	1.29	0.13
P	15	K-series	12.83	11.50	8.65	0.54
Cl	17	K-series	0.25	0.23	0.15	0.04
K	19	K-series	0.48	0.43	0.25	0.04
Ca	20	K-series	34.05	30.54	17.75	1.04
Fe	26	K-series	0.43	0.39	0.16	0.04
Au	79	M-series	8.47	7.60	0.90	0.49
		Total:	111.52	100.00	100.00	

Appendix 7 Microfacies analysis

Thin section no.	Intrabites(%)	Ostracodes (%)	Brachiopods (%)	Bryozoa (%)	Echinoderms (%)	Gastropods (%)	Cephalopods (%)	Matrix (%)	Unknown (%)	wackestone	packstone	Dolomite-stain
Bed 1:												
221.466	9.6	6.0	2.3	0	10.6	0.0	0.0	69.0	2.3		v	no
221.467	7.9	10.0	3.7	0.3	11.4	0.0	0.0	67.0	4.5	v		no
Average % BED 1ny	6.3	8.0	2.8	0.15	11.0	0,0	0.0	68.0	3.4			
Bed 2:												
221.468	6.0	16.0	5.3	1.3	14.3	0.0	0.0	53.0	4.0		v	no
221.469	2.3	14.6	5.3	0.3	20.0	0.0	0.0	54.3	2.6		v	no
221.470	7.0	14.3	1.0	0.0	22.3	0.0	0.0	54.3	1.0		v	no
Average % BED 2	5.1	15.0	3.9	0.5	18.9	0.0	0.0	53.9	2.5			
Bed 3:												
221.471	6.0	10.6	1.0	0.0	11.6	0.0	0.0	68.3	2.3		v	selectively dolomitized micrite in packstone, subhedral, micrite-core
221.472	6.3	8.0	0.3	1	25.6	0.0	0.6	54.3	3.6		v	selectively dolomitized micrite in packstone, subhedral, micrite-core
Average % BED 3	6.2	9.3	0.65	0.5	18.6	0.0	0.3	61.3	3.0			
Bed 4:												selectively dolomitized micrite in packstone, subhedral, micrite-core
221.473	13.0	5.0	1	3.6	23.3	0.0	0.0	52.6	1.3		v	selectively dolomitized micrite in packstone, subhedral, micrite-core
221.474	7.6	13.0	0.6	1.3	17.0	0.0	0.0	56.3	4.0		v	selectively dolomitized skeletal fragments and micrite in packstone, subhedral, micrite-core
221.475	8.6	13.3	1.3	0.6	12.6	0.0	0.0	60.6	2.6		v	selectively dolomitized skeletal fragments and micrite in packstone, subhedral, micrite-core
221.476	4.6	12.3	0.0	0.0	8.3	0.0	0.0	73.3	1.3	v		selectively dolomitized skeletal fragments and micrite in packstone, subhedral, micrite-core
221.477	20.0	5.6	1.0	0.0	4.6	0.0	0.0	67.6	1.3		v	selectively dolomitized micrite in packstone, subhedral-anhedral, micrite-core
Average % BED 4	10.8	9.8	0.78	1.1	13.2	0,0	0,0	62.1	2.1			
Bed 5:												
221.478	15.3	8.6	2.9	0.0	10.6	0.0	0.0	60.3	2.0		v	selectively dolomitized micrite in packstone, subhedral, micrite-core
221.479	6.0	6.0	1.3	0.0	4.0	0.0	0.3	81.3	0.6		v	selectively dolomitized micrite in packstone, subhedral, micrite-core
221.480	5.6	11.0	0.6	0.6	4.0	0.0	0.0	75.0	2.0		v	dolomitized micrite in packstone, subhedral, micrite-core
221.481	4.6	11.0	1.0	0.0	6.0	0.0	0.3	74.0	0.6		v	dolomitized micrite in packstone, subhedral, micrite-core
Average % BED 5	8.5	9.15	1.45	0.15	6.2	0.0	0.15	72.7	1.3			
Bed 6:												
221.403	4.3	6.6	0.3	0.0	7.0	0.0	9.0	68.6	1.3		v	selectively dolomitized micrite in packstone, subhedral-anhedral, micrite-core
221.404	13.0	10.3	0.0	0.0	17.0	0.0	0.0	59.0	0.6		v	selectively dolomitized micrite in packstone, subhedral, thick micrite-core
221.405	10.6	22.0	1.3	0.0	12.3	0.0	0.0	53.0	0.6		v	Selectively dolomitized micrite in packstone
221.406	10.6	16.0	3.6	0.0	11.0	0.0	0.0	57.6	0.6		v	selectively dolomitized micrite in packstone, subhedral, micrite-core
221.407	8.3	16.3	1.0	0.0	11.6	0.0	0.0	61.3	1.3		v	selectively dolomitized micrite in packstone, subhedral, micrite-core
Average % BED 6	9.36	14.2	1.2	0.0	11.8	0.0	1.8	59.9	0.9			